# Human Lower Limb Dynamic Analysis Using Wearable Sensors and Its Applications to a Rehabilitation Robot

Cao Enguo

A dissertation submitted to
Kochi University of Technology
in partial fulfillment of the requirements
for the degree of

Doctor of Philosophy

Graduate School of Engineering
Kochi University of Technology
Kochi, Japan

September 2012

# Abstract

In many countries in which the phenomenon of population aging is being experienced, motor function recovery activities have aroused much interest. In this dissertation, a sit-to-stand rehabilitation robot utilizing a double-rope system was introduced, and the performance of the robot was evaluated by analyzing the dynamic parameters of human lower limbs. For the robot control program, a trajectory control method and an impedance control method with a training game were developed to increase the effectiveness and frequency of rehabilitation activities, and a calculation method was developed for evaluating the joint moments of hip, knee, and ankle. Test experiments were designed, and ten subjects were requested to stand up from a chair with assistance from the rehabilitation robot. In the experiments, body segment rotational angles, trunk movement trajectories, rope tensile forces, ground reaction forces (GRF) and centers of pressure (COP) were measured by sensors, and the moments of ankle, knee and hip joint were real-time calculated using the sensor-measured data. The experiment results showed that the sit-to-stand rehabilitation robot using the trajectory control method could assure the accomplishment of the standing-up process in comfortable postures, and decrease the condition of joint moments. Furthermore, using the impedance control method could recognize the intended movement of patients, and train the motor function of lower limbs more effectively. And at last, using the game control method could encourage collaboration between the brain and limbs, and allow for an increase in the frequency and intensity of rehabilitation activities.

Direct measurement of tensile force of muscles locate at the inner part of limbs is not convenient in the present medical situation. For supporting the medical diagnoses in rehabilitation activities, a new quantitative method for estimating dynamics and muscle forces

of human lower limb is presented based on a developed sit-to-stand training robot and AnyBody Modeling System. The sit-to-stand training robot adopts a double-ropes control method to offer assistance in the rehabilitation activities, meanwhile in the robot system the rotational motions of body segments could be measured by wearable motion sensors, and tri-axial ground reaction force and center of pressure could be measured by a miniature type force plate. The AnyBody Modeling System professionally concerns on musculoskeletal kinematic modeling and analysis, a minimum fatigue criterion way is employed to assure that the human body would maximize its endurance and precisely, and quantitative results of muscle forces could be calculated through an inverse dynamics method in the system. In this study a musculoskeletal model composed of thigh, shank, foot, four rotational joints, and fifteen muscles was established in the AnyBody Modeling System and the geometry information of the model with magnification coefficient were determined from the anatomy datum of human lower limb. Then test experiments were implemented and four volunteers were requested to stand up from a chair in self-selected speed, and the dynamics parameters of body segments were real-time measured by the sensors in the training robot. At last the measured dynamics data were applied on the musculoskeletal model, and the quantitative muscle forces of lower limb were calculated out through the inverse dynamics method. Furthermore for validating the muscle force results, the qualitative muscle activation level was also measured in the test experiments by electromyography (EMG) method, and the measured EMG results showed a considerable comparability with the calculated AnyBody results. The dynamics and muscle forces results also showed that the rehabilitation training robot could improve conditions of lower limb muscles effectively, the sensors could give a great performance in measuring motions and GRF, and variation tendency of the muscle force results have fact significance in the sit-to-stand process. Therefore, the method for estimating muscle forces appears to be a practical means to determine dynamics parameters in musculoskeletal analysis of human limb, and the system may be applied as a convenient

instrument in clinical settings.

Human foot is a complex musculoskeletal system. A new quantitative method for dynamics analysis of muscle forces of ankle joint during human walking was presented based on a developed wearable motion, ground reaction force sensor system and AnyBody Modeling System. In the AnyBody Modeling System, which professionally concerns on musculoskeletal kinematic modeling and analysis, quantitative results of muscle forces can be calculated through an inverse dynamics method. In this study, a musculoskeletal model composed of the shank and multiple-units foot was established in the AnyBody Modeling System, and an experiment was implemented with the wearable sensor system on six volunteers during their normal gait. Tension forces of muscles of ankle joint were calculated through the inverse dynamics analysis, and the results matched the muscle activation level tendency of electromyography method, which was implemented in the experiment as a contradistinction. The method for estimating muscle forces of ankle joint in the study may be used as a convenient instrument for on-the-spot medical applications.

## Key words

Muscle Force, Standing-up, AnyBody, EMG**,** Ankle, Knee, Hip, Dynamic, Rehabilitation, Robot, Control Method, Joint Moment

# Contents

# Chapter 1

## Introduction

### 1.1 Research Backgrounds

Under the trend of population aging in many countries, the physical degeneration of aged persons leads to higher risk of deterioration of lower limb motor function, and stroke or brain injury have become common afflictions resulting in an increasing number of hemiplegics (1) (2). Meanwhile, sports injuries, traffic accidents, childhood diseases and life-style related diseases can also cause standing-up disability. A large proportion of those affected cannot recover completely under current medical conditions, and rehabilitation training has become one of the most workable methods of treatment in many situations. Therefore, motor function recovery activities have aroused widespread interest and the effectiveness of muscle strength training equipment has been greatly progressed in many countries. Furthermore, self-controlled training, which can assure frequency and intensity of rehabilitation training without need for an expert assistant, has become favored in many institutions (3).

A large proportion of those affected cannot recover completely, and rehabilitation training has become one of the most workable methods of treatment in many situations. As a result, motor function recovery activities have aroused widespread interest and the effectiveness of muscle strength training equipment has been greatly advanced in many countries (4–8). Moreover in the evaluation of rehabilitation activities, better understanding of the working of human lower limb muscles is needed for medical diagnosis, for designing rehabilitation training machines, and for making wearable artificial limbs. Therefore, it is valuable to develop a musculoskeletal model of human lower limbs for supporting the improvement of

rehabilitation machines, and an easy-operating human lower limb dynamic estimation method for evaluating the recovery effectiveness in clinical applications.

## 1.2 Development of Rehabilitation Robots and Our Goals

Balance training, limb coordination training and standing style transfer systems have provided adequate rehabilitation for many patients, and experiments have validated the practicality of these training systems (9–12). Moreover, exoskeleton robots or prosthetic limbs have played an important role in the rehabilitation field. In order to offer motive power these robots usually decide the amount of moment or force by sensing the intention of patients (13) (14), thereby raising the athletic ability of a physically weak body. But these rehabilitation activities may not ensure that training is undertaken in a natural and comfortable trajectory for the patients; moreover inadequate trajectory training may lead the injured limb to develop an unnatural trajectory. Meanwhile, rehabilitation robots with prescribed movement pattern or interactive motion rehabilitation have been developed for naturalistic motion and body weight supported training (15–18), and a gravity-balancing leg passive orthosis also performed well in trajectory training (19). But these rehabilitation systems are not capable of intelligently interpreting human intentions; they may just support an injured limb of a patient without concentrating on retraining weak points that may lead to unobvious rehabilitation effects.

Several more practical types of rehabilitation robotic devices have proved effective in helping improve limb motor function, but they may be not suitable for self-controlled training. For example, a gait rehabilitation robot with upper and lower limb connections that allows patients to update their walking velocity on various terrains, a powered lower limb orthoses for gait rehabilitation that allows practice starting, turning, stopping, and obstacle avoidance during walking over ground (20), and a bio-responsive motion system that works as a gait simulator for recovery of motion ability of the lower extremities of stroke patients (21).

However, these robots are relatively complex and difficult to set up by patients on their own, so sometimes the training can be conducted only in hospitals with an expert. These characteristics may increase the time pressure and economic pressure on patients, as rehabilitation training is normally a long-term activity. Furthermore, as for hemiplegic patients and aged persons with degenerated motor function, there is always functional disorder in some regions of brain. More and more researches studied brain mechanism during the process of motor function recovery. There is now sufficient evidence that using a rehabilitation protocol involving motor imagery practice in conjunction with physical practice of goal-directed rehabilitation tasks leads to enhanced functional recovery of paralyzed limbs among stroke sufferers (22). The brain mechanism has been studied underlying the recovery of motor functions (23–25), and its validity and merits has been verified with the achieved positive results. Therefore, rehabilitation training games that can activate collaboration between brain and limb are necessary for developing effective recovery processes. In these circumstances, development of a comfortable and effective rehabilitation system for self-training would be valuable, and dynamic analysis of human limbs for evaluating the effect and interactivity of the rehabilitation activities is essential.

## 1.3 Development of Muscle Force Estimation methods and Our Goals

Muscle force estimation is not easy because human limb is a complex musculoskeletal system and some power muscles are locating at inner part of limbs. For direct measurement of muscle forces, electromyography (EMG) method has been frequently applied as a standard clinical tool in identifying activation level of muscles, but in the EMG method the active level results of human muscles are relative large or small with the unit of % rather than quantitative values with the unit of Newton (26) (27). Moreover through surface EMG method only the activities of surface muscles could be estimated, and through needle EMG method the

invasiveness of needles may cause the reluctance of patients (28). For indirect estimation method of muscle forces, the quantitative muscle forces of human foot could be calculated. Typically, a synthesis model of the musculoskeletal system is used, which predicts individual muscle behavior when supplied with kinematic data and certain assumptions associated with objective functions (29–32). In the situation, the acquirements of motions of limbs, forces applied on limbs, and the construction of musculoskeletal model are essential (33).

Up to the present there are various methods to measure human motion, ground reaction force (GRF) and center of pressure (COP) for limb dynamics analysis. But many of them are restricted to laboratory environment and sick to adapt to different situations. The commercial motion camera system, which is regarded as the most popular instrument and a standard tool in measuring movement of human limb, could be performed only in laboratory environment and expensive for implements (34). The force plate, which is the widely used in measuring GRF with high accuracy in various fields, is limited in single stride measurement (35). In this situation, wearable sensor systems based on miniature type force sensors, acceleration sensitive units and gyroscopes play more important role in the applicability for continuously walking and climbing stairs or slopes (36) (37). For construction of musculoskeletal dynamic model, the AnyBody Modelling System, which works in a minimum fatigue criterion way, could be introduced in various applications of variable situation. The geometric data of the model could be decided based on measurements of human anatomy model, and through inverse dynamics method quantitative results of muscle forces of human foot could be calculated. Furthermore, the EMG system could be introduced to validate the calculated muscle force results (38) (39).

# Chapter 2

## A Sit-to-stand Training Robot and Its Performance Evaluation: Dynamic Analysis in Lower Limb Rehabilitation Activities

## 2.1 Summary

A sit-to-stand rehabilitation robot based on a double-rope system was developed, and the performance of the robot was evaluated by human lower limb dynamics analysis. In the robot system, precise locations of the wearable parts are unnecessary and control commands can be inputted by the patients on their own, which improved the weak point of Ref. 20-21. A trajectory control method was developed to ensure patients' comfortable postures which improved the weak point of Ref. 9-14, and an impedance control method based on the trajectory control method was developed to respect patients' moving intention which improved the weak point of Ref. 15-19. In addition, a game control method based on the impedance control method was developed to improve the coordination of brain and limbs, which achieved the advantage of Ref. 22-25. In the other hand, for evaluating the performance of the robot, dynamic parameters of human lower limb was analyzed. In the rehabilitation activities, human segments rotational angles, movement trajectories, ground reaction forces, centers of pressure and rope tensile forces were measured by a sensor system, after which the joint moments of ankle, knee and hip were real-time calculated in the control program.

## 2.2 Materials and Methods

### 2.2.1 Rehabilitation Robot for Standing-up Assistance

For providing assistance when patients stand up, a rehabilitation robot system was

developed with double ropes control method. As shown in Fig.2-1, the front rope and the back rope, which are controlled by two servo motors (MR-J2S), are connected to the patient by an easy-to-wear jacket. The lengths of ropes can be measured and recorded during real-time training by a photoelectric encoder in the sever motors, and the assistance forces of ropes can be measured by two high precision load cells. A computer program system is employed to control the motors and process the data measured by sensors (40), the angular motions of trunk, thigh, and shank are measured by the wearable motion sensors, and the ground reaction forces and center of pressure of the patient are measured by the ground reaction force sensor. During rehabilitation training, the precise locations of the three motion sensors attached on human limbs are unnecessary because all the limb segments are regarded as rotational rigid segments.

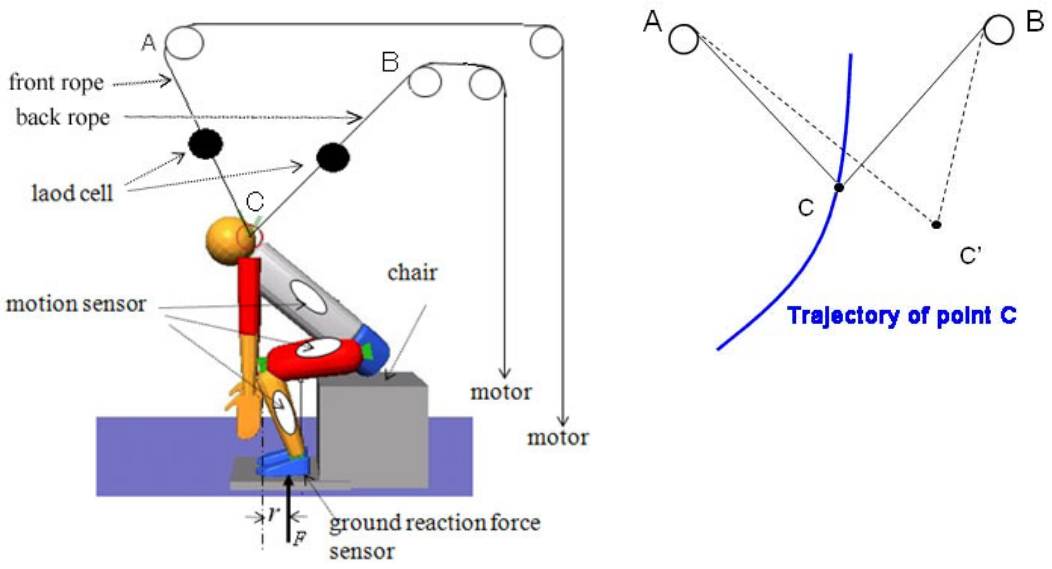


(a) (b)

Fig. 2-1. Schematic diagram of the rehabilitation robot system.

### 2.2.2 Sensor System

The wearable motion sensors were constructed with inertial elements to measure the

angular rotation of human shank, thigh, and trunk. As shown in Fig. 2-2 (a), the angular sensors recognize the gravity direction of the accelerometer as a standard direction, and the changes of accelerometer direction can arouse voltage changes in the sensors, so the angle changes can be calculated out through measuring the voltage changes. This motion sensor system is quite inexpensive compared with the conventional high-speed cameras system, and the measured data can be real-time utilized in the control program, furthermore the angular sensors can be easily fixed on body segments without precise locations because the human lower limbs are regarded as a rigid body system. A mini-type force plate was developed to real-time measure the GRF and COP. As shown in Fig. 2-2 (b), four load cells are set at the location of 1, 2, 3 and 4 of the force plate. Based on this structure, the total load (F) can be calculated by summation which is shown in Eq. (1), and the COP can be calculated with Eq. (2). Furthermore, the data measured by the force plate can be real-time utilized in the control program. In the robot system, the tensile forces of the two ropes are real-time measured by two load cells (LTZ-200KA), the length of the rope is real-time measured by a photoelectric encoder in the sever motors, and the time is calculated per 0.1 (s) by the counter of the controller in the control program.


(a) Motion Sensor (b) Force Plate

Fig. 2-2. Schematic diagram of the structure of motion and GRF sensors.

$$\mathrm{F} = F1 + F2 + F3 + F4 \tag{1}$$

$$\mathrm{COP} = L \cdot (F3 + F4) / \mathrm{F} \tag{2}$$

$L$ − Distance from location 2 to location 4.

$F1$, $F2$, $F3$, $F4$ − Forces measured by load cell 1, 2, 3, 4.

### 2.2.3 Trajectory Control Methods

To assure patients always train in their normal and comfortable postures, a trajectory control method was developed in the control program. As shown in Fig. 2-3 (a), before the patient starts to stand up the ropes move up till tight for the training preparation, and when patient intents to stand up the trajectory control method starts immediately. The rope tensile force ($T$) with a magnification coefficient ($b$) represents the movement intention of patients, decreasing $T$ means that the patient intents to stand up, while increasing $T$ means the intention of moving down. For example, after the ropes become tight in the preparation section, $T$ decreases more than 10 (N) in 0.5 (s) meaning that the patient intends to stand up and the trajectory control method starts. In the trajectory control method, working of the sensor system and the algorithm controller is based on a saved desirable trajectory, and the desirable trajectory depends on the patient's height as a researched result in our laboratory. In this way, the front and back rope move up continuously at a normal speed while following their movement trajectory points by sensing the displacements ($d$) of ropes, and the robot system can assure that the patient always trains in a satisfactorily normal trajectory. In the end of the trajectory control method, the training program arrives at the last trajectory point and motors stop when the patient stands up straightly. The trajectory control method can worked effectively for the patients who have no enough strength to finish the movement from sit position to stand position by their own.

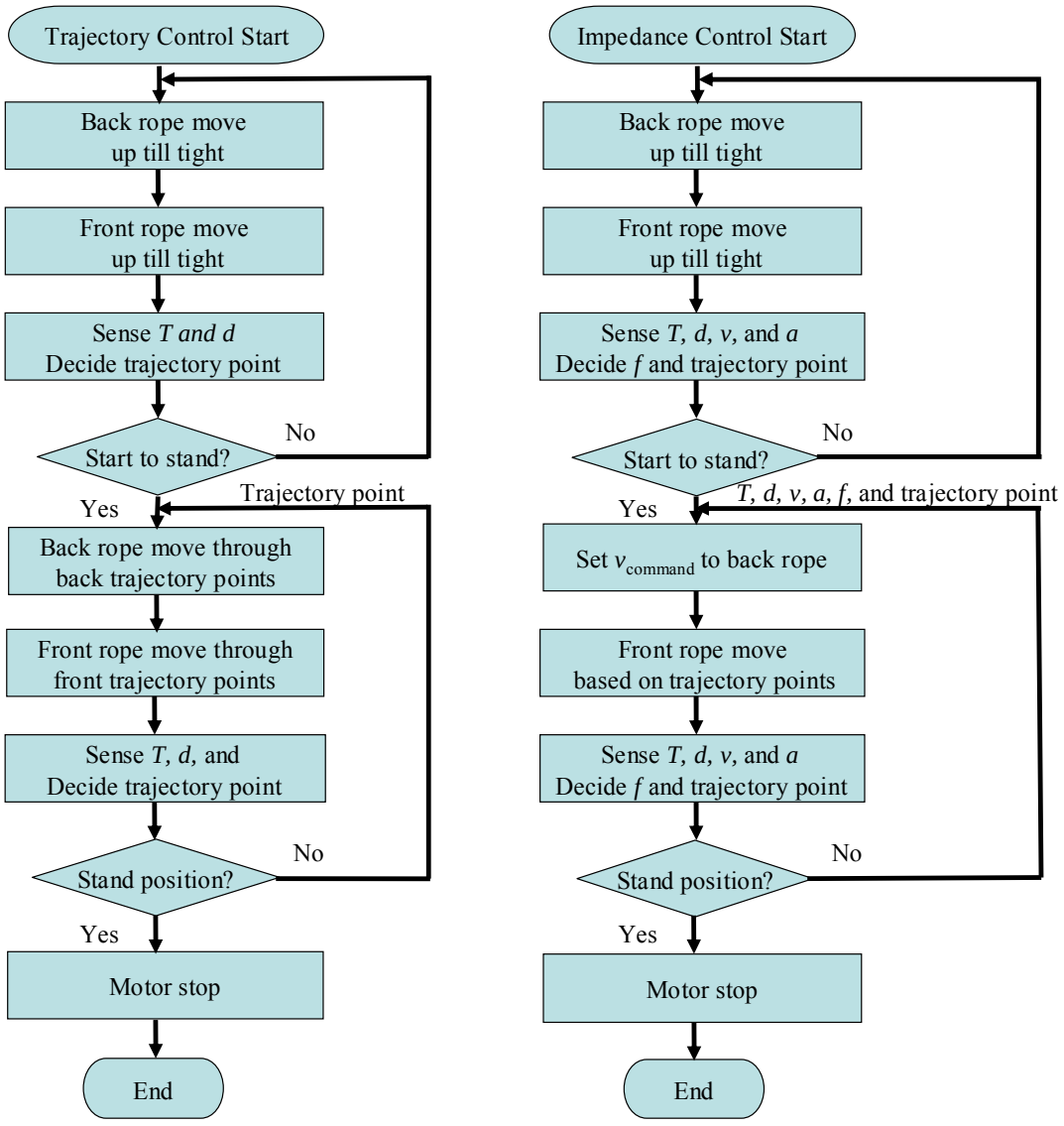


Fig. 2-3. Flow chart of trajectory control method and impedance control method.

### 2.2.4 Impedance Control Method and Game Control method

An impedance control method was developed for the control program to improve the safety and robustness of the system. The level of assisting force provided by the robot is

adjusted according to users' intention while assuring the adequate movement trajectory of body trunk. As shown in Fig. 2-1 (a), the whole hardware system is controlled by a computer program system, the front and back ropes are connected to two servo motors, and the tensile forces of the ropes are real-time measured by two high precision load cells. The assist force is real-time controlled by the back rope. The back rope can decide whether to offer assist forces or just follow the movement, because the sensor system and the algorithm controller can recognize the intended movement of the user. The back rope moves up faster when the user owns his/her own strength to stand up, moves up slower when the user needs help, or even moves down at a safe speed if the user intends to sit down. This ability ensures the rehabilitation system can spend more time training the weak posture of the user, and increases the recovery effect of the system.

Meanwhile, the movement trajectory is real-time controlled by the front rope. As shown in Fig. 2-1 (b), paired lengths of front rope and back rope decide the movement trajectory of point C, so while the length of back rope is being decided by the assist force, the adequate trajectory of point C can be controlled by adjusting the length of front rope in the control program. However, the desirable trajectories of different individuals have to be prepared in the control program. As a research result in our laboratory, there is a proportion relation between the desirable movement trajectory and the height of user. For example, when a health man stands up by himself while wearing the tautly following ropes of robot, the movement trajectory can be measured by the sensor system. If the trajectories of 1600 (mm) and 1800 (mm) heights were measured by the robot system, the trajectory of 1700 (mm) height can be calculated by averaging the two trajectories, and the lengths of front rope and back rope should be averaged separately. In this way, the trajectory of any height can be prepared in the control program.

As shown in Fig. 2-3 (b), before the user starts to stand up the ropes move up till taut in preparation for rehabilitation training, and when the user's intention to stand up is signaled the

impedance control method starts immediately. As shown in equation (3) and Table Ⅰ, the back rope tensile force (*T*) with the magnification coefficient of *b* represents the movement intention of the user. Decreasing *T* indicates that the user intends to stand up, while increasing *T* indicates an intention to crouch down. For example, 10 (N) is a small value that can be easily achieved by patients, and 0.5 (s) is a reasonable minimum action time for patients. While the ropes are already taut in the preparation phase, *T* decreasing by more than 10 (N) in 0.5 (s) indicates that the user intends to stand up and the impedance control method starts immediately. The displacement (*d*), velocity (*v*), and acceleration (*a*) of point C on body trunk are real-time calculated from the lengths of ropes and the counter of controller in the control program, and the their changes are real-time impeded with the magnification coefficients of *k*, *c*, and *u* respectively. Smaller values of *k*, *c*, and *u* indicate that the user can move up or down flexibly, but larger values indicate that the displacement, velocity, and acceleration of ropes can not change rapidly and the system is therefore more safe and stable. Desirable values of *k*, *c*, and *u* are decided by test experiments to assure that when the user stand up by himself tension on the rope can be maintained, and when the user drop down suddenly the back rope can move down at a safe speed.

$$v_{input} = (f - b \cdot T - k \cdot d - c \cdot v - u \cdot a) \cdot h \tag{3}$$

Table I Definition of terms used in Equation 3

| Terms | Definition |
|---|---|
| *T* | Back rope tensile force |
| *d* | Displacement of point C on body trunk |
| *v* | Velocity of point C on body trunk |
| *a* | Acceleration of point C on body trunk |

| | |
|---|---|
| $b$ | Magnification coefficient of $T$ |
| $k$ | Magnification coefficient of $d$ |
| $c$ | Magnification coefficient of $v$ |
| $u$ | Magnification coefficient of $a$ |
| $f$ | Insurance parameter for rope tension and standing-up accomplishment |
| $h$ | Magnification coefficient of $v_{input}$ |
| $v_{input}$ | Velocity inputted into control commands. |

Maintaining tension on the two ropes is the key requirement for the efficient working of the training system, so an insurance parameter ($f$), which is always increasing in the impedance control method, is introduced to ensure accomplishment of the standing-up process and the tension on the ropes at all times. Considering the weight of conjunction jacket, the ropes are in danger of loosing when the tensile forces are lower than 50 (N), so $f$ increases quickly to maintain the rope tension while $T$ is lower than 50 (N). Should the user stay in a weak posture for more than 10 (s), $f$ increases slowly to assist the user's upward movement at 1/5 normal standing-up speed. Here 10 (s) means that the user owns no sufficient strength to move up but only stay there, 1/5 normal standing-up speed means longer training time can be maintained on the weak postures. This control method avoids sudden collapse of the user, but does not hinder the user while he/she is training at a normal speed. Longer training times can therefore be assured if the user drops in a weak posture. As shown in Table Ⅱ, for the safety considerations, the motor stops immediately when rope length, rope tensile forces, or motion angles exceed their predetermined ranges, furthermore the rope velocity remains -1 (m/s) or 1 (m/s) when $v_{input}$ exceed -1 (m/s) or 1 (m/s) respectively. As the rope velocity is almost 1 (m/s) when a health man stands up in the robot, so this value seems quite reasonable for the safe peak value in rehabilitation activities.

Table Ⅱ Ranges of terms

| Terms | Ranges |
|---|---|
| Rope tensile forces | Each rope has the range from zero to user's weight. For safety considerations, the motors stop when exceeding. In the sitting posture, the included angle of the two ropes is about 60°, the maximum upward force of point C is about 173% of user's weight. In the standing posture, the included angle is about 120°, the maximum upward force of point C is about 100% of user's weight. |
| Rope velocity | Each rope has the range from -1 (m/s) to 1 (m/s). For safety considerations, the rope velocity remains -1 (m/s) or 1 (m/s) when exceeding. In the sitting posture, the maximum upward or downward velocity of point C is about 1.73 (m/s). In the standing posture, the maximum upward or downward velocity of point C is about 1 (m/s). |
| Rope lengths | Each rope has the range from the rope length of sitting posture to the rope length of standing posture, which is depends on user's height. For safety consideration, the motors stop when exceeding. |
| Motion angles | The motion angles of trunk, thigh, and shank have the ranges from 30°to 100°, from 0°to 100°, and from 30°to 100°respectively. Test experiments have validated that these ranges are sufficient for normal standing-up postures. For safety consideration, the motors stop when exceeding. |

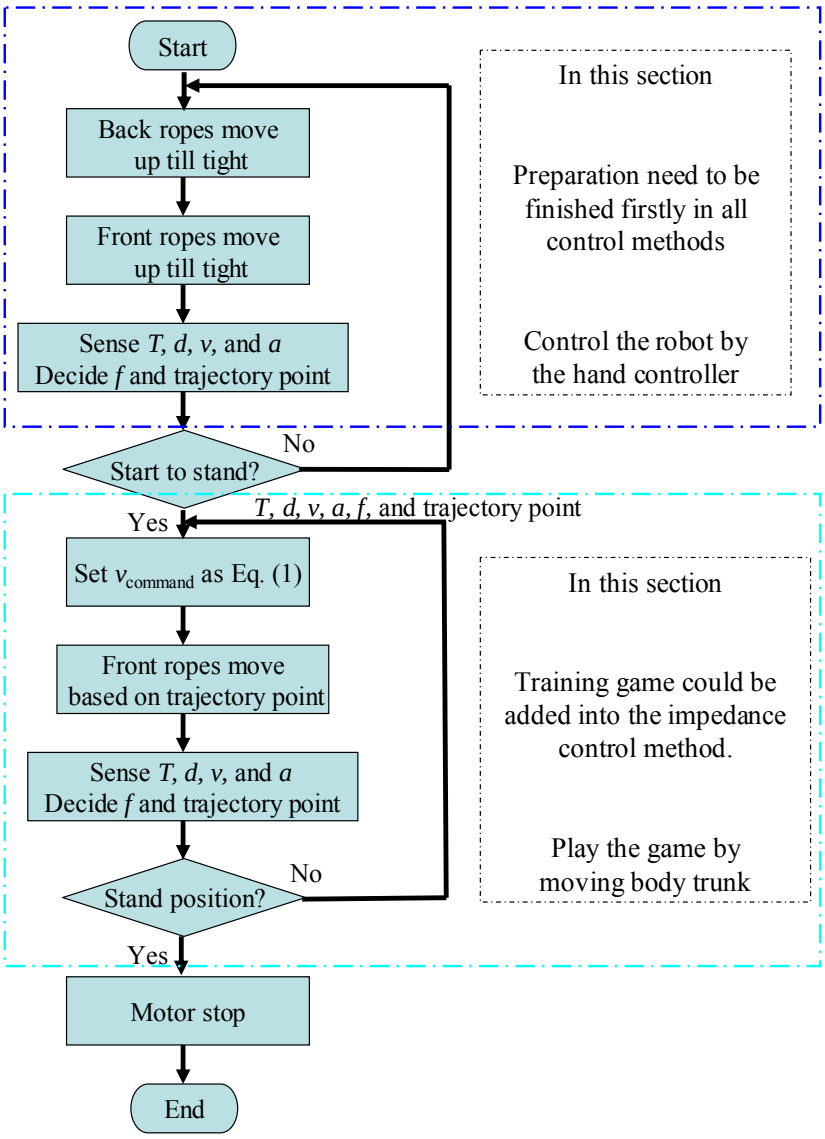


Fig. 2-4. A flow chart of impedance control method program, on which the game control method is based.

As shown in Fig. 2-4, in the game control method, a vertical direction rebound game was introduced for encouraging collaboration between brain and body in rehabilitation activities. In the game screen, the user controls a vertical blue board moving up or down to rebound a white ball, and the white ball will hit a brick and rebound back. The user can control the up-down

movement of the board by moving his body trunk up or down with the assistance of the robot, and in total it takes users about five minutes to finish the game. The game control method developed is based on the impedance control method, and additional control algorithms are developed to improve activation of the brain during the training program. In the game control method, $f$ is always increasing but only returns to 0 when $T$ decreases more than 50 (N) in 0.5 (s). Here 0.5 (s) is a reasonable minimum action time for patients, and 50 (N) means a partly motor ability of patients. The system therefore allows the user to squat down at a safe speed only after the user showed a partly standing-up ability. Therefore, users who can not offer any force are unsuitable for the game control method, and they should first do rehabilitation training using the impedance control method.

### 2.2.5 Calculation of Joint Moments

Different types of sensors can measure force and movement of human body segments, but joint moments are difficult to directly measure by sensors as it relates to many other parameters of human body. However, joint moment is one of the most important parameters in evaluating the motor function of human limbs, and it can reflect accurately the effectiveness of rehabilitation activities (41). Therefore, in this paper the joint moments of hip, knee, and ankle are calculated based on the data measured by the sensor system. As shown in Fig. 2-5 (a), the magnitude and location of $F$ can be acquired from GRF and COP data measured by the force plate. $\theta_1$, $\theta_2$, and $\theta_3$ can be acquired from the angle data measured by the three wearable motion sensors, $L_1$, $L_2$, and $L_3$ can be acquired by the lower limb lengths of users, and $m_1$, $m_2$, and $m_3$ can be estimated by the weight of users and the mass percentage law of human body, which is shown in Fig. 2-5 (b). Moreover, the parameters $p$, $q$, and $w$ are introduced to indicate the mass centre locations of foot, shank, and thigh respectively (41). As all the data are real-time measured by the sensor system of the rehabilitation robot, the joint moments can be real-time calculated in the computer control program. Finally the joint moments ($M$) of ankle,

knee and hip can be represented by the equation (4), (5), and (6).

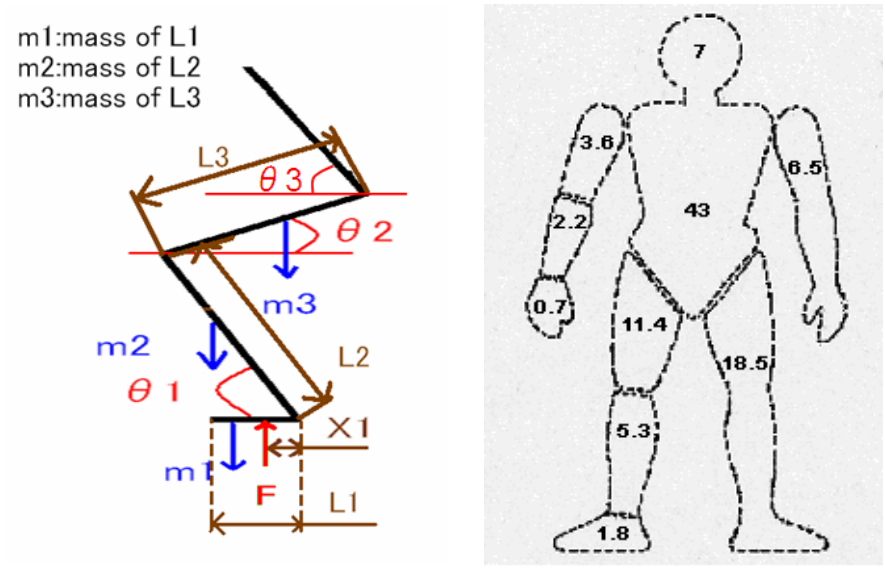


(a) (b)

Fig. 2-5. A diagram illustrating dynamic and mass division in the human body.

$$M_{ankle} = F x_1 - p L_1 m_1 g \tag{4}$$

$$\begin{aligned} M_{knee} &= F[L_2 \cos(\theta_1) - x_1] - qL_2 \cos(\theta_1) m_2 g \\ &\quad - [L_2 \cos(\theta_1) - pL_1] m_1 g \end{aligned} \tag{5}$$

$$\begin{aligned} M_{hip} &= F[L_3 \cos(\theta_2) - L_2 \cos(\theta_1) + x_1] - wL_3 \cos(\theta_2) m_3 g \\ &\quad - [L_3 \cos(\theta_2) - qL_2 \cos(\theta_1)] m_2 g \\ &\quad - [L_3 \cos(\theta_2) - L_2 \cos(\theta_1) + pL_1] m_1 g \end{aligned} \tag{6}$$

$p$ – Parameter of mass centre locations of foot.

$q$ – Parameter of mass centre locations of shank.

$w$ – Parameter of mass centre locations of thigh.

## 2.3 Experimental Study

### 2.3.1 Experiment Method

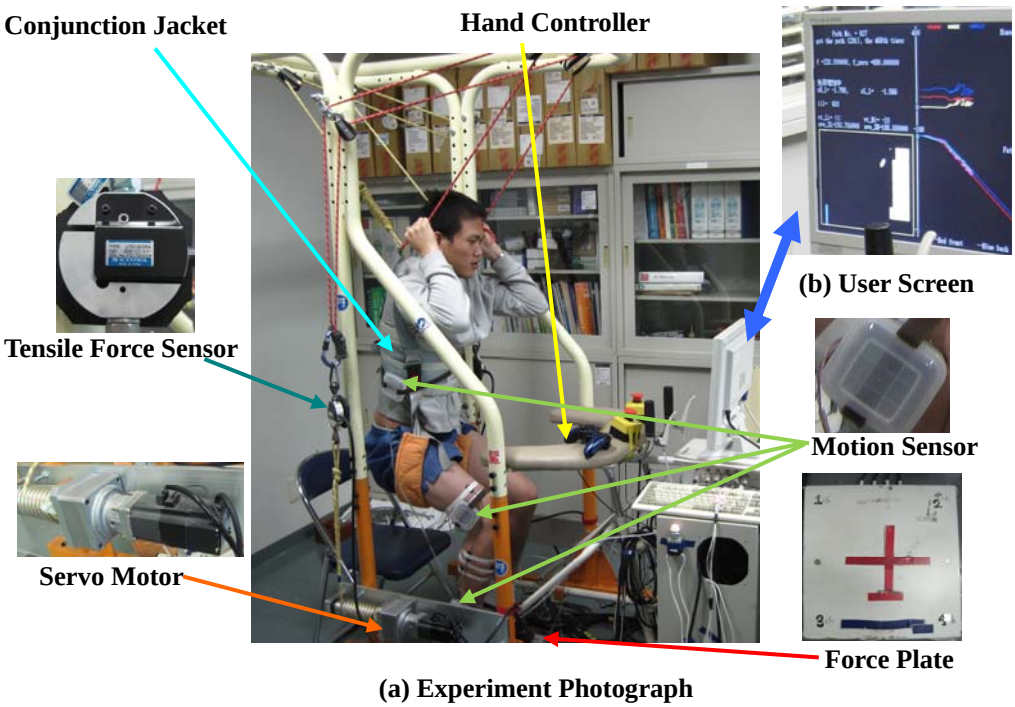


Fig. 2-6. Photograph of a subject in the rehabilitation experiment.

For analyzing the dynamic parameters of human lower limb and the effectiveness of the rehabilitation system, test experiments were designed for ten subjects (age: 26±5 years, height: 167±10 cm, mass: 52±9 kg) who have no history of musculoskeletal pathology or injury. As shown in Fig. 2-6 (a), the subjects were requested to stand up from a chair at self-selected speeds using, respectively, the self-supported standing method, the trajectory control method, the impedance control method and the game control method. In the start posture, the subject's elbow joints were in contact with the homologous knee joints, while in the terminal posture the

subject's legs were straight. In the experiment the subjects were attached to the training robot by a conjunction jacket, and they were requested to always keep their feet on the force plate. The three wearable motion sensors were fixed by belts on the trunk, thigh, and shank respectively. Precision location of the motion sensors attached to limbs is unnecessary because all the limb segments are regarded as rigid segments. Moreover, the conjunction jacket and wearable sensors are easy to wear without expert assistance, and control commands can be inputted with a hand controller. While the subjects were standing up, the movement trajectories, rope tensile forces, COP, GRF, and angular motions of trunk, thigh, and shank were real-time measured, and the joint moments of hip, knee, and ankle were real-time calculated out in the control program. As shown in the user screen of Fig. 2-6 (b), control parameters, training game, joint moments, and movement trajectory were displayed in the upper left, lower left, upper right, and lower right area of the screen respectively. In the self-standing experiment the subjects stood up on their own while the ropes followed the body movements and remained taut. In the trajectory control method and the impedance control experiments the subjects hypothesized that their legs were injured and that they had not enough strength to stand up independently, in order to see whether the trainer system could assist them in completing the process of standing-up. And in the game control experiment, the subjects moved their body trunk up or down to control a blue board on a screen to move up or down, which he/she used to rebound a white ball, somewhat like a game of squash. Before the experiment, the objective and method of the experiment were explained to the subjects, and their written and oral consent to the experiment was obtained. This experiment had been pre-approved by the ethics committee of the Department of Intelligent Mechanical System Engineering, Kochi University of Technology.

### 2.3.2 Experimental Results

As body parameters and individualities are different among different subjects, the

experiment results were not in perfect accordance. However, similar tendencies were found. As shown in Fig. 2-7, photograph represented five postures in 0%, 30%, 50%, 70%, and 100% of standing-up process (SP). To make the figures clear, the experiment results of three subjects using the impedance control method were shown from Figs. 2-8 to Fig. 2-12. The horizontal axis indicated one SP cycle, which is a posture series. In the control program, one posture can be recognized multiple times, which means one posture can be trained by longer time. As shown in Fig. 2-13, training times on different posture sections were summarized. Furthermore, different individuals were represented by different colors in all the figures.

0% 30% 50% 70% 100%

Fig. 2-7. Photograph of five postures in 0%, 30%, 50%, 70%, 100% of standing-up process (SP).

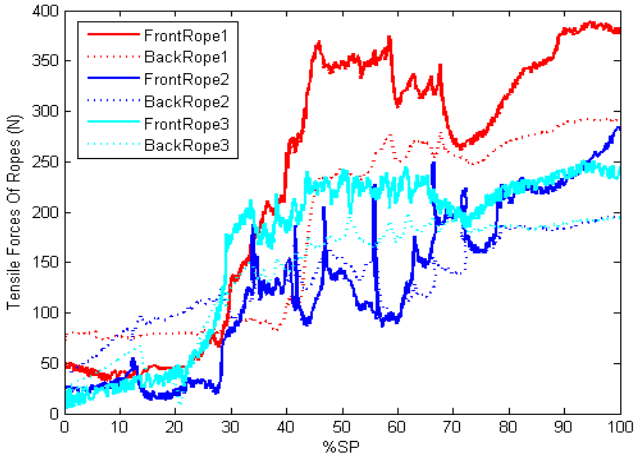


Fig. 2-8. Rope tensile forces of three subjects in impedance control method.

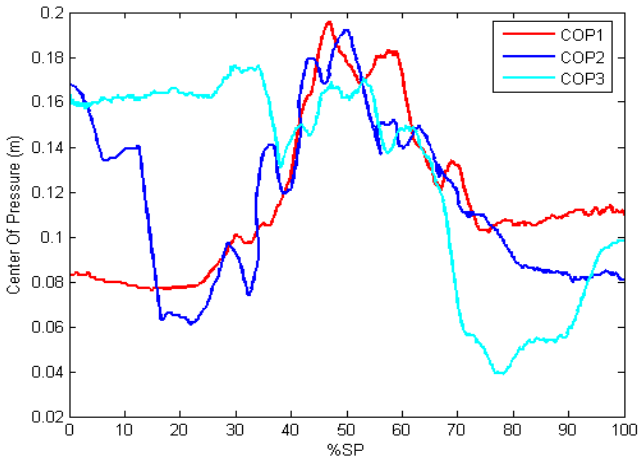


Fig. 2-9. COP of three subjects in impedance control method.

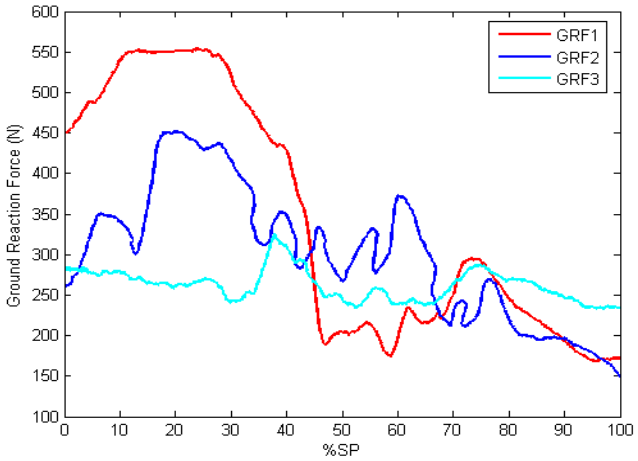


Fig.2-10. GRF of three subjects in impedance control method.

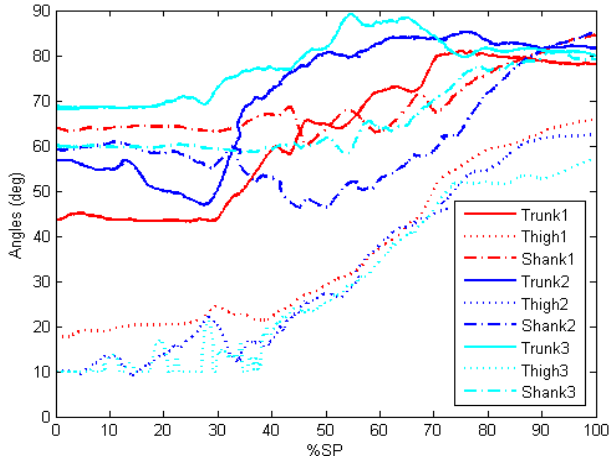


Fig. 2-11. Motion angles of three subjects in impedance control method.

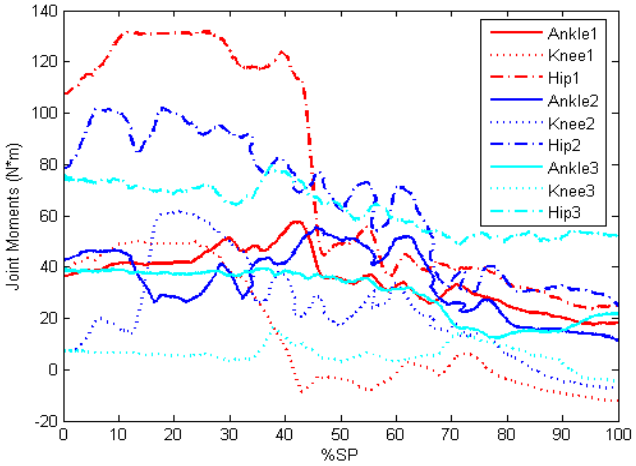


Fig. 2-12. Joint moments of ankle, knee, and hip of three subjects in impedance control method.

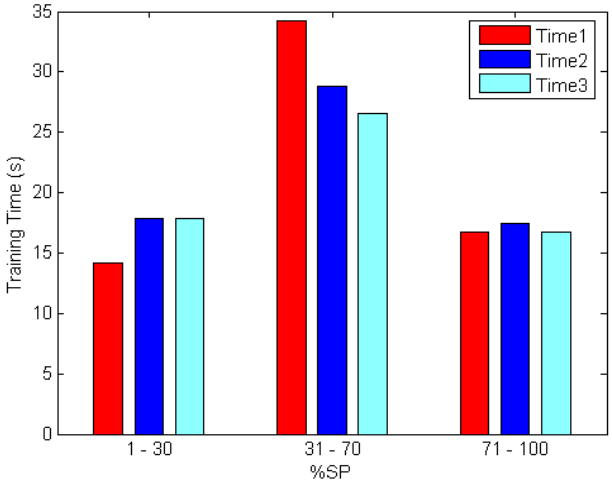


Fig. 2-13. Training times of different posture sections of three subjects in impedance control method.

For analyzing kinetics principles between trajectory control method and impedance control method, experiment results in one standing-up process cycle of two subjects were shown from Fig. 2-14 to Fig. 2-18. Furthermore for analyzing the kinetics differences among self-supported standing method (SSM), trajectory control method (TCM) and impedance control method (ICM), experiment results in one SP of the one subject were shown from Fig. 2-19 to Fig. 2-24.

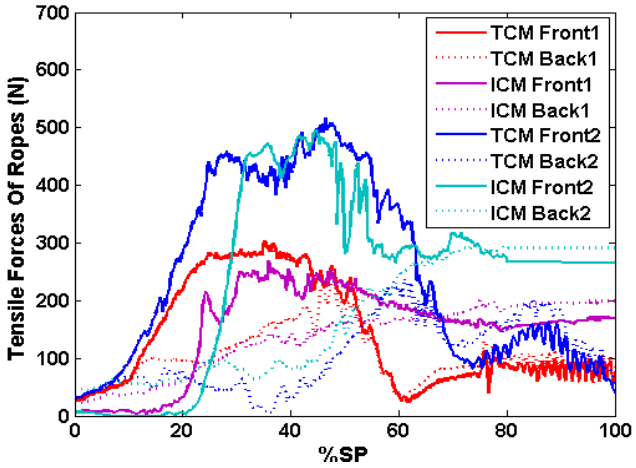


Fig. 2-14. Rope tensile forces of two subjects in TCM and ICM.

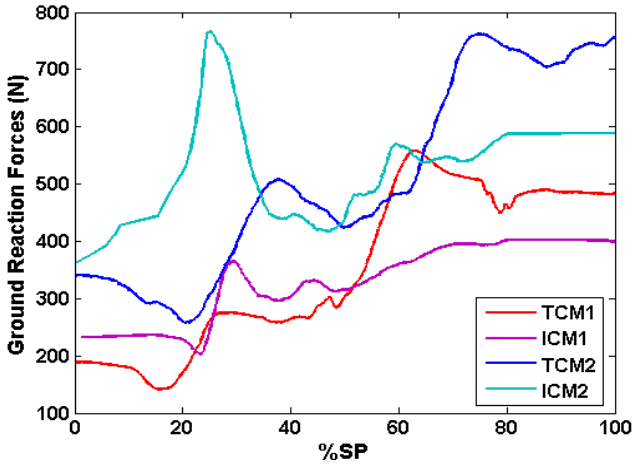


Fig. 2-15. GRF of two subjects in TCM and ICM.

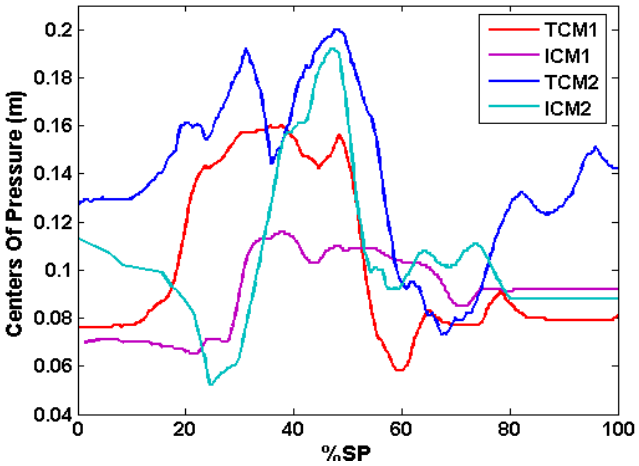


Fig. 2-16. COP of two subjects in TCM and ICM.

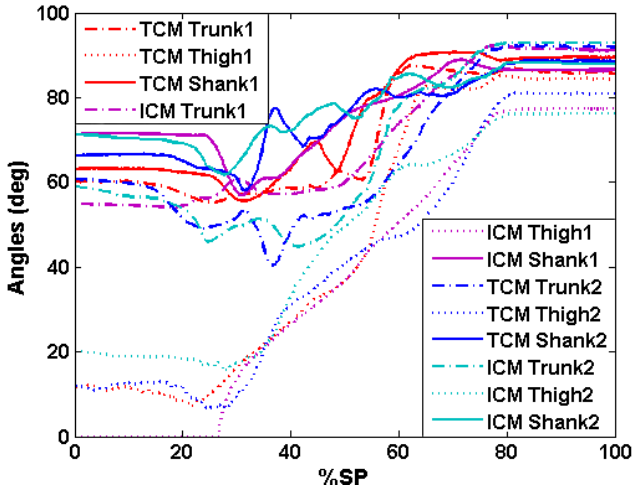


Fig. 2-17. Motion angles of shank, thigh, and trunk of two subjects in TCM and ICM.

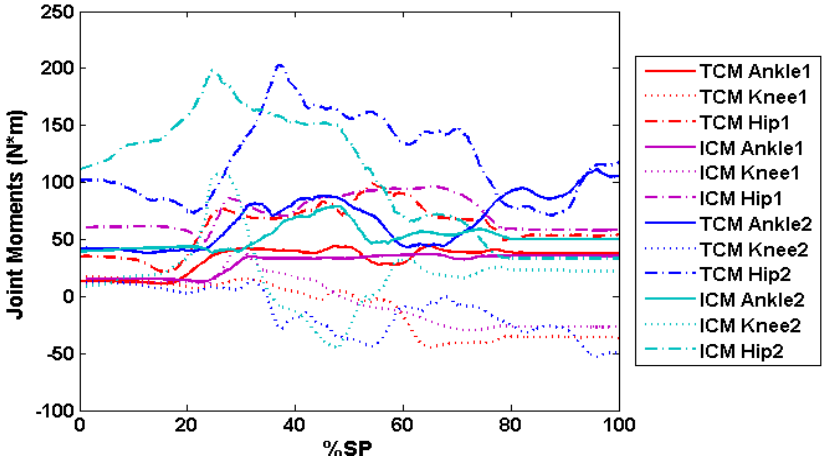


Fig. 2-18. Joint moments of ankle, knee, and hip of two subjects in TCM and ICM.

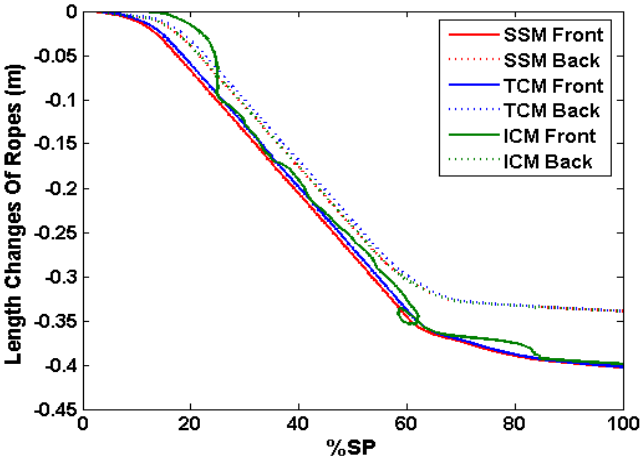


Fig. 2-19. Comparison results of rope movement trajectories among SSM, TCM and ICM.

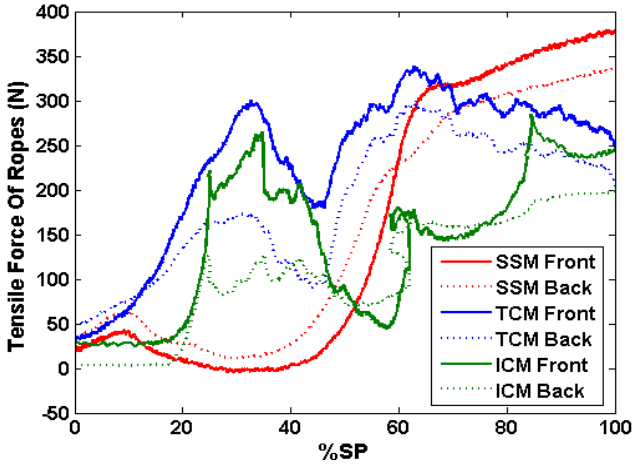


Fig. 2-20. Comparison results of rope tensile forces among SSM, TCM and ICM.

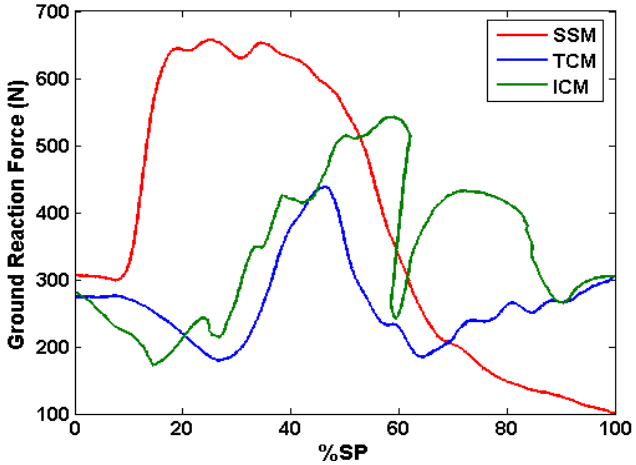


Fig. 2-21. Comparison results of GRF among SSM, TCM and ICM.

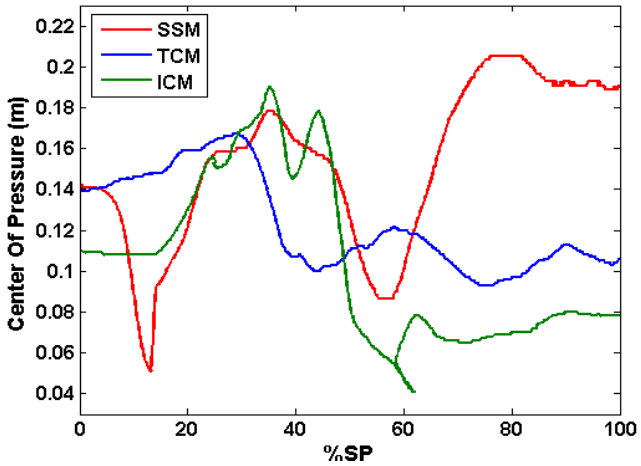


Fig. 2-22. Comparison results of COP among SSM, TCM and ICM.

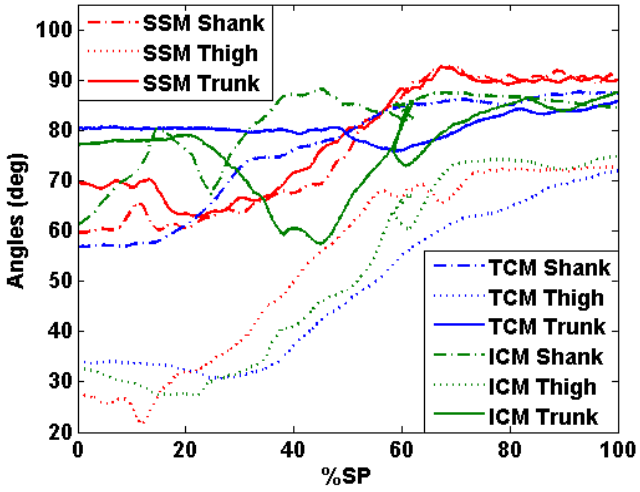


Fig. 2-23. Comparison results of motion angles of shank, thigh and trunk among SSM, TCM and ICM.

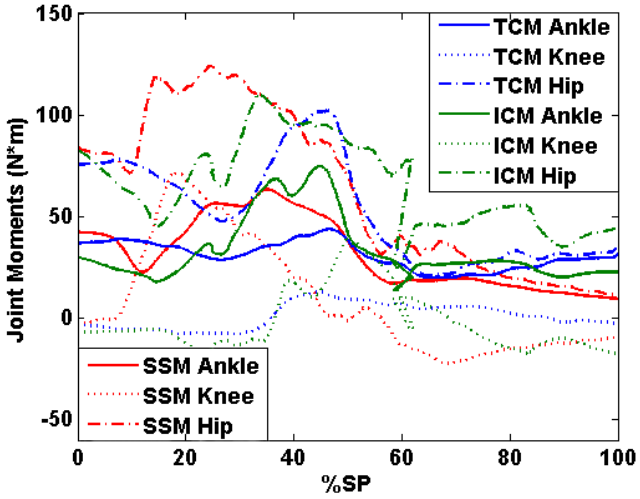


Fig. 2-24. Comparison results of joint moments of ankle, knee and Hip among SSM, TCM and ICM.

All the motion angle and joint moment parameters of lower limb were compared between TCM and ICM. As shown in Table Ⅲ and Table Ⅳ, RMS is the root of the mean of the square differences, R is the correlation coefficient, and $e_{max}$ is the maximum error. And at the right side of the table, the overall average of each parameter with six subjects was given.

TABLE Ⅲ ANALYSIS RESULTS OF LIMB MOTIONS

| Angles \ Subjects | | **1** | **2** | **3** | **4** | **5** | **6** | **Avg.** |
|---|---|---|---|---|---|---|---|---|
| | RMS | 7.88 | 6.37 | 7.69 | 7.32 | 8. 29 | 7.83 | 7.56 |
| $\theta$ | R | 0.92 | 0.91 | 0.78 | 0.87 | 0. 79 | 0.93 | 0.87 |
| Shank | $e_{max}$ | 18.82 | 17.61 | 22.46 | 18.08 | 21.53 | 15.46 | 18.99 |
| | RMS | 10.88 | 8.16 | 5.30 | 9.39 | 9.84 | 7.67 | 8.54 |
| $\theta$ | R | 0.98 | 0.95 | 0.98 | 0.89 | 0.96 | 0.93 | 0.95 |
| Thigh | $e_{max}$ | 17.11 | 13.47 | 10.14 | 16.24 | 13.03 | 11.79 | 13.63 |
| | RMS | 4.81 | 7.55 | 9.75 | 5.73 | 8.65 | 8.37 | 7.48 |
| $\theta$ | R | 0.88 | 0.89 | 0.58 | 0.92 | 0.79 | 0.84 | 0.82 |
| Trunk | $e_{max}$ | 14.14 | 16.85 | 22.66 | 9.94 | 17.89 | 20.48 | 16.99 |

Analysis results of the motion angles of shank, thigh, and trunk in the standing-up experiments on six subjects.

TABLE Ⅳ ANALYSIS RESULTS OF JOINT MOMENTS

| *M* \ Subjects | | **1** | **2** | **3** | **4** | **5** | **6** | **Avg.** |
|---|---|---|---|---|---|---|---|---|
| | RMS | 17.32 | 6.05 | 13.95 | 19.58 | 14.76 | 9.39 | 13.51 |
| *M* | R | 0.57 | 0.85 | 0.74 | 0.53 | 0.77 | 0.79 | 0.71 |
| Ankle | $e_{max}$ | 55.80 | 9.16 | 32.61 | 66.28 | 45.52 | 18.37 | 37.96 |
| | RMS | 41.81 | 13.56 | 11.22 | 38.50 | 27.09 | 21.43 | 25.60 |
| *M* | R | 0.71 | 0.77 | 0.80 | 0.73 | 0.78 | 0.81 | 0.77 |
| Knee | $e_{max}$ | 99.64 | 32.65 | 30.18 | 76.84 | 55.26 | 38.87 | 55.57 |
| | RMS | 47.67 | 15.01 | 24.08 | 39.65 | 30.42 | 29.43 | 31.04 |
| *M* | R | 0.55 | 0.79 | 0.74 | 0.61 | 0.72 | 0.78 | 0.70 |
| Hip | $e_{max}$ | 83.83 | 37.14 | 55.34 | 82.17 | 54.83 | 38.45 | 58.63 |

Analysis results of the joint moments of ankle, knee, and hip in the standing-up experiments on six subjects.

To analyze the dynamic parameters of human lower limbs in different control regimes, the contrastive experiment results of one subject using, respectively, the self-standing method, the impedance control method, and the game control method were shown from Fig. 2-25 to Fig. 2-30. To make the figures clear, data from different control methods were drawn with different colors.

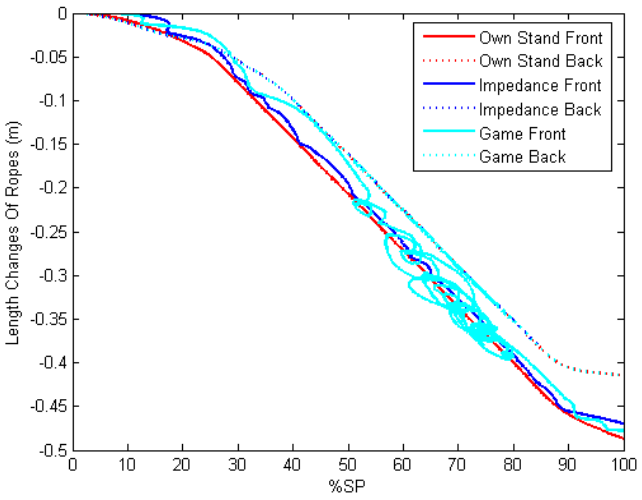


Fig. 2-25. Movement trajectories of one subject recorded during three control methods.

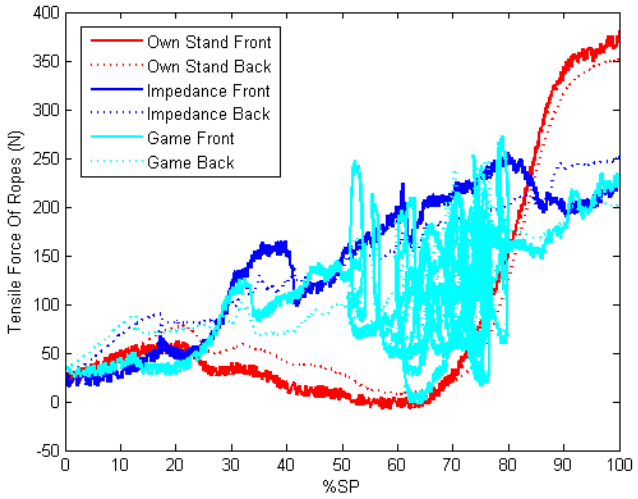


Fig. 2-26. Rope tensile forces of one subject recorded during three control methods.

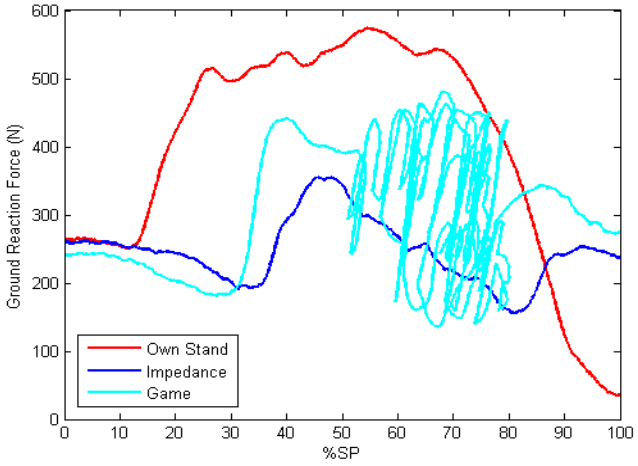


Fig. 2-27. GRF of one subject recorded during three control methods.

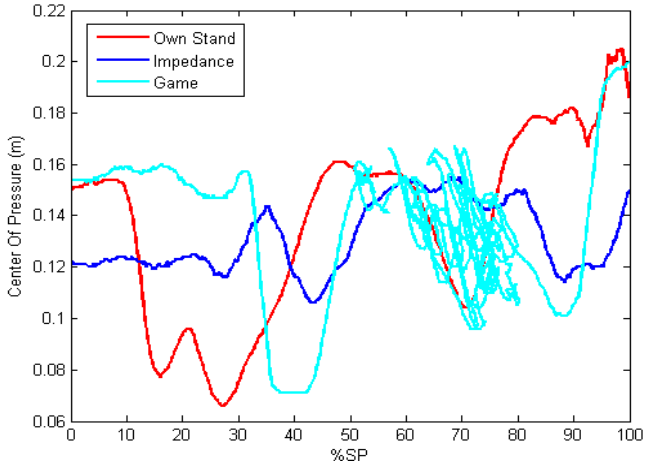


Fig. 2-28. COP of one subject recorded during three control methods.

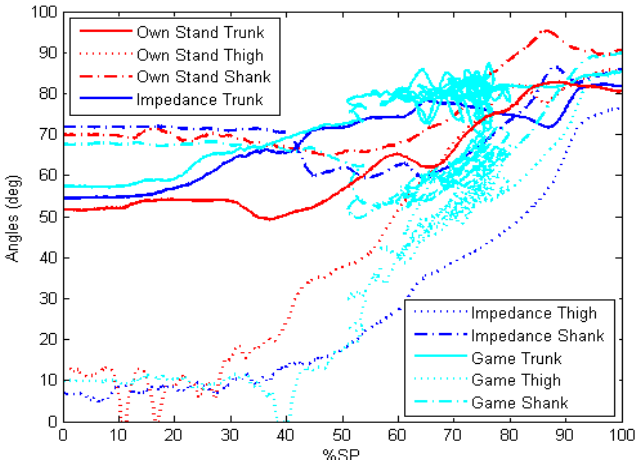


Fig. 2-29. Motion angles of shank, thigh, and trunk of one subject recorded during three control methods.

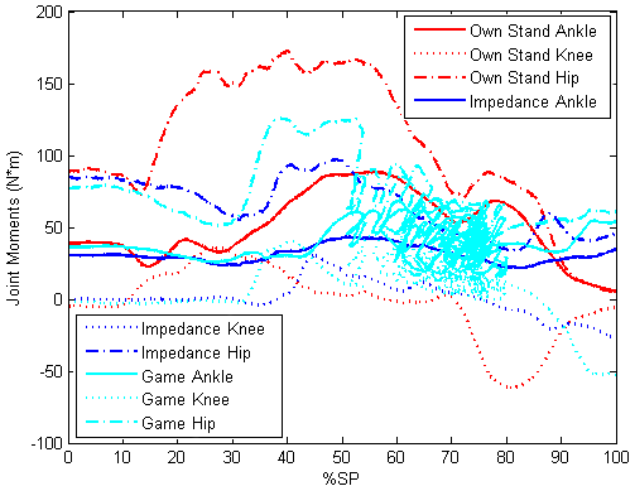


Fig. 2-30. Joint moments of ankle, knee, and hip of one subject recorded during three control methods.

## 2.4 Discussions

The experiment results of three subjects in impedance control method were shown from Figs. 2-8 to Fig. 2-13. As shown in Fig. 2-8, from 30% to 70% of SP, the tensile forces of front ropes were higher than the back ropes. As shown in Fig.2-9, the COP showed a similar tendency to the tensile forces of the front ropes. The reason is that in our experiment we found that when a healthy man stands up from a chair the center of gravity of the human body always firstly moves forward and then moves back. Therefore in our training process, the front rope worked to keep a natural standing-up trajectory, so it offered a higher tensile force than the back rope in order to assure the forward movement of the gravity center. Whereas, the tensile forces of back rope increased gradually, meaning that the subjects stood up naturally and gradually in the SP. As shown in Fig.2-10, from 0% to 30% of SP, the GRF showed higher values when the subjects intended to stand up by their own, and after 30% of SP, the GRF decreased when the subjects felt more difficulty in standing and got more help from the robot. This is because the control program was designed to move up more gradually or even move down when subjects have insufficient strength, but to move up at a faster rate to maintain

tension when subjects own sufficient strength to move up by their own. Therefore, vibratory values from 30% to 70% of SP indicate that the subjects were weak during this section and got more assistance from the robot. As shown in Fig.2-11, $\theta_1$, $\theta_2$, and $\theta_3$ grew continuously higher but only showed more vibrations in the weak posture section from 30% to 70% of SP. And in Fig. 2-12, the joint moments of hip, knee, and ankle vibrated in the weak posture section from 30% to 70% of SP, and showed higher values from 0% to 30% of SP when the subject intended to stand up on their own. In the experiment, the peak joint moment values of hip, knee, and ankle were, respectively; 132.1 (N·m) occurring in the 26.1% of SP of subject 1, 61.7 (N·m) occurring in the 21.0% of SP at subject 2, and 57.5 (N·m) occurring in the 41.9% of SP of subject 1. As shown in Fig. 2-13, the training time on weak posture section was longer than other posture sections. In the weak posture section from 31% to 70% of SP, the training times were 34.2 (s), 28.8 (s), and 26.6 (s) on subject 1, 2, and 3, so the training times could be calculated as 8.55 (s/10%), 7.20 (s/10%), and 6.65 (s/10%). From 1% to 30% of SP, the training times could be calculated as 3.55 (s/10%), 4.47 (s/10%), and 4.47 (s/10%). From 71% to 100% of SP, the training times could be calculated as 4.17 (s/10%), 4.35 (s/10%), and 4.17 (s/10%). Furthermore, all dynamic parameters vibrated up and down more often in the weak posture section than in other posture sections. Therefore, the robot system spent more time concentrating on training the weak posture section.

To make the analysis clear, from Fig. 2-14 to Fig. 2-18 the weak standing position period was defined approximately as the section from 30% to 70% of SP on the two subjects that because the subjects felt more difficulty and the peak joint moments appeared in this period. As shown in Fig. 2-14, the force values of front ropes were higher than the respective back ropes on each subject, and this difference was larger in TCM than in ICM. Furthermore as shown in Fig.2-16 the COP would move forward when force difference between the two ropes occurred. In our experiment we found that the gravity center of a human body always moves forward and then moves backward when a healthy person stands up from a chair. Therefore, in

our training process while the front rope was working on a normal standing-up trajectory, it would offer larger assistance force to assure the forward movement of the gravity center in the weak standing position period. Especially in TCM the movement of body was more passive, so larger force was applied to front rope to drive the forward movement of COP. As shown in Fig. 2-15, the GRF went up and dropped down sharply at the beginning and ending section of weak standing position period respectively, that because in weak standing position period the subject had to exert more force on the foot to stand up. As shown in Fig. 2-17, the movement tendencies were similar between the two subjects because that the training activity kept working on subjects' normal movement trajectories. Especially in TCM the $\theta 1$, $\theta 2$, and $\theta 3$ all grew progressively larger but only vibrated more in the weak standing position period because that the control program is designed to move up slower and keep more training time when subjects meet difficulties. Finally, as shown in Fig. 2-18, joint moments varied more intensely in the weak standing position period, and the peak joint moment values of hip, knee, and ankle were 203.2 (N·m), 106.8 (N·m), and 111.2 (N·m) respectively.

From Fig. 2-19 to Fig. 2-24, the weak standing position was defined approximately from 15% to 65% of SP on the 3rd subject. As shown in Fig. 2-19, in the three methods the movement trajectories of back ropes were generally in accordance that because the trajectory of the back rope is regarded as a standard movement in the SP. Whereas, the trajectory of front rope in ICM fluttered more than in SSM and TCM, that is because when the tensile forces were less than 50 (N), the back rope moved up faster than normal speed, and the front rope followed the corresponding saved desirable trajectory points and showed some hysteresis quality. For example, in the beginning period of SP, the tensile force on the ropes was less than 50 (N) when the subject started to stand up by himself. And at about 60% of SP, the subject dropped down and then moved up again, so when the front rope followed the saved trajectory points with hysteresis a trajectory cycle was drawn. In Fig. 2-20 rope tensile forces was the largest in TCM and the smallest in SSM, in Fig. 2-21 the GRF was the smallest in ICM and the

largest in SSM while varying more sharply in the weak standing position period, and in Fig. 2-22 the front rope forces were much larger than back rope forces while the COP was moving forward, therefore, it could be concluded that the greatest assistance effect had been provided by the front rope in TCM. As shown in Fig. 2-23 and Table Ⅲ, among the three methods the variations of $\theta 1$, $\theta 2$, and $\theta 3$ showed similarities with small RMS and large correlation coefficient, which matched the similarities of the human normal and comfortable standing-up trajectories. Furthermore the average correlation coefficient is higher than 0.82 between different SP. Finally, as shown in Fig. 2-24 and Table Ⅳ, the joint moments of hip, knee, and ankle all showed larger values in SSM than in the other two control methods, validating the theory that the TCM and ICM can improve the condition of joint moments of subjects effectively. Moreover the joint moments varied more frequently in ICM than in TCM, which make lower correlation coefficients and higher max errors, and the largest average RMS was 31.04 while the peak joint moment was similar. Therefore, the ICM can increase the frequency of the rehabilitation training that may be beneficial to the recovery effect.

Contrastive experiment results of one subject for the SSM, ICM and game control method (GCM) were shown from Fig. 2-25 to Fig. 2-30. As shown in Fig. 2-25, the movement trajectories were represented by the changes in rope length. In the three methods, the movement trajectories of back rope were in general accordance because the trajectory of back rope was regarded as a standard movement in the SP. The trajectory of front rope in the ICM showed an unobvious larger fluctuation than in the SSM. This is because while the subjects were standing up on their own in the ICM, the tensile forces were less than 50 (N), so the back rope moved up faster than normal speed, and the front rope followed the saved corresponding trajectory points and showed a hysteresis. Moreover, in the GCM, the front rope would make hysteresis when the subjects stood up by themselves; and the front rope would make a cycle when the subjects squatted down by themselves to play the training game. Nevertheless, the collective trajectories of front rope were still mainly in agreement, which means the human

body always moved through a comfortable trajectory in the rehabilitation activity. As shown in Fig. 2-26 both the tensile forces of back rope and front rope showed higher values in the ICM and in the GCM, and as shown in Fig. 2-27 and Fig. 2-28, the GRF and COP showed conspicuously higher values and higher range of variation in the SSM. This is because in the ICM an assist force was provided and it made the GRF and COP grew slowly and stably. In the GCM - although the values fluttered up and down while playing the training game - the values of GRF was still lower than in the SSM, meaning the assist forces in the ICM and the GCM could decrease the load on the human body. In Fig. 2-29, the variations of $\theta_1$, $\theta_2$, and $\theta_3$ showed similarities across the three experiment methods, and this was in accordance with the similarity in the variations of the movement trajectories. And as shown in Fig. 2-30, the three joint moments of hip, knee, and ankle were higher in the SSM than the other two methods, and the values vibrated up and down in the GCM, demonstrating that the ICM could decrease the joint moments effectively, and the GCM could stimulate both enthusiasm for training and frequency of training while the brain and body collaborate with each other. Furthermore, no matter how many times the human body moved up and down in the GCM, the peak values of the joint moments were still lower than the values in the SSM, showing that the GCM was effective in assuring that rehabilitation activities were performed safely.

## 2.5 Conclusions

A sit-to-stand rehabilitation robot was developed, and human lower limb dynamic parameters were analyzed for evaluating the performance of the robot. The trajectory control method and the impedance control methods could be applied to a self-supported home training program allowing subjects to control the training program safely and independently. The analysis results showed that the trajectory control method based on the standing-up rehabilitation robot could assure the safe accomplishment of sit-to-stand process, maintain a

comfortable training posture by working through natural movement trajectories, and decrease joint moments by providing assist forces on ropes. As a more effective control method, the impedance control method could also enhance training effectiveness by concentrating on training the weak posture section of users. Furthermore, the game control method, which is developed based on the impedance control method, could activate the collaboration of brain and limb and increase the frequency and intensity of rehabilitation activities. In short, the trajectory control method can be used effective for the patients who can not complete the movement from sitting position to standing position by themselves, and the impedance control method can be used effective for the patients who can complete the sit-to-stand movement by themselves but with less stabilization, furthermore the game control method can be used effective for the patients who need to increase the training frequency and intensity after finishing the impedance control method training.

Further study is needed to identify the type and effect of the rehabilitation activities, more studies are necessary to determine the reliability and validity of the control methods among more diverse groups, especially in clinical populations. And a more integrated 3D robot control method and muscle activation evaluation method can be developed for limb rehabilitation and medical diagnosis in the future.

# Chapter 3

## A Novel Approach for Muscle Force Analysis in Human Standing-up Process Based on a Rehabilitation Robot

## 3.1 Summary

A new quantitative method for performing dynamics analysis of human lower limb to estimate muscle forces was developed. A rehabilitation robot was developed for offering assistance and measuring dynamic parameters during the standing-up process. In the rehabilitation activities, rotational motions of trunk, thigh and shank were measure by three wearable motion sensors, and ground reaction force and center of pressure were measured by a miniature type force plate. In AnyBody Modeling System, a lower limb musculoskeletal model including thigh, shank, foot, four joints and fifteen muscles was developed, and the sensor-measured motion and force data of lower limb were imported into the musculoskeletal model. Quantitative muscle forces of lower limbs were calculated out using an inverse dynamics analysis method. Furthermore, for validating the muscle force results, the EMG method was adopted in the sit-to-stand experiment and the muscle activation levels were directly measured.

## 3.2 Materials and Methods

### 3.2.1 Sensor System in the Rehabilitation System

As shown in Fig.2-1 (a), a double rope rehabilitation system was developed for training human lower limb motor functions. The level of assisting force provided by the robot is adjusted according to users' intention while assuring the adequate movement trajectory of body

trunk. The assist force is real-time controlled by the back rope. The back rope can decide whether to offer assist forces or just follow the movement while maintaining the rope tension, as the sensor system and the algorithm controller can recognize the intended movement of the user. The back rope moves up faster when the user owns his/her own strength to stand up, moves up slower when the user needs help, or even moves down at a safe speed if the user intends to sit down. This ability ensures the rehabilitation system can spend more time training the weak position of the user, and increases the recovery effect of the system. Meanwhile, the movement trajectory is real-time controlled by the front rope. As shown in Fig. 2-1 (b), paired lengths of front rope and back rope decide the movement trajectory of point C, so while the length of back rope is being decided, the trajectory of point C can be controlled by adjusting the length of front rope. As a research result in our laboratory, the desirable movement trajectories to different height of users were saved in the control program. So while the length of back rope is being decided by the assist force and real-time measured by sensor, an adequate normal trajectory of user can be controlled by real-time adjusting the length of front rope in the control program. An impedance control method is developed to control two servo motors, and the motors are connected directly with the front and back ropes. The rope tensile forces are real-time measured by two high precision load cells fixed on the ropes, and the rope lengths are real-time measured by a photoelectric encoder in the motors. In rehabilitation training activities, the GRF and COP are real-time measured by a ground reaction force sensor, and angular motions of trunk, thigh, and shank are real-time measured by three wearable sensors constituted with accelerometers and gyroscopes. Additionally the whole hardware system is connected and controlled by a computer program system.

### 3.2.2 Musculoskeletal Model in AnyBody Modeling System

The AnyBody Modeling System is not only a professional musculoskeletal modeling

system, but also a kinematics and kinetics analysis system, and in the system the inverse dynamics method is adopted for estimating muscle forces. In the human body, muscles are activated by the central nervous system (CNS) based on a complicated electro-chemical process. Determining the activation that realizes a desired movement requires an extremely intricate control algorithm. AnyBody imitates the workings of the CNS by computing backwards from the movement and load specified to the necessary muscle forces in a process known as inverse dynamics. Maximum synergism would be the case where all muscles capable of a positive contribution to balancing the external load work together, in such a way that the maximum relative load on any muscle in the system is as small as possible. So in AnyBody a minimum fatigue criterion way is employed because fatigue is likely to occur first in the muscle working on the maximum relative load, it makes physiological sense that the body might work that way. It means that the body would maximize its endurance and precision, this criterion might decide survival of the fittest in an environment where organisms are competing with each other for limited resources.

To conduct dynamic analysis of human limbs, in AnyBody system environment a two-dimensional musculoskeletal model of human lower limb was created, and the geometric structure of the model was decided based on the human anatomy datum. As shown in Fig. 3-1, the coordinates of revolute joints of hip, knee, ankle, toe and muscle joint points are determined by measuring datum of the human lower limb (42). To make the model suit to different individuals, a size factor is indicated based on the height of users. Because the Vastus Medialis (VM), Vastus Lateralis (VM), and Vastus Intermedius (VI) own similar locations in the coordinate plane, in the model one resultant muscle is built in the front of thigh to simulate the muscles of VM&VL&FE. For the same reason, another two resultant muscles are built in the shank to simulate the muscles of Flexor Hallucis Longus & Flexor Digitorum Longus (FHL&FDL), and Extensor Hallucis Longus & Extensor Digitorum Longus (EHL&EDL). To sum up, thirteen muscles are involved in the model, they are Psoas Major (PM), Gluteus

Maximus (GM), Vastus Rectus (VR), VM&VL&VI, Biceps Femoris (BF), Anterior Tibialis (AT), Gastrocnemius (GAST), Soleus (SOL), Peroneus Longus (PL), Peroneus Brevis (PB), Posterior Tibialis (PT), FHL&FDL, and EHL&EDL. All muscles are built with the maximum strength of 5000 N. Furthermore, the setting of fixed hip joint avoids the dynamic affects produced by the training machine, and makes GRF the only external load on the model. The model worked as an integrated kinetics system after all the units were combined by joints and muscles.

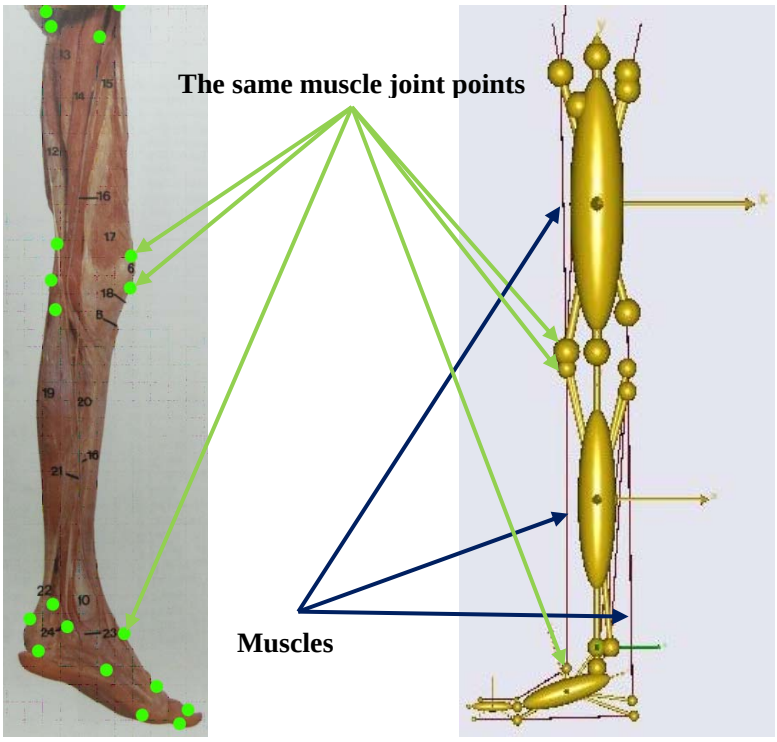


Fig. 3-1. Method for obtaining coordinates of elements on AnyBody model.

(a) Human anatomy model for obtaining geometric data of human lower limb.

(b) Musculoskeletal model in AnyBody Modeling System, whose coordinates were determined based on measuring geometric data of (a).

### 3.2.3 Inverse Dynamics Method for Calculating Muscle Forces

For calculating muscle forces of lower limb, the sensor measured motion and GRF data were imported into the AnyBody Modeling System. And the motion data driving the movement of the model are shown as follows:

$$\Delta\phi_{\text{thigh}} = \phi_{\text{thigh}} \tag{7}$$

$$\Delta\phi_{\text{shank}} = \phi_{\text{shank}} - \phi_{\text{thigh}} \tag{8}$$

$$\Delta\phi_{\text{foot}} = \phi_{\text{foot}} - \phi_{\text{shank}} \tag{9}$$

Thigh, shank, and foot in the model are driven by $\Delta\phi_{\text{thigh}}$, $\Delta\phi_{\text{shank}}$, $\Delta\phi_{\text{foot}}$ respectively. Because each angular motion data ($\phi_{\text{thigh}}$, $\phi_{\text{shank}}$, $\phi_{\text{foot}}$) are measured in general coordinate system and all the parts in the model are regarded as rigid bodies, the relative angular motion data ($\Delta\phi_{\text{thigh}}$, $\Delta\phi_{\text{shank}}$, $\Delta\phi_{\text{foot}}$) can be calculated by the quantitative subtraction. Furthermore, in the standing-up process we assume that no relative movement occurs on the toe joint and the value of $\Delta\phi_{\text{foot}}$ is regard as zero all the time.

The GRF, COP and angular motion data measured by the wearable sensor system were imported into the developed lower limb model of AnyBody Modeling System to calculate muscle forces through an inverse dynamic method. To simulate the true situation of standing-up process, one group of GRF and COP data is transferred into two groups of force data, and applies on two loading points located on the bottom plane of foot model. In single standing-up process, loads were transferred from posterior foot to the anterior foot then to posterior foot continuously and the whole force process was simulated. This transformation can perfectly imitate the GRF variation and COP shifting because the foot model is regarded as

a rigid body system; furthermore actually human foot receives GRF mainly on similar loading points too. The tangential loads applied on loading points were neglected because in the standing-up process the body trunk mainly moves on up and down directions. In this way the whole external force process is conducted. The model works as an integrated kinetics system after all bone units are combined by joints and muscles, and the quantitative muscle forces are calculated through the inverse dynamic analysis method.

### 3.2.4 Validation of Muscle Force Result by EMG Method

The motions of human lower limb are motivated by complex teamwork of muscles, but only several muscles were involved in the EMG experiment, that because only the muscles visible in skin surface and offering primary motive power in standing-up process are possible and worthy for directly analyzing. As shown in Fig. 3-2, the personal-EMG system (P-EMG-0403A01) includes dry type sensor system, filter box and data process system, and based on this system the EMG method was adopted to directly measure muscle activation level of VM&VL&VI, GAST and SOL. The dry type muscle sensors, which works on a myoelectricity difference principle, could sensing the muscle activation level while being pasted on the innervations zone of muscle surface. The raw EMG results were filtered and rectified by the filter box and the data process system into integral EMG results that could represent the muscle activation levels (43). Both the raw EMG and the integral EMG were real time recorded and displayed by the data process system, furthermore the integral EMG results were introduced in the validation with muscle force results calculated by AnyBody Modeling System. Furthermore, one hundred percent standard voluntary contractions (100%SVC) were defined as standard isolation of muscle activity in the respective muscle tests for the normalization of EMG signal

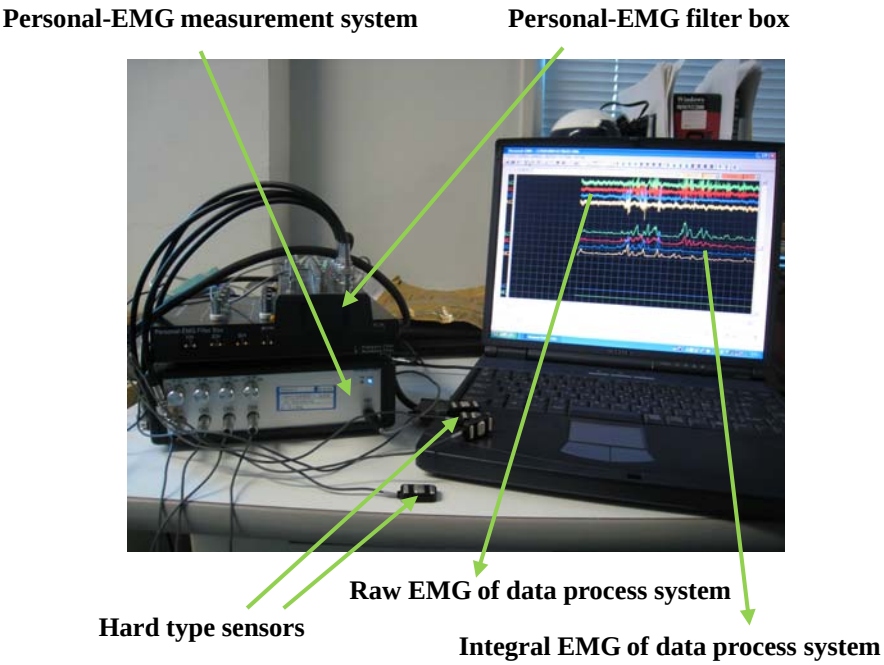


Fig. 3-2. Personal-EMG system for directly measuring the activation levels of lower limb muscles.

## 3.3 Experimental Study

### 3.3.1 Experiment Method

Test experiments were designed to validate the effectiveness of the muscle force analysis approach on four subjects (age: 25±3 years, height: 170±5 cm, mass: 61±12 kg) who have no history of musculoskeletal pathology or injury. As shown in Fig. 3-3, the subjects were requested to stand up from a chair at self-selected speed using, respectively, own-standing method without assistance and impedance control method with the assistance of the rehabilitation robot. In the start position, the subject's elbow joints were in contact with the homologous knee joints, while in the terminal position the subject's legs were straight. In the experiment the subjects were attached to the training robot by a conjunction jacket, and they

were requested to keep their feet on the force plate. The three wearable motion sensors were fixed by belts on the trunk, thigh, and shank respectively. Precision location of the motion sensors attached to limbs is unnecessary because all limb segments are regarded as rigid segments. While the subjects were standing up, the angular motions of trunk, thigh, and shank were real-time measured with the unit of degree ( ° ). And the GRF and COP were real-time measured with the unit of, respectively, Newton (N) and millimeter (mm). The EMG method was adopted to directly measure muscle activation levels of VM&VL&VI, AT, GAST and SOL, and the measured data were real time recorded by the personal-EMG application system.

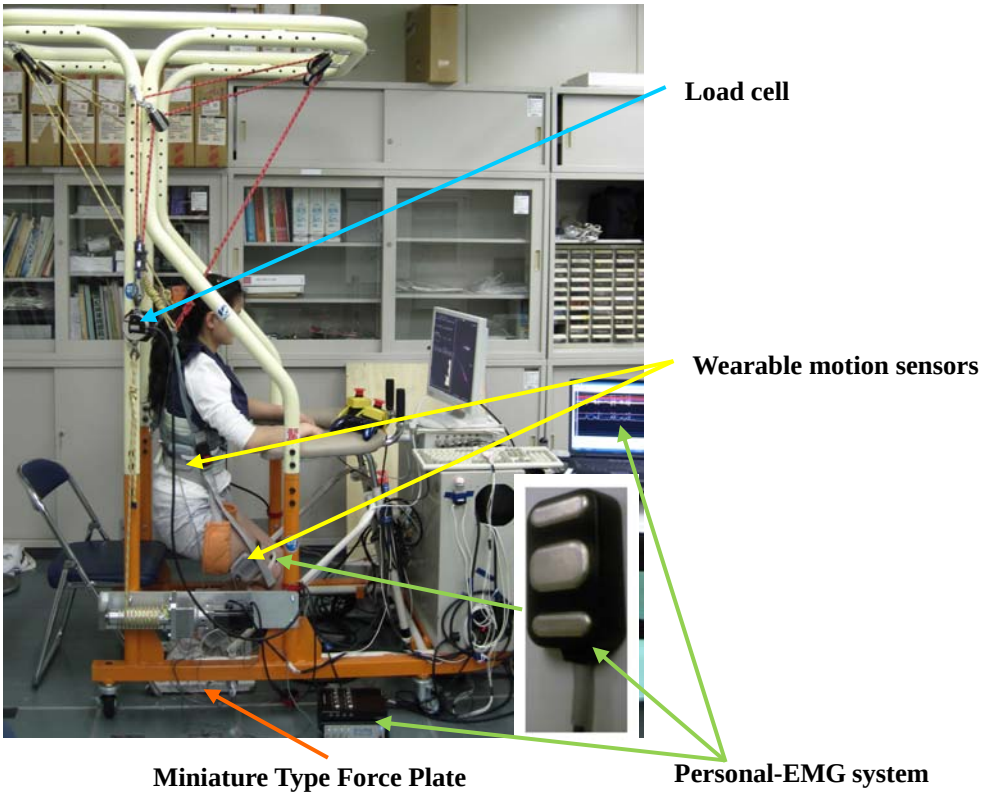


Fig. 3-3. Photograph of a subject in the standing-up experiment.

The next step was importing the motion and GRF data into AnyBody Modeling System for the calculation of muscle forces. In AnyBody system, the GRF and COP data were

transformed into two forces data on two locations, which imitated GRF variation and COP shifting perfectly. In addition, the motion data ($\Delta\phi_{\text{thigh}}$, $\Delta\phi_{\text{shank}}$, $\Delta\phi_{\text{foot}}$) were imported into the model to drive the movement of the body segments. As shown in Fig. 3-4, in AnyBody system environment the standing-up process and the muscle activation process were demonstrated visually in a easy-understood way, and the muscle forces and joint moments were calculated out through the inverse dynamics method while lower limb muscles collaborated with each other in the standing-up process. Before the experiment, the objective and method of the experiment were explained to the subjects, and their written and oral consent to the experiment was obtained. This experiment had been pre-approved by the ethics committee of the Department of Intelligent Mechanical System Engineering, Kochi University of Technology.

### 3.3.2 Experimental Results

As the complex kinetic system of standing-up process (SP) depends on a high degree of collaboration, in AnyBody Modeling System the muscle forces of lower limb were calculated based on a minimum fatigue criterion way. In the AnyBody process video of Fig. 3-4, the muscle activation level could be identified by the muscle bulge level, the value and direction of GRF could be discerned by the length and direction of the arrow.

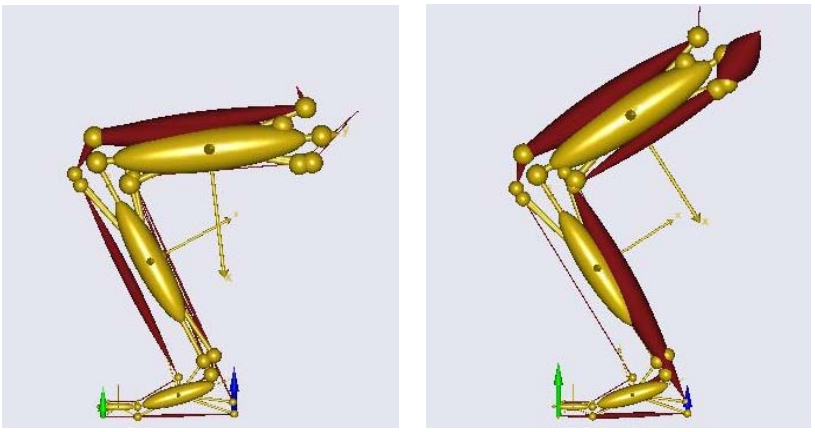

(a) 20% of standing-up process (b) 40% of standing-up process

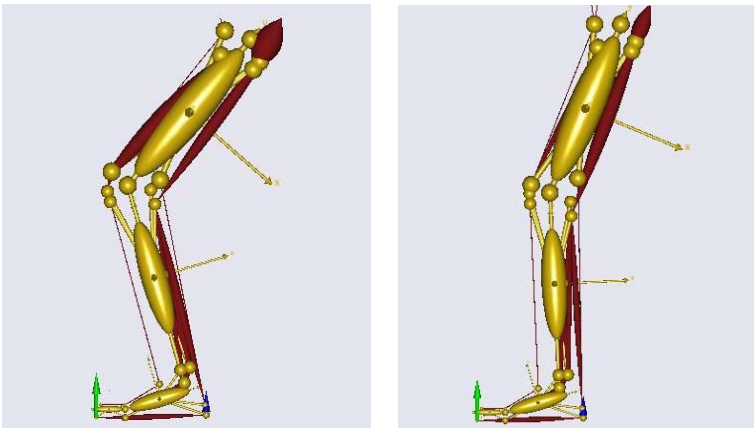

(c) 60% of standing-up process (d) 80% of standing-up process

Fig. 3-4. Screenshots of stand-up process video in AnyBody Modeling System, four postures in the process were shown.

The COP, GRF, and motion angles of body segments of four subjects are shown from Fig. 3-5 to Fig. 3-7, the quantitative muscle force results of VM&VL&VI, AT, GAST, PL and SOL of four subjects are shown in Fig. 3-8, and the size factors of subjects' height are summarized in Table Ⅴ. In Fig. 3-8, in order to represent the law of muscle force variations clearly, the *X*-axis is chosen to show the percentage of SP while the *Y*-axis indicates the muscle force in units of Newton.

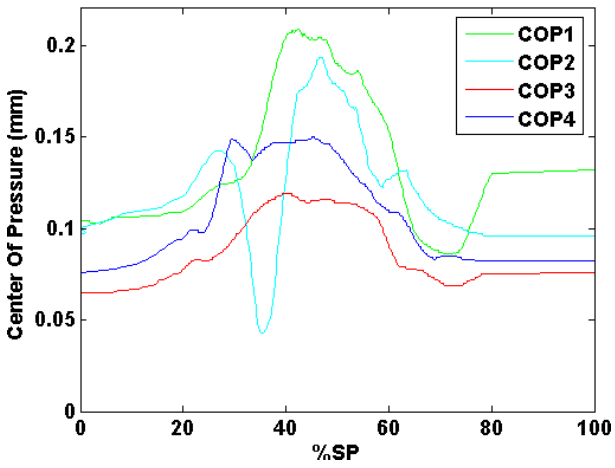


Fig. 3-5. COP of four subjects in impedance control method.

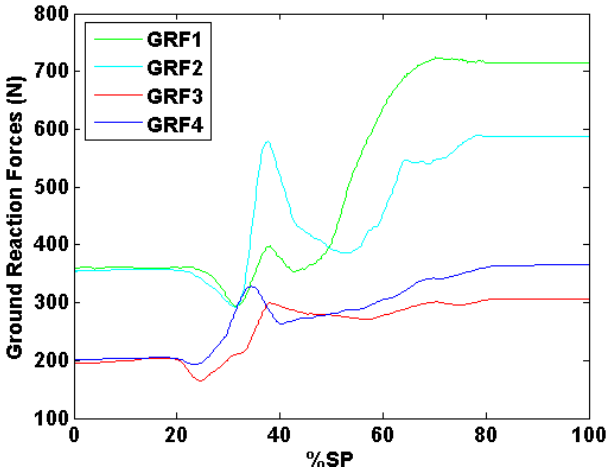


Fig. 3-6. GRF of four subjects in impedance control method.

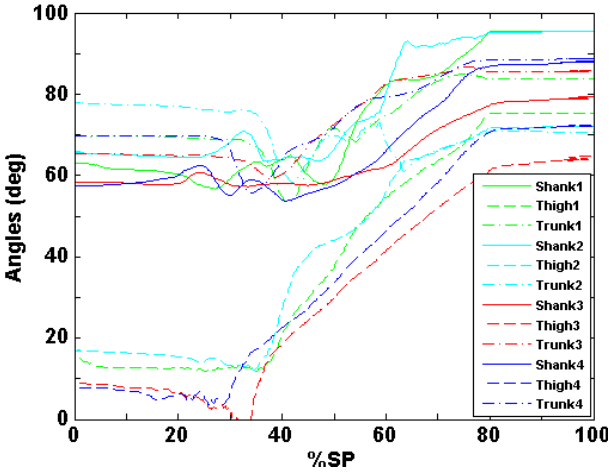


Fig. 3-7. Motion angle results of four subjects in impedance control method.

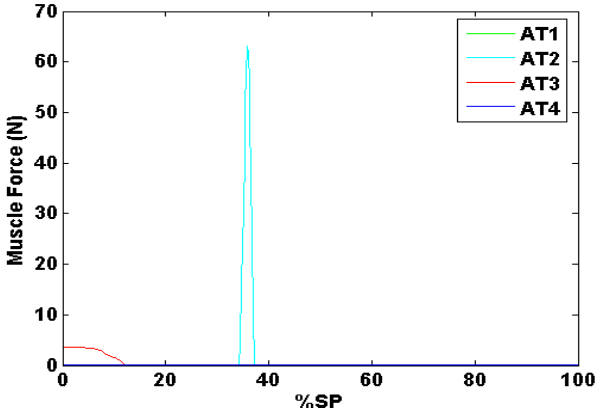


(a) Muscle forces diagrams of AT of four subjects

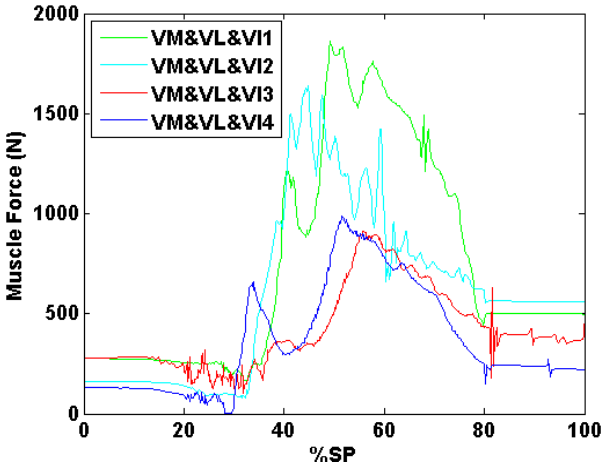


(b) Resultant muscle forces diagrams of VM&VL&VI of four subjects

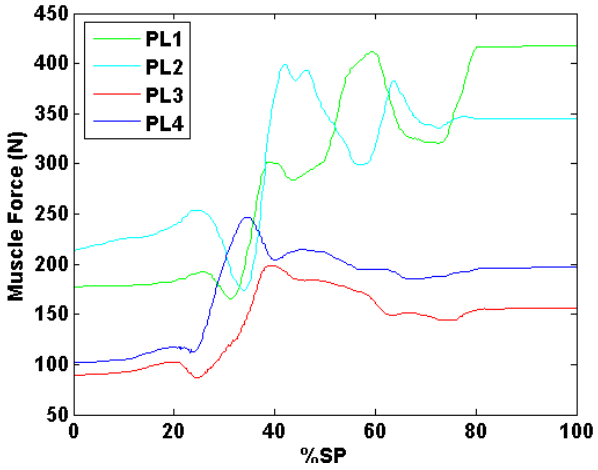


(c) Muscle forces diagrams of PL of four subjects

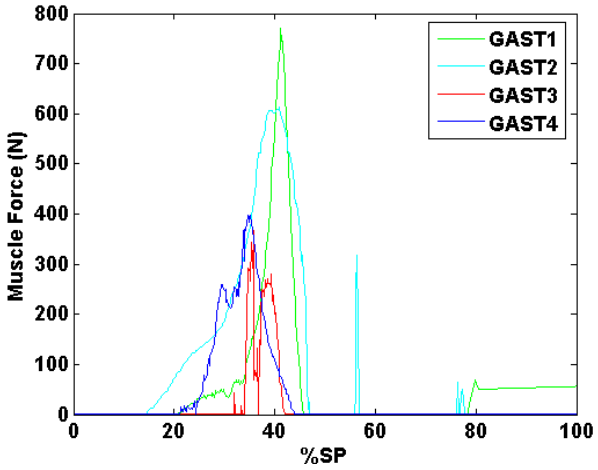


(d) Muscle forces diagrams of GAST of four subjects

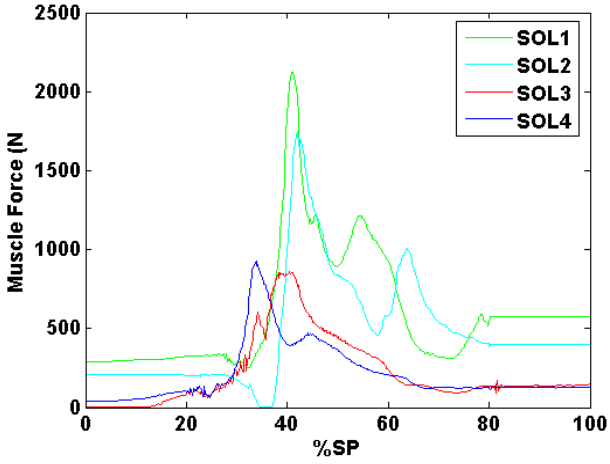


(a) Muscle forces diagrams of SOL of four subjects

Fig. 3-8. Muscle force results of four subjects in impedance control method.

Table Ⅴ List of heights of the four subjects adopted in Fig. 7.

| Subject | Size factor of AnyBody model (mm) |
|---|---|
| 1 | 1750 |
| 2 | 1740 |
| 3 | 1660 |
| 4 | 1650 |

The contrastive dynamic results of COP, GRF, motion angles of one subject using own-standing method and in impedance control method were shown from Fig. 3-9 to Fig. 3-11, and muscle force results of VM&VL&VI, AT, GAST and SOL were shown in Fig. 3-12. As quantitative muscle force results were estimated based on the rehabilitation robot and AnyBody Modeling System, EMG results were used to do the validation. As shown in Fig. 3-12 (a1), (a2), (b1), (b2), (c1), (c2), (d1) and (d2), contradistinctive analysis was conducted between calculated AnyBody results and measured EMG results; the results of AnyBody Modeling System are drawn in red while the results of EMG method are expressed in shadow. In comparison diagrams the *X*-axis represents percentage of SP, the left *Y*-axis indicates the

muscle force in units of Newton, and the right *Y*-axis indicates the percentage of standard voluntary contraction of muscles.

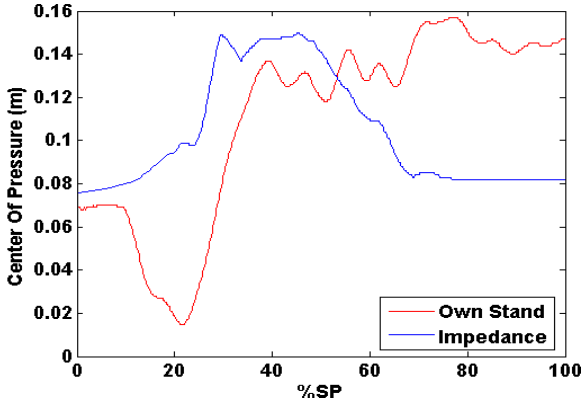


Fig. 3-9. Contradistinction COP between own-standing and impedance control method.

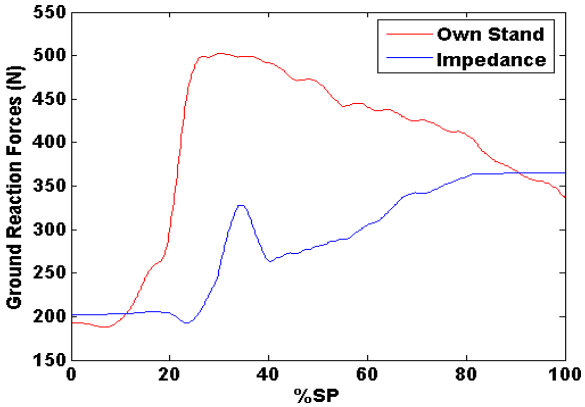


Fig. 3-10. Contradistinction COP between own-standing and impedance control method.

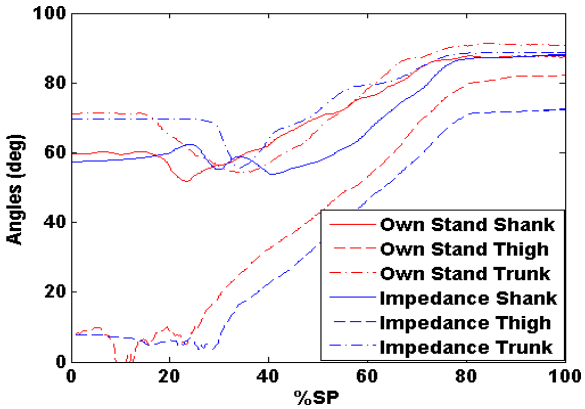


Fig. 3-11. Contradistinction motions between own-standing and impedance control method.

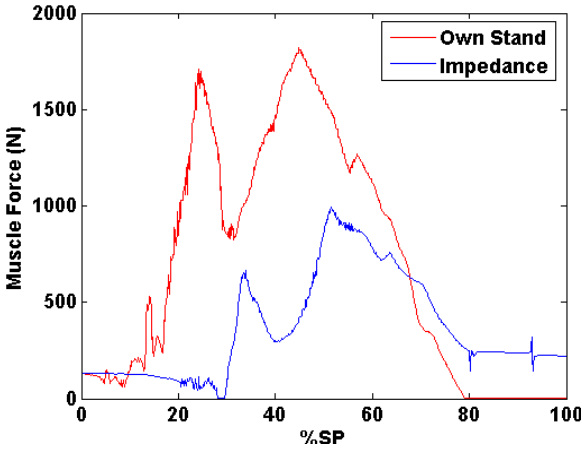


(a) Contradistinction of VM&VL&VI

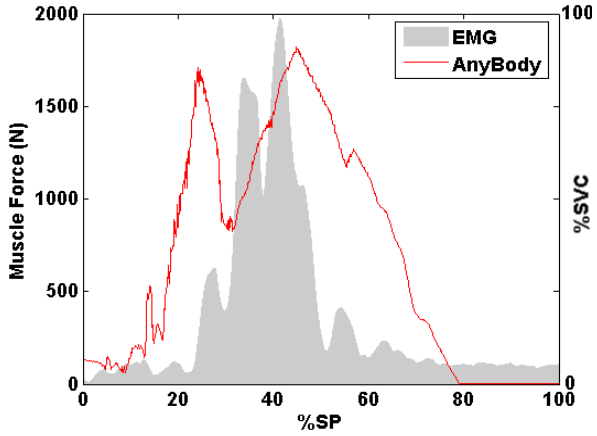


(a1) VM&VL&VI of own-standing

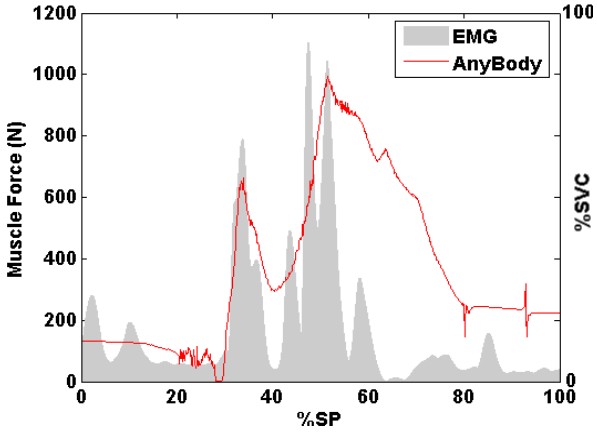


(a2) VM&VL&VI of impedance control

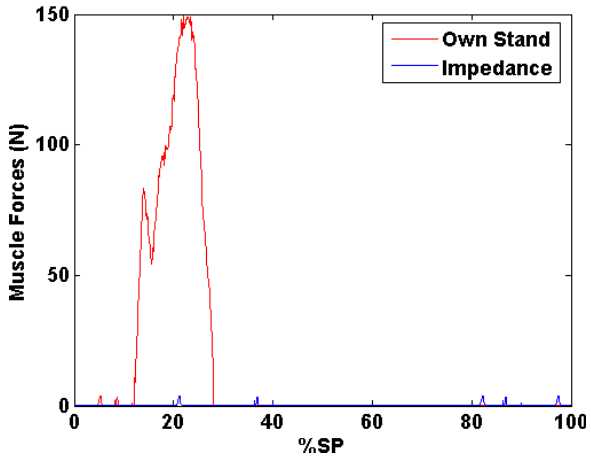


(b) Contradistinction of AT

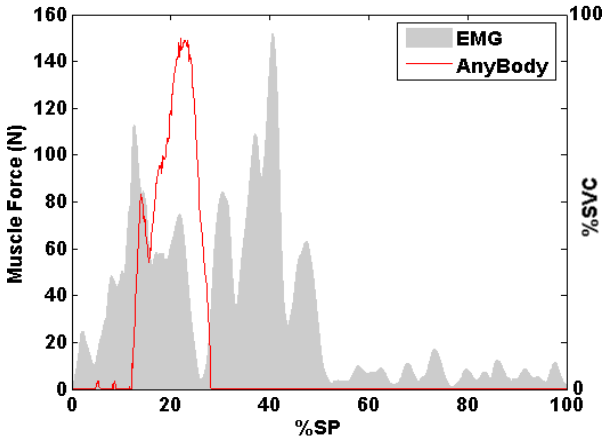


(b1) AT of own-standing

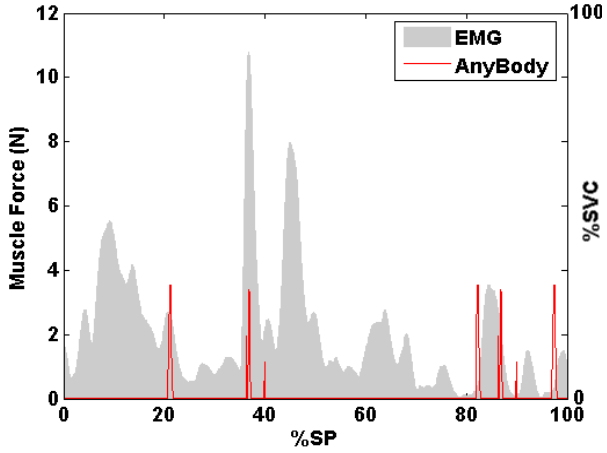


(b2) AT of impedance control

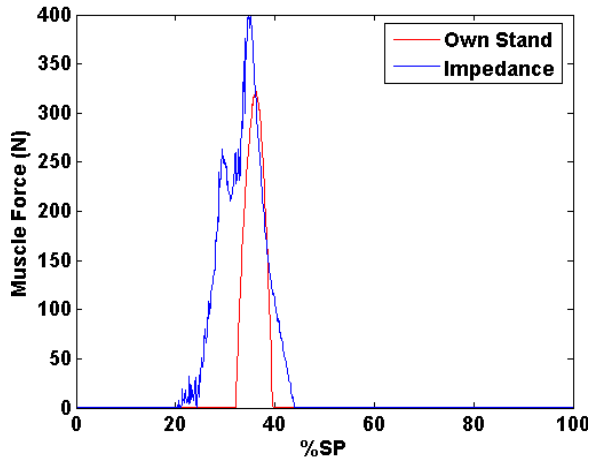


(c) Contradistinction of GAST

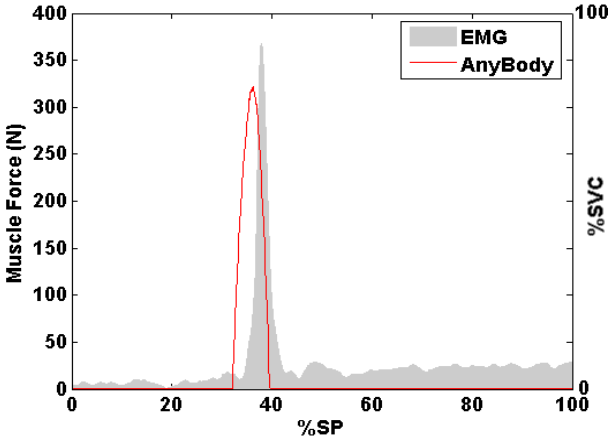


(c1) GAST of own-standing

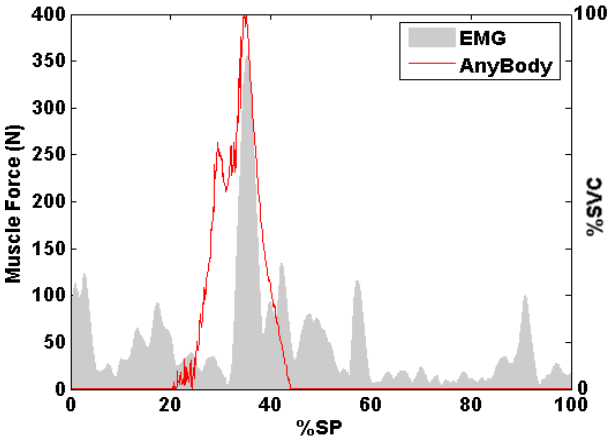


(c2) GAST of impedance control

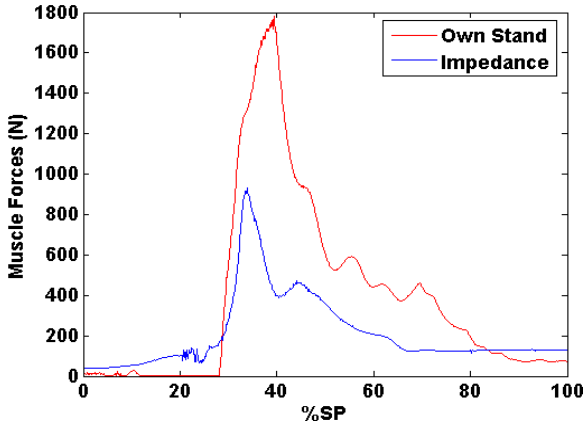


(d) Contradistinction of SOL

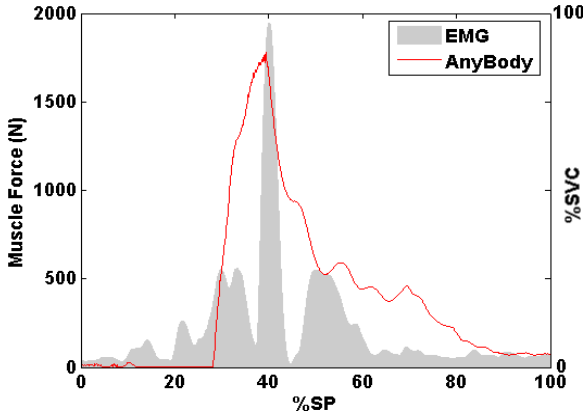


(d1) SOL of own-standing

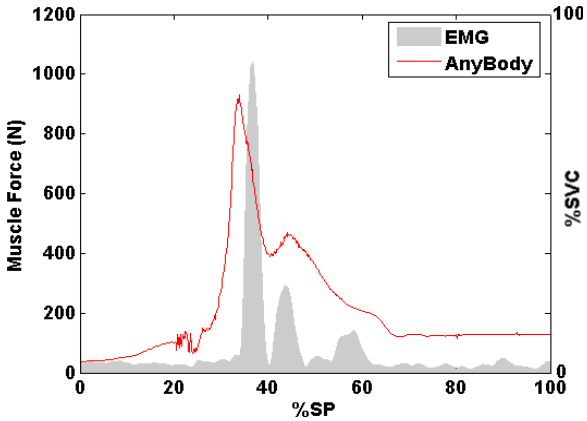


(d2) SOL of impedance control

Fig. 3-12. Contradistinction muscle force and EMG results between in own-standing method and in impedance control method.

## 3.4 Discussions

As shown from Fig. 3-5 to Fig. 3-8, experiment results of four subjects were shown in one SP cycle. As shown in Fig. 3-5, COP increased from 20% of SP and decreased from 60% of SP, because the gravity center of human body always moves forward and then backward when a healthy man stands up from a chair. As shown in Fig. 3-6 and Fig. 3-7, the GRF, $\theta_1$, $\theta_2$, and $\theta_3$ all grew continuously, but only vibrated from 20% to 60% of SP. This is because the subjects experienced more difficulty in this period and higher muscle forces were required. As shown in Fig. 3-8 (a), AT showed near-zero values but only a 60 (N) pulse at 38% of SP on subject 2, because the COP transformed to the posterior part of foot only in 38% of SP, and simultaneously, AT offered a force to balance the moment of the ankle joint simultaneously. As shown in Fig. 3-8 (b), (c), (d) and (e), at 0%-20% of SP, all muscles showed relatively low values only to maintain balance in the preparation posture. At 20%-40% of SP, VL&VM&VI started to increase in parallel with the increases in motion angles of body segments, PL started to increase in parallel with the increase of GRF, and GAST and SOL showed obvious increases in parallel with the COP transformation from the middle part of the foot to anterior part of the foot. At 40%-60% of SP, VL&VM&VI continued growing along with the increases of motion angles of body segments for pushing the human body moving upward, but GAST and SOL showed decrescendo values in parallel with the backward transformation of COP, moreover PL varied in parallel with the effect of GRF. At 60%-80% of SP, VL&VM&VI showed decrescendo values to complete the standing process, and GAST and SOL showed vibrated and lower values because the COP vibrated in a relatively small range in this period. However, PL increased by the effect of increasing GRF and vibrated by the effect of vibrating COP. At 80%-100% of SP, the human body reached a stable standing posture and all muscle forces showed stable and lower values just to maintain the balance of the body. Therefore, it seems AT, GAST and SOL were mainly responsible for the movement balance of ankle joint,

VL&VM&VI was mainly responsible for the upward movement of body trunk, PL was mainly responsible for the balance of human body. Together, they composed a cooperative muscle dynamic system in the SP.

As shown from Fig. 3-9 to Fig. 3-12, contrastive experiment results of one subject were shown between in own-standing method and in impedance control method. As shown in Fig. 3-9 and Fig. 3-10, by the assist effects of the rehabilitation robot, the COP were more stable, and the GRF showed conspicuously lower and gradually increasing values in impedance control method compared with own-standing method. And as shown in Fig. 3-11, the variations in $\theta_{1,}$ $\theta_{2,}$ and $\theta_{3}$ showed similarities in the two experiment methods because the subject moved along similar normal trajectories. As shown in Fig. 3-12 (a), (a1) and (a2), in the own-standing method, GRF appeared on the posterior part of foot at the beginning of SP. To balance the moment of ankle joint the force of AT increased and showed higher value in the 10%-30% of SP. However, in the impedance control method, AT was not activated because the GRF first appeared in the middle of the foot due to the effects of the rehabilitation robot. As shown in Fig. 3-12 (b), (b1) and (b2), VL&VM&VI showed lower and hysteretic values in impedance control method than in own-standing method, because a previous upward movement of the body trunk was provided by the robot. As shown from Fig. 3-12 (c) to (d), GAST showed similar variation in the two control method. SOL, on the other hand, showed lower values in the impedance control method than in the own-standing method, because the COP transformation had smaller ranges in the impedance control method. Therefore, the rehabilitation robot could improve the dynamic conditions and decrease the muscle forces of lower limb effectively. Furthermore as shown in Fig. 3-12 (a1), (a2), (b1), (b2), (c1), (c2), (d1) and (d2), validation analysis was performed between AnyBody method and EMG method. Although the EMG muscle activation results were relative values in units of %SVC while the AnyBody muscle force results were quantitative values in units of Newton, prominent similarity could be found in the contradistinction.

## 3.5 Conclusions

A new quantitative approach for estimating muscle forces of lower limb based on inverse dynamics technology was presented. The rehabilitation robot provided effective assistance in the standing-up process, and the sensors performed effectively in measuring dynamic parameters of lower limbs. The measured data can be imported into the musculoskeletal model in AnyBody Modeling System. In the model the quantitative muscle forces were calculated through an inverse dynamics method, and the variation in the muscle force results showed practical sense for the SP. Furthermore, the EMG method was used to directly measure muscle activation level for validation, and the muscle activation results of EMG method matched the muscle force results of AnyBody model. This approach appears to be a practical means of determining muscle force in musculoskeletal analysis of human limb rehabilitation.

# Chapter 4

## Estimate Muscle Forces of Ankle Joint with Wearable Sensors

## 4.1 Summary

A new quantitative method for performing multiple-units foot dynamics analysis to estimate muscle forces of ankle joint was developed. A pair of instrument shoes was developed to measure rotational movements of multiple parts of foot, tri-axial GRF and coordinates of the center of pressure; additionally, a wearable motion sensor (3DM-GX1) was used to measure orientations of shank and thigh. In AnyBody Modeling System a model of multiple-units foot and shank with three joints and ten muscles was developed and the quantitative muscle forces were calculated by musculoskeletal inverse dynamics analysis. To validate our estimation results of muscle forces, EMG method was adopted in the experiment and the muscle activation level was directly measured.

## 4.2 Materials and Methods

### 4.2.1 Measurement of Motion and GRF of Limbs by Wearable Sensor System

Angular motions of shank and thigh were measured by two wearable sensors with acceleration sensitive units and gyroscopes. And angular motions, GRF and COP of multiple-units foot were measured by a pair of developed instrument shoes with both force sensors and motion sensors. The measured data were expressed in a general coordinate system which was aligned with the orientation of the shoe, and located on the contacting plane between the shoe and the floor. As shown in Fig. 4-1, the Z-axis was made vertical, and the

Y-axis was chosen to represent the anterior-posterior direction of the shoe on the interface plane contacting with the ground, while the X-axis was chosen such that the global coordinate system would be right-handed (44). Accurate location of the sensors is not necessary because the limb segments are regarded as rigid bodies in the study.

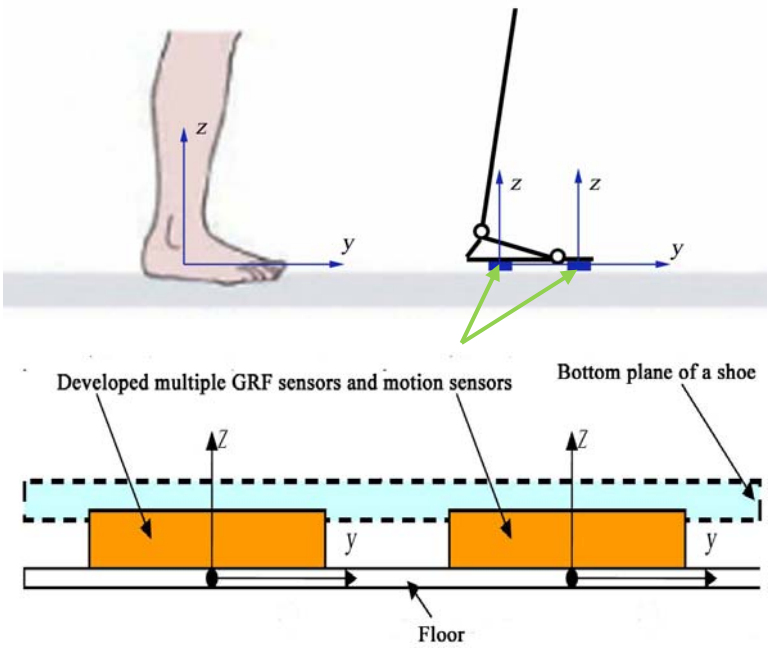


Fig. 4-1. Ordinate system of an instrument shoe with multiple sensors to obtain GRF, COP and angular motion of multiple-units foot.

In this way the dispersion force on the bottom of shoe was expressed by concentrated GRF and COP, and the measured electrical data of angular motion, GRF and COP of multiple-units foot were transmit into a signal process box, which took the responsibility for wave filtering, data consolidation and transmission, as shown in Fig. 4-2. The signal process box also played a role of signal synchronization by sending a start pulse to the wearable sensor system combined on the leg, as all the sensors have the same sampling frequency. The motion

of shank was measured because muscles joint points in shank have non-separable relationship with the muscles driving the foot, and the process of gait is relied on the co-operation of these muscles. The angular motion of thigh was not involved in the calculation of muscle forces of the foot because there are no muscles connect from thigh to the foot directly, although the motion of thigh was measured in this experiment for the future research. In the wearable motion and GRF sensor system, all the sensors had the sampling frequency of 100 Hz, and the GRF, COP, multiple-units foot and shank rotations had the units of Newton (N), millimetre (mm) and degree (°) respectively. Totally four groups of GRF, two group of COP and four groups of angular of multiple-units foot was measured by the instrument shoes, moreover one groups of angular of shank and one groups of angular of thigh were measured by the wearable sensors.

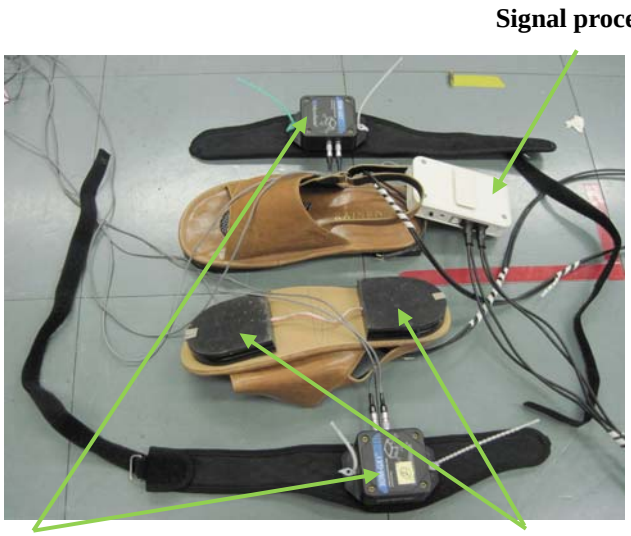


Fig. 4-2. The instrument shoes and two wearable sensors designed to obtain GRF, COP and angular motions of lower limbs during successive walking trial.

### 4.2.2 Establishment of Dynamic Model in AnyBody Modeling System

In human body muscles are activated by the central nervous system base on a complicated electro-chemical process. Determining the activation that realizes a desired movement requires an extremely intricate control algorithm. The AnyBody Modelling System is not only a professional musculoskeletal modelling system, but also a kinematics and kinetics analysis system, in which inverse dynamics method is adapted to quantitatively estimate muscle forces. AnyBody imitates the workings of the central nervous system by computing backwards from the movement and load specified by the user to the necessary muscle forces in a process known as inverse dynamics. Maximum synergism would be the case where all muscles capable of a positive contribution to balancing the external load work together, in such a way that the maximum relative load of any muscle in the system is as small as possible. It means that the body would maximize its endurance and precisely, this criterion might decide survival of the fittest in an environment where organisms are competing with each other for limited resources. So in AnyBody a minimum fatigue criterion way is employed because fatigue is likely to happen first in the muscle working on the maximum relative load, and it makes physiological sense that the body might work that way.

To implement dynamic analysis of human foot, a multiple-units foot and shank model was created in AnyBody Modelling System. As shown in Fig. 4-3, the coordinates of knee, ankle, and toe joints and muscle joint points were determined by measuring datum of the human lower limb. The shank was also built in the model for attaching muscles between foot and shank; furthermore the angular acceleration of the shank has influences on tensile forces of these muscles in the inverse dynamics method. To simulate the true situation of human walking, the GRF were implemented on three loading points locating on the bottom of foot model, and the loads applied on loading points contain both pressure and tangential forces as shown in Fig. 3 (c).

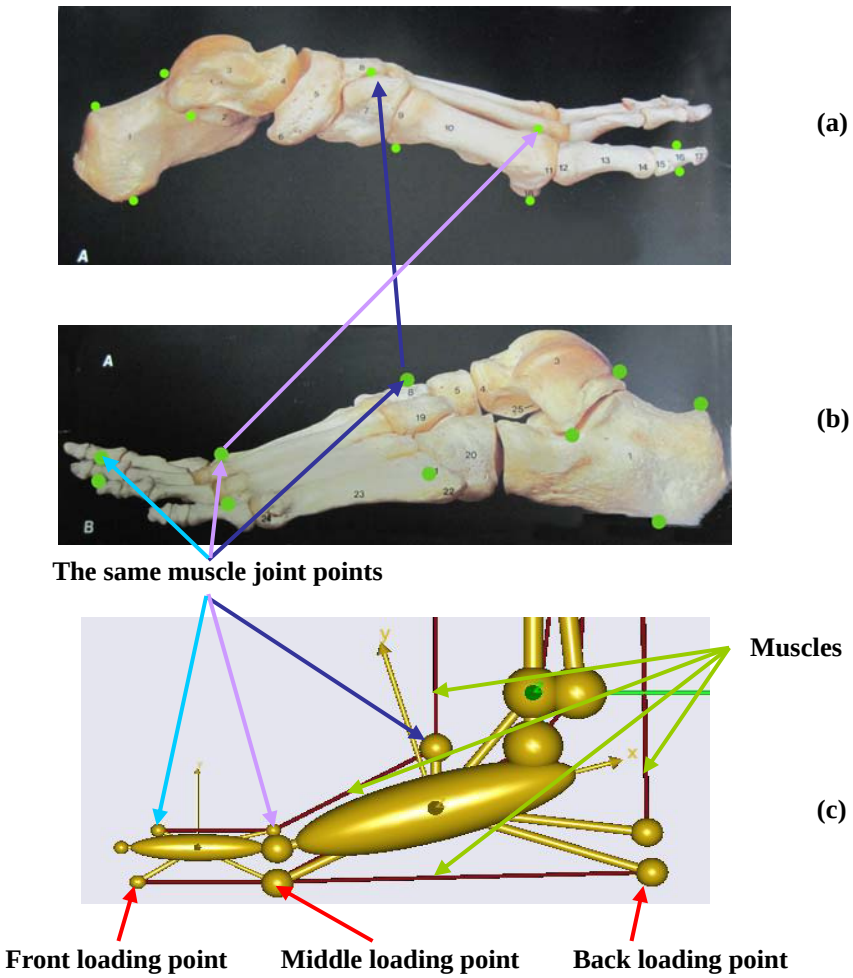


Fig. 4-3. Method for obtaining coordinates of multiple-units foot model in AnyBody System.

(a) (b) Human anatomy scan graph for obtaining geometric data of human foot.

(c) Musculoskeletal multiple-units foot model in AnyBody Modeling System.

The main working muscles involved in the model were Anterior Tibialis (ANT TIB), Gastrocnemius (GAST), Soleus (SOL), Peroneus Longus (PL), Peroneus Brevis (PB), and Posterior Tibialis (POST TIB). Because the locations of Flexor Hallucis Longus (FHL) and Extensor Hallucis Longus (EHL) are similar with Flexor Digitorum Longus (FDL) and Extensor Digitorum Longus (EDL) respectively in the coordinate plane, one resultant muscle

was built in the anterior parts of the model to simulate the muscles of FHL&FDL, and another resultant muscle was built in the posterior parts of the model to simulate the muscles of EHL&EDL. All muscles were built with the maximum strength of 5000 N. Totally seventeen muscle points were created to join muscles, four joints of hip, knee, ankle and toe were created to restrict the activity freedom degree, and three loading points were created to load the GRF and COP. The model worked as an integrated kinetics system after all the units were combined by joints and muscles. The foot model was established based on a rigid barefoot as the instrument shoes nearly have no elasticity, and to make the model suit for different individuals, the size factor was indicated based on the length of human foot.

### 4.2.3 Calculation of Muscle Force by Importing the Sensor Measured Data

The GRF, COP and angular motion data measured by the wearable sensor system were imported into the developed multiple-units foot and shank model of AnyBody Modelling System to calculate muscle forces of human foot through an inverse dynamic method. To simulate the true situation of human walking, one group of GRF and COP was transferred into two forces on different location based on Eq. (10) and Eq. (11), in this way the measured two groups of GRF and COP data were transferred into three forces data applied on three loading points on the bottom plane of foot model. In single gait cycle, loads were transferred from posterior foot to the anterior foot continuously and the whole force process was simulated. This transformation can perfectly imitate the GRF variation and COP shifting because the multiple-units foot is regarded as a rigid body system, furthermore real human foot receives GRF mainly on similar points too. The loads applied on loading points contain both pressure and tangential forces. The pressure force of GRF was expressed on the *Z*-direction, and the $COP_z$ ($x_0$, $y_0$, $z_0$) on this direction is defined by Eq. (10), and the tangential force of GRF was expressed on the *Y*-direction, and the $COP_y$ ($x_0$, $y_0$, $z_0$) on this direction is defined by Eq. (11).

$$x_0 = 0, \qquad y_0 = \frac{\sum F_z \bullet y}{\sum F_z}, \qquad z_0 = 0 \tag{10}$$

$$x_0 = 0, \qquad y_0 = \frac{\sum F_y \bullet y}{\sum F_y}, \qquad z_0 = 0 \tag{11}$$

$F_z$ — A force on *Z*-direction.
$F_y$ — A force on *Z*-direction.
$x$ — *X*-axis coordinate values of the force.
$y$ — *Y*-axis coordinate values of the force.

As shown in Fig. 4-4, the angular motion data of shank, the posterior foot and the anterior foot were measured in general coordinate system as $\phi_{\text{shank}}$, $\phi_{\text{heel}}$, $\phi_{\text{toe}}$. Because all the parts in the model were regarded as rigid bodies, the relative angular motion ($\Delta\phi_{\text{shank}}$, $\Delta\phi_{heel}$, $\Delta\phi_{\text{toe}}$) could be calculated by quantitative subtraction. Furthermore in AnyBody Modelling System, the shank, the posterior foot and the anterior foot were driven by $\Delta\phi_{\text{shank}}$, $\Delta\phi_{heel}$, $\Delta\phi_{\text{toe}}$ respectively as shown in Eq. (12), (13), (14). After all the model units were combined by joints and driven by imported motion data, the AnyBody musculoskeletal model worked as an integrated kinetics system and quantitative muscle forces were calculated out through inverse dynamic process.

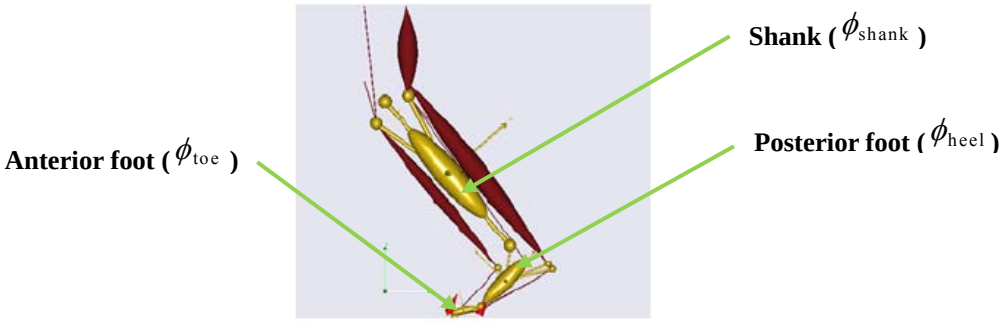


Fig.4-4. Angular motion data of shank, the posterior foot and the anterior foot were measured in general coordinate system as $\phi_{\text{shank}}$, $\phi_{\text{heel}}$, $\phi_{\text{toe}}$.

$$\Delta\phi_{\text{shank}} = \phi_{\text{shank}} \tag{12}$$

$$\Delta\phi_{\text{heel}} = \phi_{\text{heel}} - \phi_{\text{shank}} \tag{13}$$

$$\Delta\phi_{\text{toe}} = \phi_{\text{toe}} - \phi_{\text{heel}} \tag{14}$$

### 4.2.4 Validation of Muscle Force Results by EMG Method

The main muscles of human shank and foot were illustrated in Fig. 4-5, the motions of human limb are motivated by complex teamwork of these muscles, but only several of these muscles were involved in the EMG experiment, that because only the muscles visible in skin surface and offering primary motive power in walking process are possible and worthy for directly analysing. As shown in Fig. 4-6, personal-EMG system (P-EMG-0403A01) includes hard type sensor system, filter box and data process system. The EMG method was adopted to directly measure muscle activation level of ANT TIB, PL, GAST and SOL.

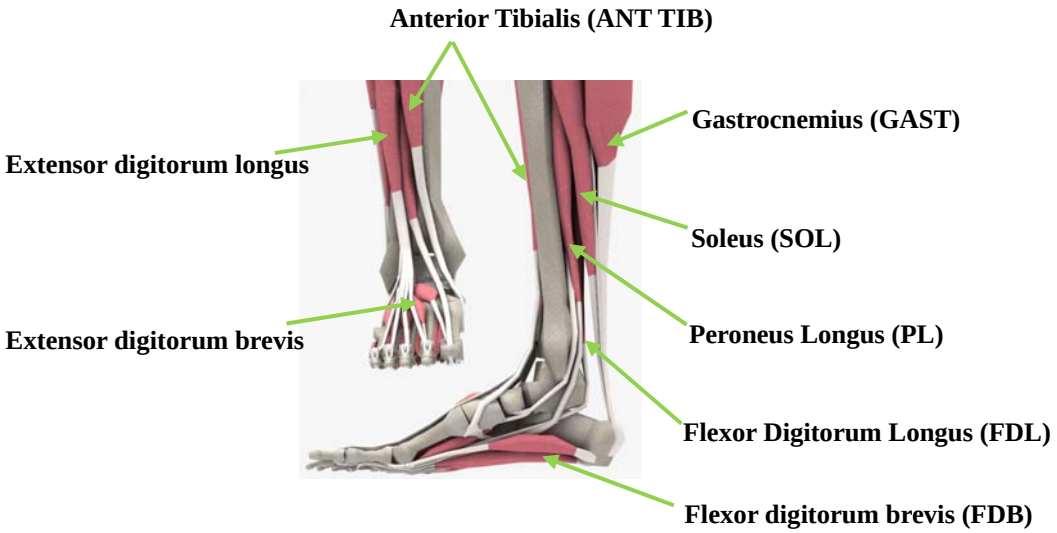


Fig.4-5. Illustration of main muscles of human shank and foot.

The raw EMG results were filtered and rectified by the filter box and the data process system into integral EMG results that could represent the muscle activation levels. Both the raw EMG and the integral EMG were real time recorded and displayed by the data process system, furthermore the integral EMG results were introduced in the validation with muscle force results calculated by AnyBody Modelling System. Furthermore, one hundred percent maximum voluntary contractions (100%MVC) were defined as maximum isolation of muscle activity in the respective muscle tests for the normalization of EMG signal.

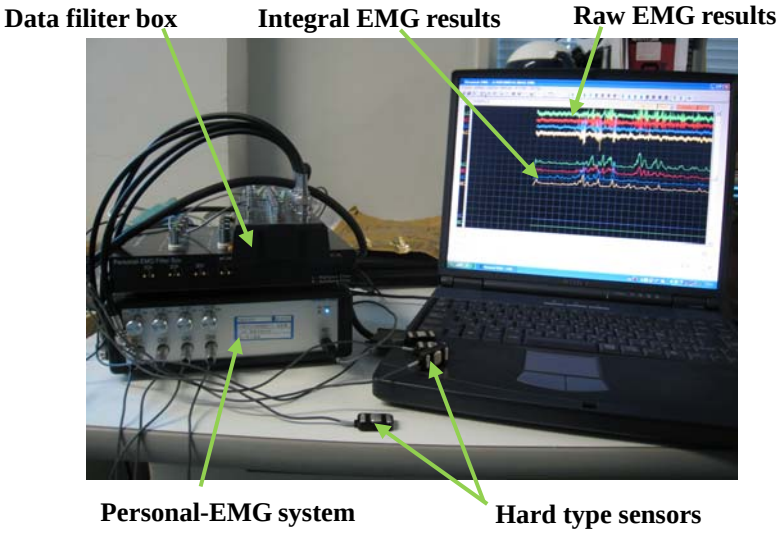


Fig.4-6. Personal-EMG system adopted to directly measure muscle activation levels in human lower limb.

## 4.3 Experimental Study

### 4.3.1 Experiment Method

The first experiment step is acquisition motion and GRF information of human lower limbs in gait cycle, six adult volunteers (age: 29.5±4 years, weight: 74±8.5 kg.) who had no

musculoskeletal disease history were required to performed their normal speed gait in the experiment. The distance of the performance was four meters, duration time was ten seconds. As shown in Fig. 4-7, three-dimensional angular motion of thigh, shank, posterior part and anterior part of the multiple-units foot were measured with the unit of degree (°), and three-dimensional GRF and two-dimensional COP were measured by the instrument shoes with the unit of Newton (N) and millimetre (mm) respectively. Because all the limb parts were regarded as rigid segments, precise location of wearable sensors which attached on human limbs was unnecessary, so was the size adjustable of the instrumented shoes for the same reason. The sampling frequency of all sensors were regulated as 100 Hz, signal synchronization was realized by the signal process box which would send a pulse to wearable sensors attached on shank and thigh. To remove noise, low-pass filtering was performed on obtained signals with the cut-off frequency of 10 Hz.

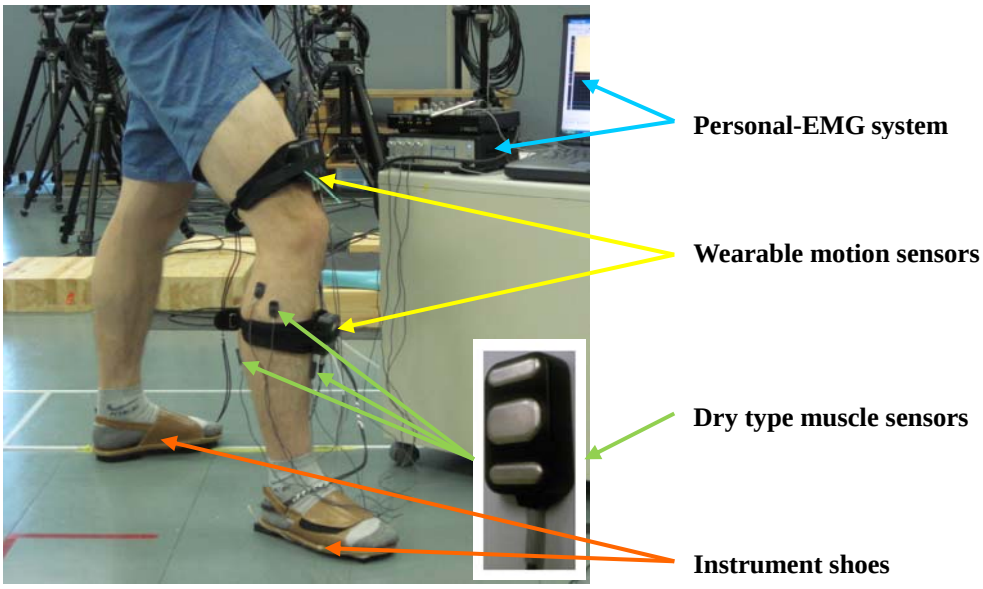


Fig. 4-7. Prototype of a volunteer wearing instrument shoes, wearable motion sensors and muscle sensors of personal-EMG in the experiment.

To directly measure muscle activation levels of ANT TIB, PL, GAST and SOL, the personal-EMG system and dry type muscle sensors were adopted in the experiment. The dry type muscle sensors, which works on a myoelectricity difference principle, could sensing the muscle activation level while being pasted on the neurosis zone of muscle surface. Furthermore the measured raw EMG results were real time filtered and rectified into integral EMG results by the personal-EMG application system, and both raw EMG results and integral EMG results were real time displayed for easy checking and adjusting. As shown in Fig. 4-8, we divided one gait cycle into four steps: contacting step, supporting step, leaving step and swing step. The contacting step starts from the heel contacting the ground and ends in the whole foot bottom plane stamping on the ground, the supporting step represents the process of gravity movement from posterior to anterior while one foot supporting the whole weight, the leaving step stands for the action from the heel leaving the ground to the whole foot leaving the ground, and the swing step means the foot swing forward process without contacting the floor.

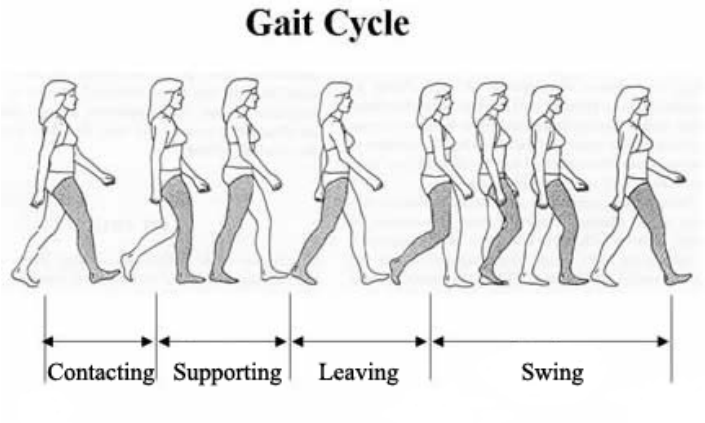


Fig. 4-8. One gait cycle was divided into contacting step, supporting step, leaving step and swing step.

The second experiment step was calculating the muscle forces in AnyBody Modelling System. For preparation, the measured motion and GRF data of lower limb were transferred

into the form that is adequate to the AnyBody system. As a rigid body system, the relative angular motion data ($\Delta\phi_{shank}$, $\Delta\phi_{heel}$, $\Delta\phi_{toe}$) were imported into the model to drive the movement of the shank and the multiple-units foot. The measured GRF data were transformed into three forces on three loading points to imitate GRF variation and COP shifting. As shown in Fig. 4-9, in *Z*-axis the entire pressure GRF data got by sensors was drawn as $F_z$, and GRF transformation data applied on three loading points were drawn as $F_z$-Front, $F_z$-Middle and $F_z$-Back. Furthermore in *Y*-axis, the entire tangential GRF data were transformed into $F_y$-Front, $F_y$-Middle and $F_y$-Back with the same algorithm. In order to make the foot model suitable for different individual, the size factors of foot length were adopted. As shown in Table Ⅵ, the size factors of five volunteers were summarized. Finally, the muscle forces and joint moment, while ankle joint muscles collaborating with each other in normal walking, were calculated through the inverse dynamics method in AnyBody Modelling System. This experiment has been approved by the ethics committee of the Department of Intelligent Mechanical System Engineering, Kochi University of Technology.

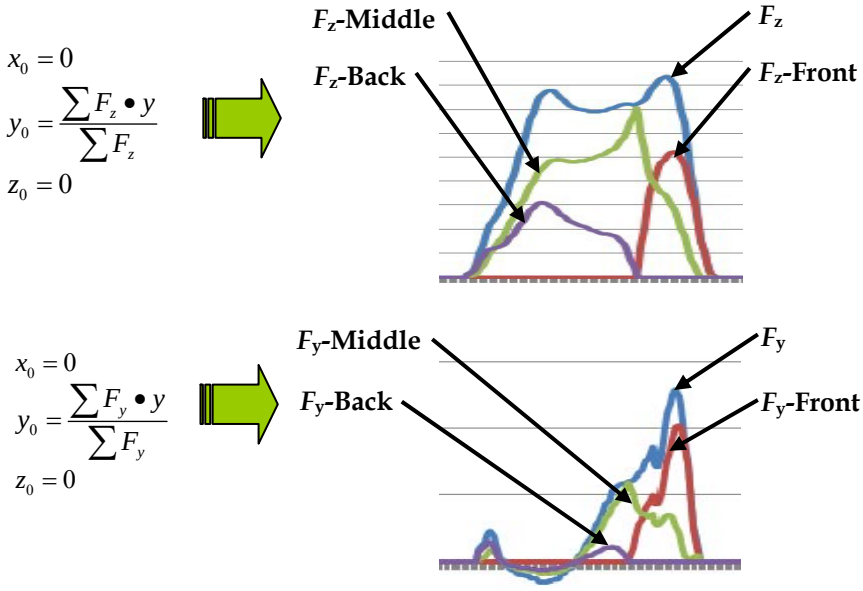


Fig. 4-9. The GRF were transferred into three forces on three loading points to imitate GRF variation and COP shifting in gait cycle.

Table Ⅵ. List of size factors of the six subjects adopted in Fig. 4-7.

| Subject | Size factor of AnyBody foot model (mm) |
|---|---|
| 1 | 235 |
| 2 | 240 |
| 3 | 240 |
| 4 | 260 |
| 5 | 265 |
| 6 | 260 |

### 4.3.2 Experimental Results

As the complex kinematic walking system requires a high collaboration, in AnyBody Modeling System the muscle forces of ankle joint were calculated based on a minimum fatigue criterion way. In the AnyBody gait process video of Fig. 4-10, the muscle activation level could be identified by the muscle bulge level, the value and direction of GRF could be discerned by the length and direction of the arrow. The quantitative force results of ANT TIB, POST TIB, GAST, SOL, resultant EHL&EDL and resultant FHL&FDL of six subjects in their normal gait were shown in Fig. 4-11. To represent the law of muscle force changes clearly, the *X*-axis was chosen as the percentage of gait cycle while the *Y*-axis indicated the muscle force with the unit of Newton. The muscles connecting from thigh to shank were excluded because those muscles provide no contribution in the ankle joint rotation.

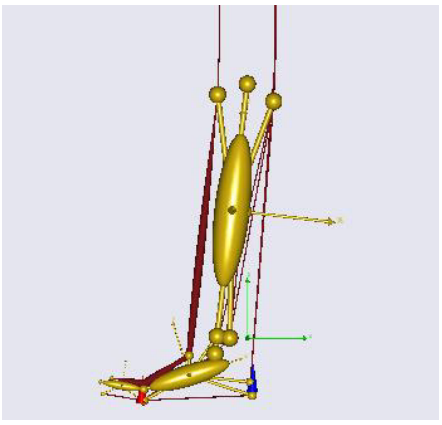

(a) Screenshot in contacting step

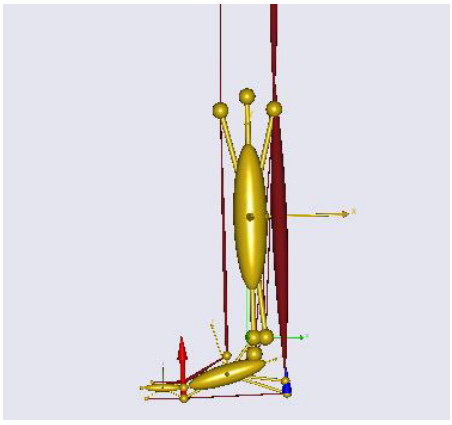

(b) Screenshot in supporting step

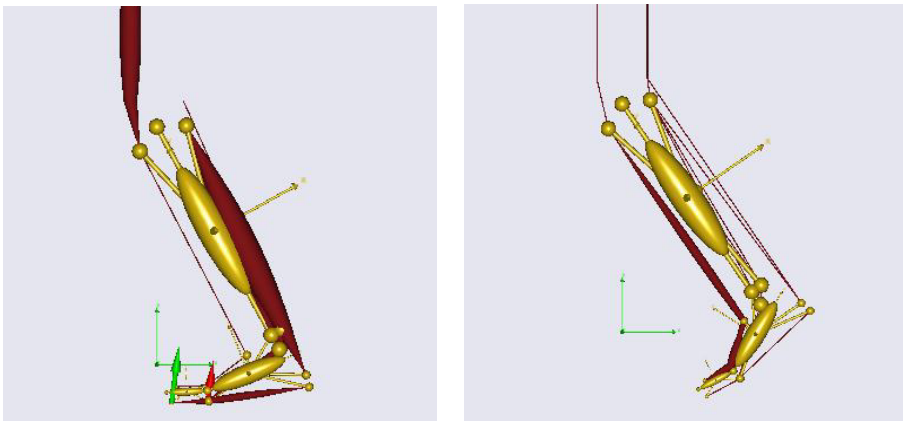

(c) Screenshot in leaving step (d) Screenshots in swing step

Fig. 4-10. Screenshots of gait video in AnyBody Modelling System, four postures in one gait cycle were shown.

As quantitative muscle force results were estimated base on wearable sensor system and AnyBody Modeling System, EMG results had been used to do the comparison, but in EMG method the muscle activation result was relatively large or small with the unit of %MVC. As shown in Fig. 4-12, contradistinctive analysis was implemented between calculated AnyBody results and measured EMG results, the muscle forces of subject 2, 3 and 4 obtained from the AnyBody Modeling System were drawn in red while the results from EMG method were expressed in shadow. In comparison diagrams the *X*-axis represented percentage of gait cycle while the *Y*-axis indicated the percentage of maximum voluntary contraction of muscles. All models were based on rigid barefoot as the instrument shoes nearly have no elasticity. Furthermore for making the discussion clearly, the step division figure of gait cycle was expressed on the top of each diagram.

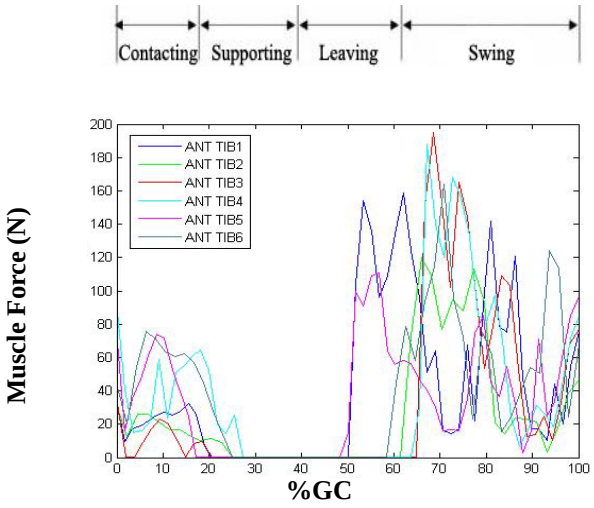


(a) Muscle forces diagrams of ANT TIB of six subjects

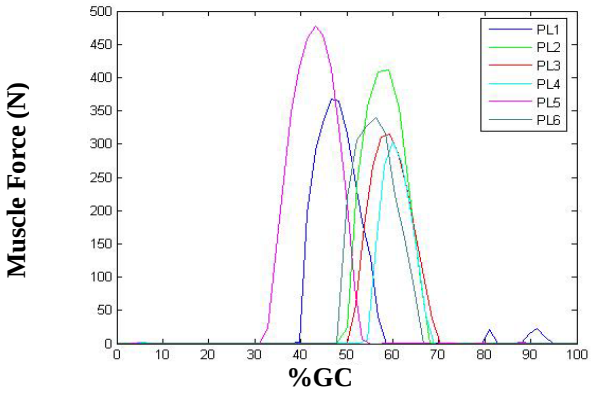


(b) Muscle forces diagrams of PL of six subjects

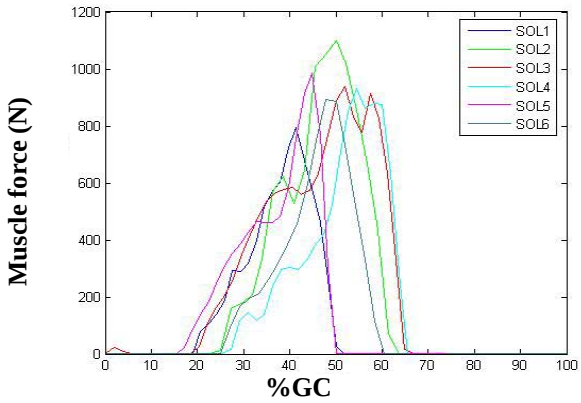


(c) Muscle forces diagrams of SOL of six subjects

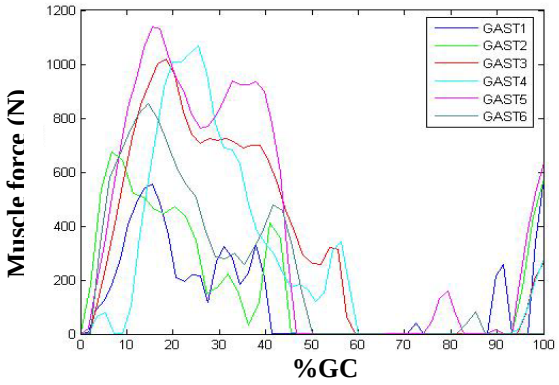


(d) Muscle forces diagrams of GAST of six subjects

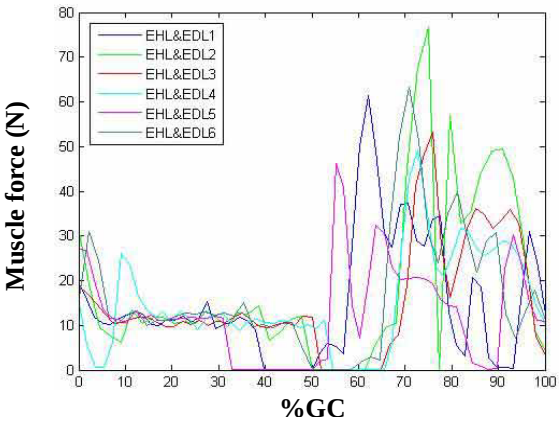


(e) Resultant muscle forces diagrams of EHL&EDL of six subjects

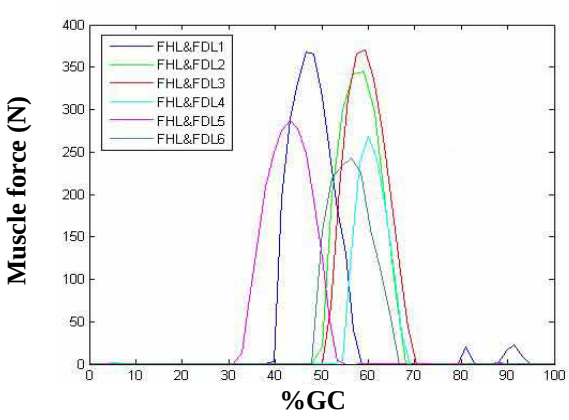


(f) Resultant Muscle forces diagrams of FHL&FDL of six subjects

Fig. 4-11. Muscle forces results of ANT TIB, PL, SOL, GAST, resultant FHL&FDL, and resultant EHL&EDL of six subjects of AnyBody Modeling System.

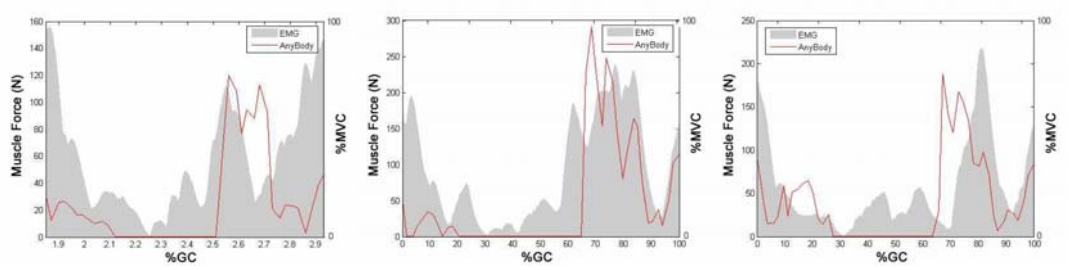


(a) ANT TIB 2 (b) ANT TIB 3 (c) ANT TIB 4

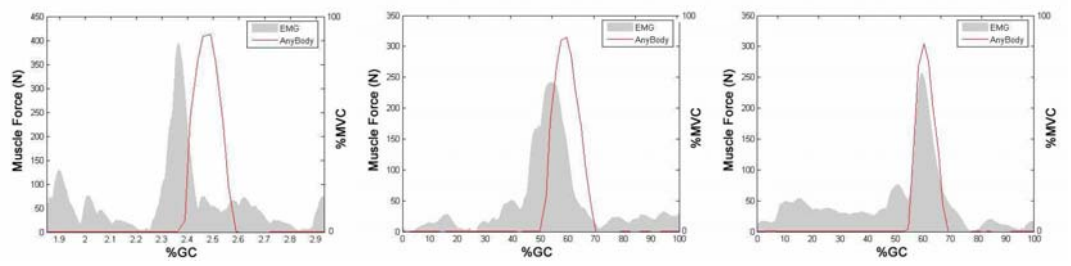


(d) PL 2 (e) PL 3 (f) PL 4

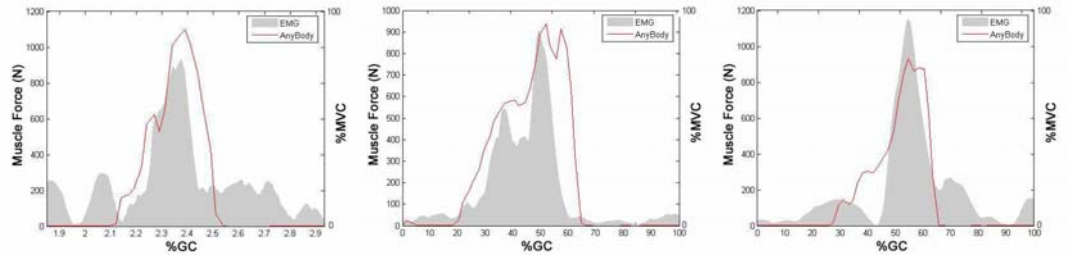


(g) SOL 2 (h) SOL 3 (i) SOL 4

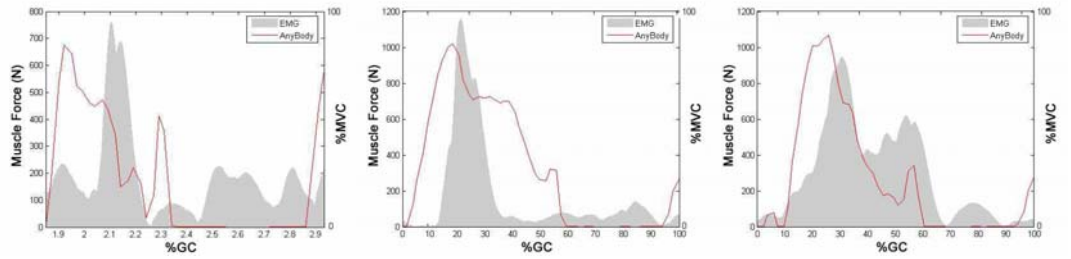


(j) GAST 2 (k) GAST 3 (l) GAST 4

Fig. 4-12. Comparison diagrams of muscle activation results of ANT TIB, PL, SOL and GAST in one gait cycle. The quantitative muscle forces (N) obtained by the AnyBody Modeling System were drawn in red while the maximum voluntary contractions results (%MVC) from EMG method were expressed in shadow.

## 4.4 Discussions

As muscle force results were estimated base on wearable sensor system and AnyBody Modeling system, EMG results had been used to do the comparison because in EMG method the muscle activity result is relatively large or small. As shown in Fig. 4-11, AnyBody results of six volunteers was exhibited, furthermore reality sense for walking process and similarity could be found among different individuals. And in Fig. 4-12, contradistinctive analysis was implemented between calculated results of AnyBody and measured results of EMG method, similar comparability could be found although the two result had some differences.

In the first contacting step, backwards and vertical GRF appeared while the heel contacting the floor, the muscle force of ANT TIB and resultant EHL&EDL which locate on the front of shank grew up to balance the moment of ankle joint. Similarly in the last swinging step, all muscles had relatively small values except ANT TIB and resultant EHL&EDL which offered forces to drive the limb swing till next gait cycle start. As shown in Fig. 4-11 (a), (e) and Fig. 4-12 (a), (b), (c), the value of both AnyBody results and EMG results were relatively high in the beginning and ending period of the gait cycle, whereas the AnyBody results were keeping nearly zero and the EMG results were only keeping relatively smaller values in the middle steps of the gait cycle.

In the supporting step, the load transformation from posterior foot to anterior foot caused the obvious increasing of tensile forces of SOL and GAST, and the peak value of GAST occurred in this step, whereas the ANT TIB and resultant EHL&EDL offered decrescendo force values in this step as shown in Fig. 4-11 and Fig. 4-12. While in the leaving ground step, muscles in posterior of shank continued to increase for pushing human body moving forward and upward till the whole foot separated from the ground and start to swing, force curves of resultant FHL&FDL and PL had similar tendencies, they had similar period of rising parts and descending parts, moreover, the peak value of PL, SOL and resultant FHL&FDL also occurred

in this step as shown in Fig. 4-11 (b), (c), (f) and Fig. 4-12. The Achilles tendon force were calculated by summating muscle forces of SOL and GAST. In our results by summating muscle forces of Fig. 4-11 (c) and (d), the largest peak Achilles tendon force was 1536 N occurred in 41.37% gait cycle of volunteer 5, while the smallest was 935 N in 39.66% gait cycle of volunteer 1, that were in good agreement with reported peak Achilles tendon force 1430±500 N (45).

The calculated muscle forces results of AnyBody have realistic meaning and tendency comparability with the EMG results got in the same experiment. Furthermore in the future the muscle forces can be made into vector quantity instead of scalar quantity by 3D technology in AnyBody Modeling System, and more veracious and accurate model can be established as the wearable angular and GRF data collecting sensor system owns the capability of three-dimensional measuring.

## 4.5 Conclusions

A new quantitative method for estimating muscle forces of human ankle joint based on inverse dynamics technology was presented. The developed wearable motion and force sensors gave a great performance in measuring angular displacement and GRF of human limbs. The data measured by wearable sensors could apply on bionic dynamic limbs in AnyBody Modeling System, which professional concerns on musculoskeletal kinematics and kinetics modeling and analysis. In this way the quantitative muscle forces of ankle joint were calculated and the variation tendency of these force results showed reality sense for walking process analysis. The EMG method, which by now is known as the most accepted method in estimating muscle forces in human musculoskeletal analysis, was involved in the experiment to do the validation. Moreover the muscle forces results of AnyBody model matched the muscle activation levels tendency of EMG method. This method for dynamics analysis of

human foot appears to be a practical means to determine muscle forces in musculoskeletal analysis of human limb. The method introduced in this paper is implemental for on-the-spot medical applications, as it owns the diversiform environments suitability and inexpensive implementation characteristic.

# Chapter 5

## Conclusions

### 5.1 Summary

For the rehabilitation of human lower limbs, a new estimation method of lower limb kinetics during standing-up process is presented, and a trajectory control method and a impedance control method with training game based on a rehabilitation robot are developed to assure safely and effective training for patients. During the standing-up process, body segment rotational angles, movement trajectories, ground reaction forces, center of pressure and rope tensile forces are real-time measured by the robot sensor system, and the joint moments of ankle, knee and hip are calculated in real-time control program. Test experiments were performed on ten subjects, in the experiment the robot system were connected to the subject by easy-to-wear jackets and all control commands were controlled by the subjects own. The experimental results validate the theory that both the trajectory control method and the impedance control method can assure the accomplishment of the standing-up process, maintain a comfortable training posture by working through natural movement trajectories, and decrease joint moments by providing assist forces on ropes. Furthermore, using the impedance control method, the intended movement of patients can be recognized, and the motor function of lower limbs can be trained more effectively by concentrating the training on the weak standing position of patients. The game control method are developed based on the impedance control method, the robot under the game control method could activate the collaboration of brain and limb, and increase the frequency and intensity of rehabilitation activities. Therefore, the control methods are suitable for self-supported home training, and can be applied to assess kinetics

parameters during the standing-up process and improve the rehabilitation of patients in clinical settings.

As it is inconvenient to directly measure tension forces of muscles attaching on limbs, a new quantitative approach for estimating muscle forces of lower limb based on inverse dynamics technology was presented. Firstly muscle force estimation in human standing-up process was presented based on a rehabilitation robot and AnyBody Modeling System. The rehabilitation robot was developed for offering assistance and measuring dynamic parameters of body segments. In the rehabilitation experiment, ground reaction force, center of pressure, and rotational motions of trunk, thigh and shank were real-time measured by the sensors of the robot system. Meanwhile, the AnyBody Modeling System was adopted for calculating muscle forces of lower limbs. In AnyBody Modeling System, a musculoskeletal model composed of thigh, shank, foot, four joints and fifteen muscles was developed. The sensor measured GRF, COP and motion data were imported into the model, then the tension forces of muscles of lower limb were calculated through an inverse dynamics method. Furthermore for the validation of the rehabilitation experiment, the activation levels of muscles were also directly measured by an electromyography system. The experiment results showed that the rehabilitation robot provided effective assistance in the standing-up process, and the sensors performed effectively in measuring dynamic parameters of lower limbs. In AnyBody Modeling System, the variation in the muscle force results showed practical sense for the standing-up process. Furthermore, the muscle activation results of EMG method matched the muscle force results of AnyBody model. Therefore, this approach appears to be a practical means of determining muscle force in musculoskeletal analysis of human limb rehabilitation. Secondly muscle force estimation in human walking process was presented based on a wearable sensor system and AnyBody Modeling System. Test experiments were also performed. The experiment results showed that developed wearable motion and force sensors gave a great performance in measuring angular displacement and GRF of human limbs. The data measured

by wearable sensors could apply on bionic dynamic limbs in AnyBody Modeling System, which professional concerns on musculoskeletal kinematics and kinetics modeling and analysis. In this way the quantitative muscle forces of ankle joint were calculated and the variation tendency of these force results showed reality sense for walking process analysis. The EMG method was also involved in the experiment to do the validation, and the muscle forces results of AnyBody model matched the muscle activation levels tendency of EMG method. The method introduced in this dissertation is implemental for on-the-spot medical applications, as it owns the diversiform environments suitability and inexpensive implementation characteristic.

## 5.2 Future Work and Prospect

For the research of human dynamic analysis based on the rehabilitation robot, further study is needed to identify the type and effect of the rehabilitation activities, more studies are necessary to determine the reliability and validity of the control methods among more diverse groups, especially in clinical populations. And a more integrated 3D robot control method and human dynamic evaluation method can be developed for limb rehabilitation and medical diagnosis in the future. Furthermore, as shown in Fig. 5-1 the rehabilitation robot during human walking can be developed, the human lower limb dynamic parameters during gait process can be analyzed for evaluating the performance of the robot, and adequate control methods can be developed for increasing the effectiveness of rehabilitation activities. For the research of muscle force estimation of lower limb, as shown in Fig. 5-2 the lower limb dynamic parameters can be analyzed in vector quantity instead of scalar quantity by 3D technology in AnyBody Modeling System, and more veracious and accurate model can be established as the angular and GRF data collecting sensor system owns the capability of three-dimensional measuring.

Fig.5-1. Prototype of a volunteer in the gait rehabilitation experiment.

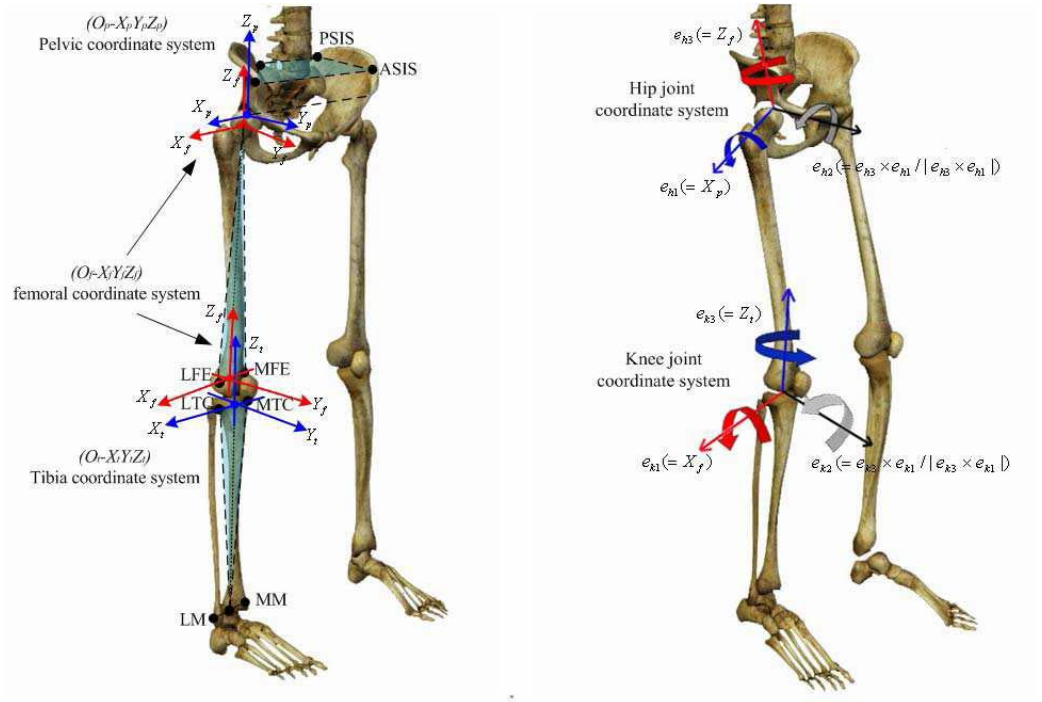


Fig.5-2. Description of coordinate system for the kinematic analysis of lower limb segments.

# REFERENCES

(1) Fent, T., Counting (On) An Aging Population, *IEEE Computing in Science & Engineering,* Vol.8, No.6 (2006), pp. 88–96.

(2) Mann, W.C., The Aging Population and Its Needs, *IEEE Pervasive Computing,* Vol.3, No.2 (2004), pp. 12–14.

(3) Van Exel, N. J. A., Koopmanschap, M. A., Scholte op Reimer, W., Niessen, L. W., and Huijsman, R., Cost-Effectiveness of Integrated Stroke Services, *QJM-J. Assoc. Physicians*, Vol.98, No.6 (2005), pp. 415–425.

(4) Allemand, Y., Stauffer, Y., Clavel, R., Brodard, R., Design of a New Lower Extremity Orthosis for Overground Gait Training with the WalkTrainer, *Proc. of 11th IEEE Intl. Conf. on Rehabilitation Robotics,* Kyoto, Japan (2009-6), pp. 550–555.

(5) Yoon, J., Novandy, B., Yoon, C. H., and Park, K. J., A 6-DOF Gait Rehabilitation Robot With Upper and Lower Limb Connections That Allows Walking Velocity Updates on Various Terrains, *IEEE/ASME Transactions on Mechatronics,* Vol.15, No.2 (2010), pp. 201–215.

(6) Noritsugu, T. and Tanaka, T., Application of Rubber Artificial MuscleManipulator as a Rehabilitation Robot, *IEEE/ASME Transactions on Mechatronics*, Vol. 2, No. 4 (1997-12), pp. 259–267.

(7) Doi, Y., Exercise apparatus for restoration of function, *J. Soc.Biomech.,* Vol. 17, No. 2 (1993), pp. 99–105.

(8) Fujie, M., Improvement of walking rehabilitation system for elderly, *Proc. IEEE Int. Conf. Robotics and Automation,* Vol. 3 (1995), pp. 32–39.

(9) Jaime, R. P., Matjacˇic´, Z., and Hunt, K. J., Paraplegic Standing Supported by FES-Controlled Ankle Stiffness, *IEEE Trans. on Neural Systems and Rehabilitation Engineering,* Vol.10, No.4 (2002), pp. 239–248.

(10) Peshkin, M., Brown, D. A., Santos-Munné, J. J., Makhlin, A., Lewis, E., Colgate, J. E., Patton, J., and Schwandt, D., 2005, KineAssist: A Robotic Overground Gait and Balance Training Device, *Proc. of IEEE 9th Intl. Conf. on Rehabilitation Robotics,* Chicago. USA (2005-7), pp. 241–246.

(11) Mori, Y., Okada, J., and Takayama, K., Development of a Standing Style Transfer System 'ABLE' for Disabled Lower Limbs, *IEEE /ASME Trans. on Mechatronics,* Vol.11, No.4 (2006), pp. 372–380.

(12) Vallery, H., Ekkelenkamp, R., Buss, M., and Kooij, H., Complementary Limb Motion Estimation based on Interjoint Coordination: Experimental Evaluation, *Proc. of IEEE 10th Intl. Conf. on Rehabilitation Robotics,* Noordwijk. Netherlands (2007-6), pp. 798–803.

(13) Tsukahara, A., Hasegawa, Y., and Sankai, Y., Standing-Up Motion Support for Paraplegic Patient with Robot Suit HAL, *IEEE 11th Int. Conf. on Rehabilitation Robotics,* Kyoto. Japan (2009-6), pp. 211–217.

(14) Riener, R., Lünenburger, L., Jezernik, S., Anderschitz, M., Colombo, G., and Dietz, V., Patient-Cooperative Strategies for Robot-Aided Treadmill Training: First Experimental Results, *IEEE Trans. on Neural Systems and Rehabilitation Engineering,* Vol.13, No.3 (2005), pp. 380–394.

(15) Aoyagi, D., Ichinose, W. E., Harkema, S. J., Reinkensmeyer, D. J., and Bobrow, J. E., A Robot and Control Algorithm That Can Synchronously Assist in Naturalistic Motion During Body-Weight-Supported Gait Training Following Neurologic Injury, *IEEE Trans. on Neural Systems and Rehabilitation Engineering,* Vol.15, No.3 (2007), pp. 387–400.

(16) Kuzelicki, J., Kamnik, R., Burger, H., and Bajd, T., Robot Assisted Standing-Up in Persons with Lower Limb Prostheses, *Proc. of 23rd IEEE/EMBS Annual Conf. on Engineering in Medicine and Biology Society*, Vol.2 (2001), pp. 1332–1335.

(17) Veneman, J. F., Kruidhof, R., Hekman, E. E. G., Ekkelenkamp, R., Asseldonk, E. H. F. V., and Kooij, H., Design and Evaluation of the LOPES Exoskeleton Robot for Interactive Gait Rehabilitation, *IEEE Trans. on Neural Systems and Rehabilitation Engineering,* Vol.15, No.3 (2007), pp. 379–386

(18) Neckel, N. D., Nichols, D., and Hidler, J. M., Joint Moments Exhibited by Chronic Stroke Volunteers While Walking with a Prescribed Physiological Gait Pattern, *Proc. of IEEE 10th Intl. Conf. on Rehabilitation Robotics,* Noordwijk. Netherlands (2007-6), pp. 771–775.

(19) Banala, S. K., Agrawal, S. K., Fattah, A., Krishnamoorthy, V., Hsu, W. L., Scholz, J., and Rudolph, K., Gravity-Balancing Leg Orthosis and Its Performance Evaluation, *IEEE Trans. on Robotics,* Vol.22, No.6 (2006), pp. 1228–1239.

(20) Ferris, D. P., Sawicki, G. S., and Domingo, A., Powered lower limb orthoses for gait rehabilitation, *Top Spinal Cord Inj Rehabil.,* Vol.11, No.2 (2005), pp. 34–49.

(21) Hirata, R., Sakaki, T., Okada, S., Nakamoto, Z., Hiraki, N., Okajima, Y., Uchida, S., Tomita, Y., and Horiuchi, T., BRMS:Bio-Resposive Motion System (Rehabilitation System for Stroke Patients), *Proc. of IEEE/RSJ Intl. Conf. on Intelligent Robots and Systems EPFL,* Lausanne. Switzerland, Vol.2 (2002), pp. 1344–1348.

(22) Prasad, G., Herman, P., Coyle, D., McDonough, S., and Crosbie, J., Using Motor Imagery Based Brain-Computer Interface for Post-stroke Rehabilitation, *Proceedings of the 4th International IEEE EMBS Conference on Neural Engineering,* Antalya. Turkey (2009-5), pp. 258–262.

[23] Kato, H., Izumiyama, M., Koizumi, H., Takahashi, A., Itoyama, Y., Near-infrared spectroscopic topography as a tool to monitor motor reorganization after hemiparetic stroke: A comparison with functional MRI, *Stroke*, Vol. 33, No. 8 (2002), pp. 2032-2036.

[24] Watanabe, A., Matsuo, K., Kato, N., Kato, T., Cerebrovascular Response to Cognitive Tasks and Hyperventilation Measured by Multi-Channel Near-Infrared Spectroscopy, *Journal of Neuropsychiatry Clin Neurosci*, Vol. 15, No. 4 (2003), pp. 442-449.

[25] Imai, I., Takeda, K., Shiomi, T., Taniguchi, T., Kato, H., Sensorimotor cortex activation during mirror therapy in healthy right-handed subjects: A study with near-infrared spectroscopy, *Journal of Physical Therapy Science*, Vol. 20, No. 2 (2008), pp. 141-145.

(26) Lee, K.S., EMG-Based Speech Recognition Using Hidden Markov Models With Global Control Variables, *IEEE Transactions on Biomedical Engineering*, Vol. 55, No. 3 (2008), pp. 930-940, ISSN 0018-9294.

(27) Merlo, A., Farina, D., and Merletti, R., A Fast and Reliable Technique for Muscle Activity Detection From Surface EMG Signals, *Transactions On Biomedical Engineering*, Vol. 50, No. 3 (2003), pp. 316-323, ISSN 0018-9294.

(28) Kizuka T., Masuda, T., Kiryu, T., and Sadoyama, T., Biomechanism Library Practical Usage of Surface Electromyogram, *Publisher of Tokyo Denki University*, ISBN 4-501-32510-0 (2009), Tokyo, Japan.

(29) Seirig, A., and Arkivar, R., The prediction of muscular load sharing and joint forces in the lower extremities during walking, *Journal of Biomechanics*, Vol. 8 (1975), pp. 89–102.

(30) Chao, E. Y.-S., and Rim, K., Application of optimization principles in determining the applied moments in human leg joints during gait, *Journal of Biomechanics*, Vol. 6 (1973), pp. 497–510.

(31) Pedotti, A., Krishnan, V., and Stark, L., Optimization of muscle-force sequencing in human locomotion, *Math. Biosci.*, Vol. 38 (1978), pp. 57–76.

(32) Hatze, H., The complete optimization of a human motion, *Math. Biosci.*, Vol. 28 (1976), pp. 99–135.

(33) Hou, Y.F., Zurada, J.M., Karwowski, W., Marras, W.S., and Davis, K., Estimation of the Dynamic Spinal Forces Using a Recurrent Fuzzy Neural Network, *IEEE Transactions on*

*Systems, Man, and Cybernetics—Part B: Cybernetics*, Vol. 37, No. 1 (2007), pp. 100-109, ISSN 1083-4419.

(34) Ferreira, J.P., Crisostomo, M.M., and Coimbra, A.P., Human Gait Acquisition and Characterization, *IEEE Transactions on Instrumentation and Measurement*, Vol. 58, No. 9 (2009), pp. 2979-2988, ISSN 0018-9456.

(35) Moustakidis, S.P., Theocharis, J.B., and Giakas, G., Subject Recognition Based on Ground Reaction Force Measurements of Gait Signals, *IEEE Transactions on Systems, Man, and Cybernetics—Part B: Cybernetics*, Vol. 38, No. 6 (2008), pp. 1476-1485, ISSN 1083-4419.

(36) Liu, K., Liu, T., Shibata, K., Inoue, Y., and Zheng, R.C., Novel Approach to Ambulatory Assessment of Human Segmental Orientation on A Wearable Sensor System, *Journal of Biomechanics*, Vol. 42, No. 16 (2009), pp. 2747-2752, ISSN 0021-9290.

(37) Boonstra, M.C., Slikke, R.M., Keijsers, N.L., Lummel, R.C., Malefijt, M.C., and Verdonschot, N., The Accuracy of Measuring the Kinematics of Rising from a Chair with Accelerometers and Gyroscopes, *Journal of Biomechanics*, Vol. 39, No. 2 (2006), pp. 354-358, ISSN 0021-9290.

(38) Bigland, B., and Lippold, O., The relationship between force, velocity, and integrated electrical activity in human muscles, *J. Physiol.*, Vol. 123 (1954), pp. 214–224.

(39) Milner-Brown, H., and Stein, R., The relation between the surface electromyogram and muscular force, *J. Physiol.*, Vol. 246 (1975), pp. 549–569.

(40) Urban, M., and Bajcsy, P., Fusion of Voice, Gesture, and Human-Computer Interface Controls for Remotely Operated Robot, *7th International Conference on Information Fusion (FUSION),* Vol.2 (2005-7), pp. 1644–1651.

(41) Bando, N., Horibe, S., Yamada, H., Morita, H., and Tanaka, K., Solid Body Link Model for the Motion of Standing Up and Capability of Evaluation of Joint Moment, *Research Report of Life Technology Research Centre,* Gifu Ken. Japan, No.2 (2006), pp. 30–37.

(42) McMinn, R.M.H., Hutchings, R.T., Logan, B.M., *A Colour Atlas of Foot and Ankle Anatomy,* (1982), p.10–21, Wolfe Medical Publications Ltd.

(43) Perry, J., Ireland, M., Gronley, J., Hoffer, M., Predictive Value of Manual Muscle Testing and Gait Analysis in Normal Ankles by Electromyography, *Foot Ankle*, Vol.6, No.5 (1986), pp.254–259.

(44) Liu, T., Inoue, Y., Shibata, K., New Method for Assessment of Gait Variability Based on Wearable Ground Reaction Force Sensor, *30th Annual International IEEE EMBS Conference Vancouver* (2008), pp. 2341-2344, ISSN 1557-170X.

(45) Finni, T., Komi, P.V., Lukkariniemi, J., Achilles Tendon Loading During Walking: Application of a Novel Optic Fiber Technique, *Eur J Appl Physiol Occup Physiol*, Vol.39, No.2 (1998), pp.289-291.

# APPENDIX

## Appendix A

### Abbreviations

**GRF** Ground Reaction Force.

**COP** Center of Pressure

**EMG** Electromyography

**SSM** Self-supported Standing Method

**TCM** Trajectory Control Method

**ICM** Impedance Control Method

**GCM** Game Control Method

**PM** Muscle of Psoas Major

**GM** Muscle of Gluteus Maximus

**VR** Muscle of Vastus Rectus

**BF** Muscle of Biceps Femoris

**ANT TIB** Muscle of Anterior Tibialis

**GAST** Muscle of Gastrocnemius

**SOL** Muscle of Soleus

**PL** Muscle of Peroneus Longus

**PB** Muscle of Peroneus Brevis

**POST TIB** Muscle of Posterior Tibialis

**VM&VL&VI** Resultant muscle of Vastus Medialis, Vastus Lateralis, and Vastus Intermedius

**FHL&FDL** Resultant muscle of Flexor Hallucis Longus and Flexor Digitorum Longus

**EHL&EDL** Resultant muscle of Extensor Hallucis Longus and Extensor Digitorum Longus

# Appendix B

## ANYBODY Code

## For Create the Lower Limb Dynamic Model of Human Gait Process

```
Main = {
  AnyFolder MyModel = {

    AnyFixedRefFrame GlobalRef = {
      AnyDrawRefFrame DrwGlobalRef =
       {ScaleXYZ = {0.1, 0.1, 0.1};
        RGB = {0,1,0};
       };
      AnyRefNode KeNode = {
        sRel = {0,0,0};
      };
      AnyRefNode XiNode = {
        sRel = {0,0.45,0};
      };
      AnyRefNode FrontNode = {
        sRel = {-0.05,0.85,0};
      };
      AnyRefNode BackNode = {
        sRel = {0.05,0.85,0};
      };
      AnyRefNode BackDown = {
        sRel = {0.05,0.5,0};
      };
      AnyRefNode FrontDown = {
        sRel = {-0.05,0.5,0};
      };
    };   // Global reference frame
      AnySeg DownLeg={
        r0 = {0, 0.225, 0};
        Mass = 5 ;
        Jii = {0.02, 0.002, 0.02};
```

```
    AnyRefNode KeDown = {
      sRel = {0,-0.225,0};
    };
    AnyRefNode XiDown = {
      sRel = {0,0.225,0};
    };
    AnyRefNode XiFront = {
      sRel = {-0.05,0.2,0};
    };
    AnyRefNode XiBack = {
      sRel = {0.05,0.2,0};
    };
    AnyRefNode Middle = {
      sRel = {0.02,0,0};
    };
    AnyRefNode Down0 = {
      sRel = {0.0225,-0.225,0};
    };
    AnyRefNode Down = {
      sRel = {0,-0.256,0};
    };
    AnyDrawSeg DrwSeg = {};
  }; // DownLeg
  AnySeg BackFoot={
    r0 = {-0.05, -0.067, 0};
    Axes0 = RotMat(16.27626*pi/180, z);
    Mass = 2 ;
    Jii = {0.0003, 0.0024, 0.0024};
    AnyRefNode KeBack = {
      sRel = {0.0675,0.051,0};
    };
    AnyRefNode Bei = {
      sRel = {0.01,0.0335,0};
    };
    AnyRefNode ZhiBack = {
      sRel = {-0.0845,0,0};
    };
    AnyRefNode GenNei = {
```

```
    sRel = {0,0,0};
  };
  AnyRefNode GenWai = {
    sRel = {0.1,-0.044,0};
  };
  AnyRefNode FMiddle = {
    sRel = {-0.09,-0.0193,0};
  };
  AnyRefNode FBack = {
    sRel = {0.096,-0.067,0};
  };
  AnyDrawSeg DrwSeg = {};
}; // BackFoot
AnySeg FrontFoot={
  r0 = {-0.172, -0.09, 0};
  Mass = 0.5;
  Jii = {0.0000125, 0.000125, 0.000125};
  AnyRefNode ZhiUp = {
    sRel = {-0.02,0.01,0};
  };
  AnyRefNode ZhiUp1 = {
    sRel = {0.039,0.01,0};
  };
  AnyRefNode ZhiDown = {
    sRel = {-0.031,-0.02,0};
  };
  AnyRefNode ZhiFront = {
    sRel = {0.039,0,0};
  };
  AnyRefNode Jian = {
    sRel = {-0.039,0,0};
  };
  AnyRefNode FMiddle = {
    sRel = {0.039,-0.02,0};
  };
  AnyRefNode FFront = {
    sRel = {-0.03,-0.02,0};
  };
```

```
      AnyDrawSeg DrwSeg = {};
   }; // FrontFoot

AnyRevoluteJoint Xi = {
   AnyRefFrame &Ground = .GlobalRef.XiNode;
   AnyRefFrame &Shank = .DownLeg.XiDown;
};
AnyRevoluteJoint Ke = {
   AnyRefFrame &Ground = .DownLeg.KeDown;
   AnyRefFrame &BackFoot = .BackFoot.KeBack;
};
AnyRevoluteJoint Zhi = {
   AnyRefFrame &Ground = .BackFoot.ZhiBack;
   AnyRefFrame &FrontFoot = .FrontFoot.ZhiFront;
};

AnyFolder Drivers = {
   AnyKinEqInterPolDriver XiMotion = {
      Type = Bspline;
      BsplineOrder = 4;
      FileName = "shankt.txt";
      AnyRevoluteJoint &Jnt = ..Xi;
      MeasureOrganizer = {0};
      Reaction.Type = {Off};
   }; // Xi driver
   AnyKinEqInterPolDriver KeMotion = {
      Type = Bspline;
      BsplineOrder = 4;
      FileName = "heelt.txt";
      AnyRevoluteJoint &Jnt = ..Ke;
      MeasureOrganizer = {0};
      Reaction.Type = {Off};
   }; // Ke driver
   AnyKinEqInterPolDriver ZhiMotion = {
      Type = Bspline;
      BsplineOrder = 4;
      FileName = "toet.txt";
      AnyRevoluteJoint &Jnt = ..Zhi;
```

```
      MeasureOrganizer = {0};
      Reaction.Type = {Off};
   }; // Zhi driver
}; // Driver folder

AnyFolder Muscles = {
   AnyMuscleModel MusMd0 = {
        F0 = 100;
   };
   AnyMuscleModel MusMd1 = {
        F0 = 500;
   };
   AnyMuscleModel MusMd2 = {
        F0 = 1000;
   };
   AnyMuscleModel MusMd3 = {
        F0 = 5000;
   };
   AnyViaPointMuscle FrontUpLeg = {
      AnyMuscleModel &MusMdl = ..Muscles.MusMd3;
      AnyRefNode &Org = ..GlobalRef.FrontNode;
      AnyRefNode &Via = ..GlobalRef.FrontDown;
      AnyRefNode &Ins = ..DownLeg.XiFront;
      AnyDrawMuscle DrwMus = {Bulging = 1; MaxStress = 500000;};
   };
   AnyViaPointMuscle BackUpLeg = {
      AnyMuscleModel &MusMdl = ..Muscles.MusMd3;
      AnyRefNode &Org = ..GlobalRef.BackNode;
      AnyRefNode &Via = ..GlobalRef.BackDown;
      AnyRefNode &Ins = ..DownLeg.XiBack;
      AnyDrawMuscle DrwMus = {Bulging = 1; MaxStress = 500000;};
   };
   AnyViaPointMuscle AntiTib = {
      AnyMuscleModel &MusMdl = ..Muscles.MusMd2;
      AnyRefNode &Org = ..DownLeg.XiFront;
      AnyRefNode &Ins = ..BackFoot.Bei;
      AnyDrawMuscle DrwMus = {Bulging = 1; MaxStress = 50000;};
   };
```

```
AnyViaPointMuscle PostTib = {
  AnyMuscleModel &MusMdl = ..Muscles.MusMd2;
  AnyRefNode &Org = ..DownLeg.XiBack;
  AnyRefNode &Via = ..DownLeg.Down;
  AnyRefNode &Ins = ..FrontFoot.FMiddle;
  AnyDrawMuscle DrwMus = {Bulging = 1; MaxStress = 900000;};
};
AnyViaPointMuscle PL = {
  AnyMuscleModel &MusMdl = ..Muscles.MusMd2;
  AnyRefNode &Org = ..DownLeg.XiBack;
  AnyRefNode &Via0 = ..DownLeg.Down0;
  AnyRefNode &Via = ..DownLeg.Down;
  AnyRefNode &Ins = ..FrontFoot.FMiddle;
  AnyDrawMuscle DrwMus = {Bulging = 1; MaxStress = 900000;};
};
AnyViaPointMuscle PB = {
  AnyMuscleModel &MusMdl = ..Muscles.MusMd2;
  AnyRefNode &Org = ..DownLeg.Middle;
  AnyRefNode &Via0 = ..DownLeg.Down0;
  AnyRefNode &Via = ..DownLeg.Down;
  AnyRefNode &Ins = ..FrontFoot.FMiddle;
  AnyDrawMuscle DrwMus = {Bulging = 1; MaxStress = 900000;};
};
AnyViaPointMuscle Sol = {
  AnyMuscleModel &MusMdl = ..Muscles.MusMd3;
  AnyRefNode &Org = ..DownLeg.XiBack;
  AnyRefNode &Ins = ..BackFoot.GenWai;
  AnyDrawMuscle DrwMus = {Bulging = 1; MaxStress = 200000;};
};
AnyViaPointMuscle Gast = {
  AnyMuscleModel &MusMdl = ..Muscles.MusMd3;
  AnyRefNode &Org = ..GlobalRef.BackDown;
  AnyRefNode &Ins = ..BackFoot.GenWai;
  AnyDrawMuscle DrwMus = {Bulging = 1; MaxStress = 200000;};
};
AnyViaPointMuscle EDL = {
  AnyMuscleModel &MusMdl = ..Muscles.MusMd0;
  AnyRefNode &Org = ..DownLeg.XiFront;
```

```
        AnyRefNode &Via = ..BackFoot.Bei;
        AnyRefNode &Via1 = ..FrontFoot.ZhiUp1;
        AnyRefNode &Ins = ..FrontFoot.ZhiUp;
        AnyDrawMuscle DrwMus = {Bulging = 1; MaxStress = 40000;};
    };
    AnyViaPointMuscle FDL = {
        AnyMuscleModel &MusMdl = ..Muscles.MusMd2;
        AnyRefNode &Org = ..DownLeg.XiBack;
        AnyRefNode &Via0 = ..DownLeg.Down0;
        AnyRefNode &Via1 = ..DownLeg.Down;
        AnyRefNode &Via2 = ..FrontFoot.FMiddle;
        AnyRefNode &Ins = ..FrontFoot.ZhiDown;
        AnyDrawMuscle DrwMus = {Bulging = 1; MaxStress = 900000;};
    };
    AnyViaPointMuscle EDB = {
        AnyMuscleModel &MusMdl = ..Muscles.MusMd0;
        AnyRefNode &Org = ..BackFoot.Bei;
        AnyRefNode &Via = ..FrontFoot.ZhiUp1;
        AnyRefNode &Ins = ..FrontFoot.ZhiUp;
        AnyDrawMuscle DrwMus = {Bulging = 1; MaxStress = 40000;};
    };
    AnyViaPointMuscle FDB = {
        AnyMuscleModel &MusMdl = ..Muscles.MusMd0;
        AnyRefNode &Org = ..BackFoot.FBack;
        AnyRefNode &Via = ..FrontFoot.FMiddle;
        AnyRefNode &Ins = ..FrontFoot.ZhiDown;
        AnyDrawMuscle DrwMus = {Bulging = 1; MaxStress = 10000;};
    };
}; // Muscles folder

AnyForce3D InterpBack = {
    // Interpolation function. The interpolated data can also be read directly from a text file
    AnyFunInterpol force1 = {
        Type = Bspline;
        BsplineOrder = 4;
        FileName = "Fzback.txt";
    };
    AnyVector Fb = force1(t);
```

```
    AnyFunInterpol force11 = {
      Type = Bspline;
      BsplineOrder = 4;
      FileName = "Fyback.txt";
    };
    AnyVector Fbb = force11(t);
    F = {Fbb[0],Fb[0],0}; // Force in Newton
    AnyRefFrame &BackFoot = Main.MyModel.BackFoot.FBack;
      AnyDrawVector drF = {
        Vec = .Fout/7000;      // Scale the length down
        Line = {
          Style = Line3DStyleFull;
          Thickness = 0.01;
          RGB = {0, 0, 1};
          End = {
            Style = Line3DCapStyleArrow;    // This specifies the end to be an arrowhead
            RGB = {0, 0, 1};
            Thickness = 0.02;    // The head begins with twice the thickness of the shaft
            Length = 0.05;
          }; //End
        }; //Line
      // attach the arrow to the hand
      AnyRefFrame &Palm = Main.MyModel.BackFoot.FBack;
      }; //drF
}; //InterpBack

AnyForce3D InterpMiddle = {
    // Interpolation function. The interpolated data can also be read directly from a text file
    AnyFunInterpol force2 = {
      Type = Bspline;
      BsplineOrder = 4;
      FileName = "Fzmiddle.txt";
    };
    AnyVector Fc = force2(t);
    AnyFunInterpol force22 = {
      Type = Bspline;
      BsplineOrder = 4;
      FileName = "Fymiddle.txt";
```

```
    };
    AnyVector Fcc = force22(t);
    F = {Fcc[0],Fc[0],0}; // Force in Newton
    AnyRefFrame &BackFoot = Main.MyModel.BackFoot.FMiddle;
      AnyDrawVector drF = {
        Vec = .Fout/7000;      // Scale the length down
        Line = {
          Style = Line3DStyleFull;
          Thickness = 0.01;
          RGB = {1, 0, 0};
          End = {
            Style = Line3DCapStyleArrow;    // This specifies the end to be an arrowhead
            RGB = {1, 0, 0};
            Thickness = 0.02;    // The head begins with twice the thickness of the shaft
            Length = 0.05;
          }; //End
        }; //Line
      // attach the arrow to the hand
      AnyRefFrame &Palm = Main.MyModel.FrontFoot.FMiddle;
      }; //drF
}; //InterpMiddle

AnyForce3D InterpFront = {
    // Interpolation function. The interpolated data can also be read directly from a text file
    AnyFunInterpol force3 = {
      Type = Bspline;
      BsplineOrder = 4;
      FileName = "Fzjian.txt";
    };
    AnyVector Fd = force3(t);
    AnyFunInterpol force33 = {
      Type = Bspline;
      BsplineOrder = 4;
      FileName = "Fyjian.txt";
    };
    AnyVector Fdd = force33(t);
    F = {Fdd[0],Fd[0],0}; // Force in Newton
    AnyRefFrame &FrontFoot = Main.MyModel.FrontFoot.FFront;
```

```
            AnyDrawVector drF = {
              Vec = .Fout/7000;      // Scale the length down
              Line = {
                Style = Line3DStyleFull;
                Thickness = 0.01;
                RGB = {0, 1, 0};
                End = {
                  Style = Line3DCapStyleArrow;    // This specifies the end to be an arrowhead
                  RGB = {0, 1, 0};
                  Thickness = 0.02;    // The head begins with twice the thickness of the shaft
                  Length = 0.05;
                }; //End
              }; //Line
            // attach the arrow to the hand
            AnyRefFrame &Palm = Main.MyModel.FrontFoot.FFront;
            }; //drF
        }; //InterpFront

    }; // MyModel

      AnyBodyStudy MyStudy = {
        AnyFolder &Model = .MyModel;
        Gravity = {0.0, -9.81, 0.0};
        nStep = 600;
        tStart= 0.00;
        tEnd= 4.90;
      }; // MyStudy
    };    // Main
```

**For Create the Lower Limb Dynamic Model of Human Standing-up Process**

```
Main = {
  AnyFolder MyModel = {
      AnyFixedRefFrame GlobalRef = {
      AnyDrawRefFrame DrwGlobalRef =
        {ScaleXYZ = {0.1, 0.1, 0.1};
         RGB = {0,1,0};
        };
      AnyRefNode KeNode = {
         sRel = {0,0,0};
      };
      AnyRefNode KuanNode = {
         sRel = {0,0.9,0};
      };
      AnyRefNode FrontNode = {
         sRel = {-0.05,1.0,0};
      };
      AnyRefNode BackNode = {
         sRel = {0.0725,0.95,0};
      };
      AnyRefNode BackDown = {
         sRel = {0.05,0.925,0};
      };
      AnyRefNode FrontDown = {
         sRel = {-0.0725,0.95,0};
      };
    };   // Global reference frame

      AnySeg UpLeg={
         r0 = {0, 0.675, 0};
         Mass = 10 ;
         Jii = {0.08, 0.008, 0.08};
         AnyRefNode XiUp = {
            sRel = {0,-0.225,0};
         };
         AnyRefNode KuanUp = {
```

```
        sRel = {0,0.225,0};
      };
      AnyRefNode KuanFront = {
        sRel = {-0.06,0.2,0};
      };
      AnyRefNode KuanBackDown = {
        sRel = {0.05,0.175,0};
      };
      AnyRefNode KuanBack = {
       sRel = {0.05,0.2,0};
     };
      AnyRefNode MiddleUp = {
        sRel = {-0.03,0.15,0};
      };
      AnyRefNode XiUpFront2 = {
        sRel = {-0.05,-0.225,0};
      };
      AnyRefNode XiUpBack = {
        sRel = {0.05,-0.165,0};
      };
      AnyDrawSeg DrwSeg = {};
};// UpLeg
AnySeg DownLeg={
      r0 = {0, 0.225, 0};
      Mass = 5 ;
      Jii = {0.02, 0.002, 0.02};
      AnyRefNode KeDown = {
        sRel = {0,-0.225,0};
      };
      AnyRefNode XiDown = {
        sRel = {0,0.225,0};
      };
      AnyRefNode XiFront = {
        sRel = {-0.05,0.2,0};
      };
      AnyRefNode XiFront2 = {
        sRel = {-0.05,0.225,0};
      };
```

```
        AnyRefNode XiBack = {
            sRel = {0.05,0.2,0};
        };
        AnyRefNode XiBack2 = {
            sRel = {0.05,0.165,0};
        };
        AnyRefNode Middle = {
            sRel = {0.02,0,0};
        };
        AnyRefNode Down0 = {
            sRel = {0.0225,-0.225,0};
        };
        AnyRefNode Down = {
            sRel = {0,-0.256,0};
        };
        AnyDrawSeg DrwSeg = {};
    }; // DownLeg
    AnySeg BackFoot={
        r0 = {-0.05, -0.067, 0};
        Axes0 = RotMat(16.27626*pi/180, z);
        Mass = 2 ;
        Jii = {0.0003, 0.0024, 0.0024};
        AnyRefNode KeBack = {
            sRel = {0.0675,0.051,0};
        };
        AnyRefNode Bei = {
            sRel = {0.01,0.0335,0};
        };
        AnyRefNode ZhiBack = {
            sRel = {-0.0845,0,0};
        };
        AnyRefNode GenNei = {
            sRel = {0,0,0};
        };
        AnyRefNode GenWai = {
            sRel = {0.1,-0.044,0};
        };
        AnyRefNode FMiddle = {
```

```
        sRel = {-0.09,-0.0193,0};
    };
    AnyRefNode FBack = {
        sRel = {0.096,-0.067,0};
    };
    AnyDrawSeg DrwSeg = {};
}; // BackFoot
AnySeg FrontFoot={
    r0 = {-0.172, -0.09, 0};
    Mass = 0.5;
    Jii = {0.0000125, 0.000125, 0.000125};
    AnyRefNode ZhiUp = {
        sRel = {-0.02,0.01,0};
    };
    AnyRefNode ZhiUp1 = {
        sRel = {0.039,0.01,0};
    };
    AnyRefNode ZhiDown = {
        sRel = {-0.031,-0.02,0};
    };
    AnyRefNode ZhiFront = {
        sRel = {0.039,0,0};
    };
    AnyRefNode Jian = {
        sRel = {-0.039,0,0};
    };
    AnyRefNode FMiddle = {
        sRel = {0.039,-0.02,0};
    };
    AnyRefNode FFront = {
        sRel = {-0.03,-0.02,0};
    };
    AnyDrawSeg DrwSeg = {};
}; // FrontFoot

AnyRevoluteJoint Kuan = {
  AnyRefFrame &Ground = .GlobalRef.KuanNode;
  AnyRefFrame &Thigh = .UpLeg.KuanUp;
```

```
};
AnyRevoluteJoint Xi = {
   AnyRefFrame &Ground = .UpLeg.XiUp;
   AnyRefFrame &Shank = .DownLeg.XiDown;
};
AnyRevoluteJoint Ke = {
   AnyRefFrame &Ground = .DownLeg.KeDown;
   AnyRefFrame &BackFoot = .BackFoot.KeBack;
};
AnyRevoluteJoint Zhi = {
   AnyRefFrame &Ground = .BackFoot.ZhiBack;
   AnyRefFrame &FrontFoot = .FrontFoot.ZhiFront;
};

AnyFolder Drivers = {
   AnyKinEqInterPolDriver KuanMotion = {
      Type = Bspline;
      BsplineOrder = 4;
      FileName = "thight.txt";
      AnyRevoluteJoint &Jnt = ..Kuan;
      MeasureOrganizer = {0};
      Reaction.Type = {Off};
   }; // Kuan driver
   AnyKinEqInterPolDriver XiMotion = {
      Type = Bspline;
      BsplineOrder = 4;
      FileName = "shankt.txt";
      AnyRevoluteJoint &Jnt = ..Xi;
      MeasureOrganizer = {0};
      Reaction.Type = {Off};
   }; // Xi driver
   AnyKinEqInterPolDriver KeMotion = {
      Type = Bspline;
      BsplineOrder = 4;
      FileName = "heelt.txt";
      AnyRevoluteJoint &Jnt = ..Ke;
      MeasureOrganizer = {0};
      Reaction.Type = {Off};
```

```
    }; // Ke driver
    AnyKinEqInterPolDriver ZhiMotion = {
      Type = Bspline;
      BsplineOrder = 4;
      FileName = "toet.txt";
      AnyRevoluteJoint &Jnt = ..Zhi;
      MeasureOrganizer = {0};
      Reaction.Type = {Off};
    }; // Zhi driver
}; // Driver folder

AnyFolder Muscles = {
    AnyMuscleModel MusMd0 = {
        F0 = 100;
    };
    AnyMuscleModel MusMd1 = {
        F0 = 500;
    };
    AnyMuscleModel MusMd2 = {
        F0 = 1000;
    };
    AnyMuscleModel MusMd3 = {
        F0 = 5000;
    };
    AnyMuscleModel MusMd4 = {
        F0 = 10000;
    };
    AnyViaPointMuscle PsoasMajor = {
      AnyMuscleModel &MusMdl = ..Muscles.MusMd3;
      AnyRefNode &Org = ..GlobalRef.FrontNode;
      AnyRefNode &Ins = ..UpLeg.KuanFront;
      AnyDrawMuscle DrwMus = {Bulging = 1; MaxStress = 200000;};
    };
    AnyViaPointMuscle GluteusMaximus = {
      AnyMuscleModel &MusMdl = ..Muscles.MusMd3;
      AnyRefNode &Org = ..GlobalRef.BackNode;
      AnyRefNode &Ins = ..UpLeg.KuanBackDown;
      AnyDrawMuscle DrwMus = {Bulging = 1; MaxStress = 200000;};
```

```
};
AnyViaPointMuscle VastusRectus = {
   AnyMuscleModel &MusMdl = ..Muscles.MusMd3;
   AnyRefNode &Org = ..GlobalRef.FrontDown;
   AnyRefNode &Via1 = ..UpLeg.KuanFront;
   AnyRefNode &Via3 = ..UpLeg.XiUpFront2;
   AnyRefNode &Ins = ..DownLeg.XiFront2;
   AnyDrawMuscle DrwMus = {Bulging = 1; MaxStress = 200000;};
};
AnyViaPointMuscle BicepsFemoris = {
   AnyMuscleModel &MusMdl = ..Muscles.MusMd3;
   AnyRefNode &Org = ..GlobalRef.BackDown;
   AnyRefNode &Via1 = ..UpLeg.KuanBack;
   AnyRefNode &Ins = ..DownLeg.XiBack2;
   AnyDrawMuscle DrwMus = {Bulging = 1; MaxStress = 200000;};
};
AnyViaPointMuscle Vastus = {
   AnyMuscleModel &MusMdl = ..Muscles.MusMd3;
   AnyRefNode &Org = ..UpLeg.MiddleUp;
   AnyRefNode &Via2 = ..UpLeg.XiUpFront2;
   AnyRefNode &Ins = ..DownLeg.XiFront2;
   AnyDrawMuscle DrwMus = {Bulging = 1; MaxStress = 200000;};
};
AnyViaPointMuscle AntiTib = {
   AnyMuscleModel &MusMdl = ..Muscles.MusMd2;
   AnyRefNode &Org = ..DownLeg.XiFront;
   AnyRefNode &Ins = ..BackFoot.Bei;
   AnyDrawMuscle DrwMus = {Bulging = 1; MaxStress = 50000;};
};
AnyViaPointMuscle PostTib = {
   AnyMuscleModel &MusMdl = ..Muscles.MusMd2;
   AnyRefNode &Org = ..DownLeg.XiBack;
   AnyRefNode &Via = ..DownLeg.Down;
   AnyRefNode &Ins = ..FrontFoot.FMiddle;
   AnyDrawMuscle DrwMus = {Bulging = 1; MaxStress = 900000;};
};
AnyViaPointMuscle PL = {
   AnyMuscleModel &MusMdl = ..Muscles.MusMd2;
```

```
    AnyRefNode &Org = ..DownLeg.XiBack;
    AnyRefNode &Via0 = ..DownLeg.Down0;
    AnyRefNode &Via = ..DownLeg.Down;
    AnyRefNode &Ins = ..FrontFoot.FMiddle;
    AnyDrawMuscle DrwMus = {Bulging = 1; MaxStress = 900000;};
};
AnyViaPointMuscle PB = {
    AnyMuscleModel &MusMdl = ..Muscles.MusMd2;
    AnyRefNode &Org = ..DownLeg.Middle;
    AnyRefNode &Via0 = ..DownLeg.Down0;
    AnyRefNode &Via = ..DownLeg.Down;
    AnyRefNode &Ins = ..FrontFoot.FMiddle;
    AnyDrawMuscle DrwMus = {Bulging = 1; MaxStress = 900000;};
};
AnyViaPointMuscle Sol = {
    AnyMuscleModel &MusMdl = ..Muscles.MusMd3;
    AnyRefNode &Org = ..DownLeg.XiBack;
    AnyRefNode &Ins = ..BackFoot.GenWai;
    AnyDrawMuscle DrwMus = {Bulging = 1; MaxStress = 200000;};
};
AnyViaPointMuscle Gast = {
    AnyMuscleModel &MusMdl = ..Muscles.MusMd3;
    AnyRefNode &Org = ..UpLeg.XiUpBack;
    AnyRefNode &Ins = ..BackFoot.GenWai;
    AnyDrawMuscle DrwMus = {Bulging = 1; MaxStress = 200000;};
};
AnyViaPointMuscle EDL = {
    AnyMuscleModel &MusMdl = ..Muscles.MusMd0;
    AnyRefNode &Org = ..DownLeg.XiFront;
    AnyRefNode &Via = ..BackFoot.Bei;
    AnyRefNode &Via1 = ..FrontFoot.ZhiUp1;
    AnyRefNode &Ins = ..FrontFoot.ZhiUp;
    AnyDrawMuscle DrwMus = {Bulging = 1; MaxStress = 40000;};
};
AnyViaPointMuscle FDL = {
    AnyMuscleModel &MusMdl = ..Muscles.MusMd2;
    AnyRefNode &Org = ..DownLeg.XiBack;
    AnyRefNode &Via0 = ..DownLeg.Down0;
```

```
        AnyRefNode &Via1 = ..DownLeg.Down;
        AnyRefNode &Via2 = ..FrontFoot.FMiddle;
        AnyRefNode &Ins = ..FrontFoot.ZhiDown;
        AnyDrawMuscle DrwMus = {Bulging = 1; MaxStress = 900000;};
      };
      AnyViaPointMuscle EDB = {
        AnyMuscleModel &MusMdl = ..Muscles.MusMd0;
        AnyRefNode &Org = ..BackFoot.Bei;
        AnyRefNode &Via = ..FrontFoot.ZhiUp1;
        AnyRefNode &Ins = ..FrontFoot.ZhiUp;
        AnyDrawMuscle DrwMus = {Bulging = 1; MaxStress = 40000;};
      };
      AnyViaPointMuscle FDB = {
        AnyMuscleModel &MusMdl = ..Muscles.MusMd0;
        AnyRefNode &Org = ..BackFoot.FBack;
        AnyRefNode &Via = ..FrontFoot.FMiddle;
        AnyRefNode &Ins = ..FrontFoot.ZhiDown;
        AnyDrawMuscle DrwMus = {Bulging = 1; MaxStress = 10000;};
      };
};// Muscles folder

AnyForce3D InterpBack = {
      // Interpolation function. The interpolated data can also be read directly from a text file
      AnyFunInterpol force1 = {
        Type = Bspline;
        BsplineOrder = 4;
        FileName = "Fzback.txt";
      };
      AnyVector Fb = force1(t);
      AnyFunInterpol force11 = {
        Type = Bspline;
        BsplineOrder = 4;
        FileName = "Fyback.txt";
      };
      AnyVector Fbb = force11(t);
      F = {Fbb[0],Fb[0],0}; // Force in Newton
      AnyRefFrame &BackFoot = Main.MyModel.BackFoot.FBack;
        AnyDrawVector drF = {
```

```
            Vec = .Fout/5000;      // Scale the length down
            Line = {
               Style = Line3DStyleFull;
               Thickness = 0.01;
               RGB = {0, 0, 1};
               End = {
                  Style = Line3DCapStyleArrow;    // This specifies the end to be an arrowhead
                  RGB = {0, 0, 1};
                  Thickness = 0.02;    // The head begins with twice the thickness of the shaft
                  Length = 0.05;
               }; //End
            }; //Line
         // attach the arrow to the hand
         AnyRefFrame &Palm = Main.MyModel.BackFoot.FBack;
         }; //drF
}; //InterpBack

AnyForce3D InterpMiddle = {
      // Interpolation function. The interpolated data can also be read directly from a text file
      AnyFunInterpol force2 = {
         Type = Bspline;
         BsplineOrder = 4;
         FileName = "Fzmiddle.txt";
      };
      AnyVector Fc = force2(t);
      AnyFunInterpol force22 = {
         Type = Bspline;
         BsplineOrder = 4;
         FileName = "Fymiddle.txt";
      };
      AnyVector Fcc = force22(t);
      F = {Fcc[0],Fc[0],0}; // Force in Newton
      AnyRefFrame &BackFoot = Main.MyModel.BackFoot.FMiddle;
         AnyDrawVector drF = {
            Vec = .Fout/7000;      // Scale the length down
            Line = {
               Style = Line3DStyleFull;
               Thickness = 0.01;
```

```
            RGB = {1, 0, 0};
            End = {
              Style = Line3DCapStyleArrow;    // This specifies the end to be an arrowhead
              RGB = {1, 0, 0};
              Thickness = 0.02;    // The head begins with twice the thickness of the shaft
              Length = 0.05;
            }; //End
          }; //Line
        // attach the arrow to the hand
        AnyRefFrame &Palm = Main.MyModel.FrontFoot.FMiddle;
        }; //drF
}; //InterpMiddle
AnyForce3D InterpFront = {
    // Interpolation function. The interpolated data can also be read directly from a text file
    AnyFunInterpol force3 = {
      Type = Bspline;
      BsplineOrder = 4;
      FileName = "Fzjian.txt";
    };
    AnyVector Fd = force3(t);
    AnyFunInterpol force33 = {
      Type = Bspline;
      BsplineOrder = 4;
      FileName = "Fyjian.txt";
    };
    AnyVector Fdd = force33(t);
    F = {Fdd[0],Fd[0],0}; // Force in Newton
    AnyRefFrame &FrontFoot = Main.MyModel.FrontFoot.FFront;
      AnyDrawVector drF = {
        Vec = .Fout/5000;     // Scale the length down
        Line = {
          Style = Line3DStyleFull;
          Thickness = 0.01;
          RGB = {0, 1, 0};
          End = {
            Style = Line3DCapStyleArrow;    // This specifies the end to be an arrowhead
            RGB = {0, 1, 0};
            Thickness = 0.02;    // The head begins with twice the thickness of the shaft
```

```
                    Length = 0.05;
                  }; //End
                }; //Line
              // attach the arrow to the hand
              AnyRefFrame &Palm = Main.MyModel.FrontFoot.FFront;
              }; //drF
    }; //InterpFront
}; // MyModel

  AnyBodyStudy MyStudy = {
    AnyFolder &Model = .MyModel;
    Gravity = {0.0, -9.81, 0.0};
    nStep = 500;
    tStart= 0.01;
    tEnd= 5.36;
  }; // MyStudy
};   // Main
```

# ACKNOWLEDGMENTS

This thesis would not be completed without the help of many enthusiastic persons. Here, I would like to mention some of the most influential people for this thesis as well as my life.

First of all, I would like to give a big thanks to my supervisor, Prof. Yoshio Inoue, who provided me with his enthusiastic suggestions and advice to support my research works. I also have appreciated your encouragement and advice for not only this project, but also my future career that I would not have obtained anywhere except from you.

I would like to thank Prof. Kyoko Shibata, Prof. Koichi Oka, Prof. Shouyu Wang and Prof. Fumiaki Takeda, who gave me so many useful suggestions and information about the project in every discussion meeting. And thank all the other members of Robotics and Dynamic Lab, who make me feel so fine and happy. Special acknowledgments to Liu tao sensei, who brought me so many helps and smiles.

I would like to thank IRC staffs, Ban sensei, Kubo sensei, Yoshida san, Yamasaki san, Fujii san and my Sakamoto san, who helped me so much on Japanese study and foreign life when I just went to Japan. I will never forget their warm heart and kindness.

Thanks also to all those people helped me to correct my written English. At last, but not at least, I address my special thanks to SSP Scholarship and Rotary Scholarship for kind supports.

# *List of Publications*

## *Academic Journal Papers*

● Enguo Cao, Yoshio Inoue, Tao Liu, Kyoko Shibata, A Sit-to-stand Training Robot and Its Performance Evaluation: Dynamic Analysis in Lower Limb Rehabilitation Activities, *Journal of System Design and Dynamics-Transactions of the JSME*, Vol. 6, No. 4, pp. 466–481, 2012.

● Enguo Cao, Yoshio Inoue, Tao Liu, Kyoko Shibata, Estimate Muscle Forces of Ankle Joint with Wearable Sensors, *Journal of Biomechanical Science and Engineering-Transactions of the JSME*, Vol. 6, No. 4, pp. 299–310, 2011.

● Kun Liu, Yoshio Inoue, Kyoko Shibata; Enguo Cao, Ambulatory Estimation of Knee-Joint Kinematics in Anatomical Coordinate System Using Accelerometers and Magnetometers, *IEEE Transactions on Biomedical Engineering*, Vol. 58, No. 2, pp. 435–442, 2011.

● Tao Liu, Yoshio Inoue, Kyoko Shibata, Enguo Cao, Ambulatory estimation of muscle forces of lower limbs in a Rehabilitation robot system, *ICIC Express Letters*, Vol. 2, No. 1, pp. 235 - 240, 2011.

● Enguo Cao, Yoshio Inoue, Tao Liu, Kyoko Shibata, A Novel Approach for Muscle Force Analysis in Human Standing-up Process Based on a Rehabilitation Robot, *Journal of Biomechanical Science and Engineering-Transactions of the JSME,* Second Review.

● Enguo Cao, Yoshio Inoue, Kyoko Shibata, Kun Liu, Tao Liu, Estimation and Analysis of Lower Limb Kinetics during Standing up Process in Trajectory Control and Impedance control methods based on a Rehabilitation Robot, *IEEE Transactions on Robotics,* Under Review.

## *Academic Book Papers*

● Enguo Cao, Yoshio Inoue, Tao Liu, Kyoko Shibata, Muscle Force Analysis of Human Foot Based on Wearable Sensors and EMG Method, *EMG Methods for Evaluating Muscle and Nerve Function / Book, Edited by: Mark Schwartz, Published by In*Tech, ISBN 978-953-307-793-2, pp. 375 – 390, 2011.

## *International Conference Proceedings*

● Enguo Cao, Yoshio Inoue, Tao Liu, Kyoko Shibata, Estimation of Lower Limb Muscle Forces During Human Sit-to-stand Process With a Rehabilitation Training System, *IEEE-EMBS International Conference on Biomedical and Health Informatics (BHI 2012),* pp. 1016 - 1019, 2012.

● Enguo Cao, Yoshio Inoue, Tao Liu, Kyoko Shibata, A Self-controlled Trainer Robot for Sit to Stand Training, *The 3rd International Symposium on Frontier Technology (ISFT 2011),* pp. 78–81, 2011.

● Enguo Cao, Yoshio Inoue, Tao Liu, Kyoko Shibata, Analysis of Muscle Forces in Lower Limbs Based on Wearable Sensors, *2010 IEEE International Conference on Information and Automation (ICIA 2010),* pp. 185–190, 2010.

● Enguo Cao, Yoshio Inoue, Tao Liu, Kyoko Shibata, A Sit-to-stand Trainer System in Lower Limb Rehabilitation, *IEEE/ASME International Conference on Advanced Intelligent Mechatronics (AIM 2011),* pp. 116–121, 2010.

● Enguo Cao, Yoshio Inoue, Kyoko Shibata, Tao Liu, Dynamics and Muscle Forces Estimation of Human Lower Limb Based on a Sit-to-stand Training Robot, *The 6th Asian Conference on Multibody Dynamics (ACMD 2012),* Accepted.